IDENTIFICATION OF SHIP COUPLED HEAVE AND PITCH MOTIONS USING NEURAL NETWORKS

JINSONG XU

IDENTIFICATION OF SHIP COUPLED HEAVE AND PITCH MOTIONS USING NEURAL NETWORKS

By

© Jinsong Xu, B.Eng.

A thesis submitted to the School of Graduate Studies

in partial fulfillment of the requirements for

the degree of Master of Engineering

Faculty of Engineering and Applied Science

Memorial University of Newfoundland

July 1997

St. John's Newfoundland Canada

Abstract

Investigation of the ship motion behavior in irregular sea states is an important step for ship seakeeping performance research. Ship motion identification from the full scale measurements is the only way to study the actual motion behavior and verify the motion predictions after ship constructions. A particular identification method for coupled heave and pitch motions was developed and validated in this research. The two-degree Random Decrement technique and the Neural Networks technique were combined in identification process.

This developed method was applied to several motion systems to test its effects. The random motion data were obtained from the ship model experiments and numerical simulations. The coupled heave and pitch Random Decrement signatures obtained from the random motion histories were used as the Neural Networks training data to identify the Random Decrement equations. The identification results were verified by comparing the predictions with the actual Random Decrement signatures, and with the free response signatures.

The application results suggested that the validation of the identified equations was mainly dependent on the nature of the Random Decrement signatures and the quality of the Neural Networks training. Only White Noise or broad-band spectrum excitations could yield the required agreement between identified Random Decrement equations and motion free response equations.

Acknowledgments

I would like to take this opportunity to express my sincere appreciation to my supervisor Dr. M.R.Haddara for his support, guidance and encouragement during my study at Memorial University of Newfoundland.

I highly appreciate Dr. J.J.Sharp's approval of the financial support and his academic instructions. I am also grateful to my course instructors Dr. L. Lye, Dr. I. Jordaan, and Dr. G. Sabin for their generous help.

Special thanks to Mr. Andrew Kuczora for his advice and assistance in the experiments.

Table of Contents

Abstract ii

Acknowledgments iii

Table of Contents iv

List of Figures vi

List of Tables viii

1. Introduction 1

2. Methods and Procedures 6

2.1 Motion Data Acquisition 6
2.1.1 Ship Model Experiments 8
2.1.2 Motion Simulation 12
2.2 Random Decrement Technique 17
2.3 Formulation of Random Decrement Equations 22
2.4 Neural Network Technique for Motion Identification 24
2.5 Verification and Analysis of Identified Equations 29

3. Results and Discussion 31

3.1 Ship Model Experiment Results 31
3.1.1 Random Decrement Signature 33
3.1.2 Neural Network Identification 37
3.1.3 Verification of Identification Results 38
3.2 Ship Model Simulation Results (JONSWAP Wave) 46
3.2.1 System Analysis for Various Damping Parameters 46
3.2.2 Identification for Light Damping System 52
3.2.3 Verification for Light Damping System 54
3.3 Ship Model Simulation Results (White Noise) 58
3.3.1 Analysis of the Random Decrement Signatures 58
3.3.2 Identification Results 60
3.3.3 Verification Results 63

4. Conclusions and Recommendations 65

References 69

Appendix A Parameter Calculations 70

Appendix B Exciting Forces Calculations 77

Appendix C Data Processing Programs 84

Appendix D Neural Network Training Program 89

Appendix E Verification Programs 94

List of Figures

FIGURE 1: BODY PLAN OF 'R-CLASS ICEBREAKER' SHIP MODEL 8
FIGURE 2: JONSWAP WAVE SPECTRUM 11
FIGURE 3: WHITE NOISE EXCITATION FORCES SPECTRUM 15
FIGURE 4: ILLUSTRATION OF TWO-DEGREE RANDOM DECREMENT TECHNIQUE 21
FIGURE 5: MULTILAYER PERCEPTRON NEURAL NETWORK 26
FIGURE 6: HEAVE RANDOM DECREMENT SIGNATURE OF GROUP ONE -- RHP21, RHP22 AND RHP23 33
FIGURE 7: PITCH RANDOM DECREMENT SIGNATURE OF GROUP ONE -- RHP21, RHP22 AND RHP23 34
FIGURE 8: HEAVE RANDOM DECREMENT SIGNATURE OF GROUP TWO -- RHP41, RHP42 AND RHP43 34
FIGURE 9: PITCH RANDOM DECREMENT SIGNATURE OF GROUP TWO -- RHP41, RHP42 AND RHP43 35
FIGURE 10: RANDOM DECREMENT SIGNATURE OF GROUP ONE & GROUP TWO 35
FIGURE 11: NEURAL NETWORK TRAINING RESULTS 38
FIGURE 12: VERIFICATION RESULTS FOR HEAVE TRIGGER 1.0CM 39
FIGURE 13: VERIFICATION RESULTS FOR HEAVE TRIGGER 0.9CM 40
FIGURE 14: VERIFICATION RESULT FOR HEAVE TRIGGER 0.8CM 40
FIGURE 15: VERIFICATION RESULTS FOR HEAVE TRIGGER 0.6CM 41
FIGURE 16: VERIFICATION RESULTS FOR HEAVE TRIGGER 0.5CM 41
FIGURE 17: VERIFICATION RESULTS FOR HEAVE TRIGGER 0.4CM 42
FIGURE 18: EXPERIMENTAL HEAVE & PITCH FREE RESPONSE SIGNATURE RPH11 43
FIGURE 19: EXPERIMENTAL HEAVE & PITCH FREE RESPONSE SIGNATURE RPH12 44
FIGURE 20: EXPERIMENTAL HEAVE & PITCH FREE RESPONSE SIGNATURE RPH13 44
FIGURE 21: COMPARISON BETWEEN EXPERIMENTAL FREE RESPONSE AND RANDOM DECREMENT PREDICTION 45
FIGURE 22: COMPARISON BETWEEN FREE RESPONSE & RANDOM DECREMENT SIGNATURE (HEAVE TRIGGER 0.7 CM) 47
FIGURE 23: COMPARISON BETWEEN FREE RESPONSE & RANDOM DECREMENT SIGNATURE (HEAVE TRIGGER 0.6 CM) 48
FIGURE 24: COMPARISON BETWEEN FREE RESPONSE & RANDOM DECREMENT SIGNATURE FOR ζ=0.20 49
FIGURE 25: COMPARISON BETWEEN FREE RESPONSE & RANDOM DECREMENT SIGNATURE FOR ζ=0.16 50
FIGURE 26: COMPARISON BETWEEN FREE RESPONSE & RANDOM DECREMENT SIGNATURE FOR ζ=0.12 50
FIGURE 27: COMPARISON BETWEEN FREE RESPONSE & RANDOM DECREMENT SIGNATURE FOR ζ=0.08 51

FIGURE 28: COMPARISON BETWEEN FREE RESPONSE & RANDOM DECREMENT SIGNATURE FOR ζ=0.04 51
FIGURE 29: COMPARISON BETWEEN FREE RESPONSE & RANDOM DECREMENT SIGNATURE FOR ζ=0.02 52
FIGURE 30: NEURAL NETWORK TRAINING RESULTS FOR LIGHT DAMPING SYSTEM SIMULATIONS 54
FIGURE 31: COMPARISON BETWEEN PREDICTIONS & RANDOM DECREMENT SIGNATURE (HEAVE TRIGGER 2.0CM) 55
FIGURE 32: COMPARISON BETWEEN PREDICTIONS & RANDOM DECREMENT SIGNATURE (HEAVE TRIGGER 1.5CM) 55
FIGURE 33: COMPARISON BETWEEN PREDICTIONS & RANDOM DECREMENT SIGNATURE (HEAVE TRIGGER 1.0CM) 56
FIGURE 34: COMPARISON BETWEEN PREDICTIONS & FREE RESPONSE (HEAVE TRIGGER 2.0CM) 56
FIGURE 35: COMPARISON BETWEEN PREDICTIONS & FREE RESPONSE (HEAVE TRIGGER 1.5CM) 57
FIGURE 36: COMPARISON BETWEEN PREDICTIONS & FREE RESPONSE (HEAVE TRIGGER 1.0CM) 57
FIGURE 37: COMPARISON BETWEEN FREE RESPONSE & RANDOM DECREMENT SIGNATURE (HEAVE TRIGGER 1.3CM) 59
FIGURE 38: COMPARISON BETWEEN FREE RESPONSE & RANDOM DECREMENT SIGNATURE (HEAVE TRIGGER 1.0CM) 59
FIGURE 39: COMPARISON BETWEEN HEAVE AUTOCORRELATION, RANDOM DECREMENT, AND FREE RESPONSE 60
FIGURE 40: HEAVE TRAINING RESULT FOR WHITE NOISE SIMULATIONS 62
FIGURE 41: PITCH TRAINING RESULT FOR WHITE NOISE SIMULATIONS 62
FIGURE 42: COMPARISON BETWEEN PREDICTIONS & RANDOM DECREMENT SIGNATURE (HEAVE TRIGGER 1.3CM) 64
FIGURE 43: COMPARISON BETWEEN PREDICTIONS & RANDOM DECREMENT SIGNATURE (HEAVETRIGGER 1.2CM) 64

List of Tables

TABLE I: HYDROSTATIC PARTICULARS FOR MODEL 'R-CLASS ICEBREAKER' 7
TABLE II: SHIP MODEL EXPERIMENTS CATEGORY 12
TABLE III : MODEL EXPERIMENTS MOTION DATA FILES 31
TABLE IV: MEAN VALUE ANALYSES 32
TABLE V: IDENTIFICATION RESULTS FOR RANDOM DECREMENT EQUATIONS 37
TABLE VI: IDENTIFICATION RESULTS FOR LIGHT DAMPING SYSTEM SIMULATIONS 53
TABLE VII: IDENTIFICATION RESULTS FOR WHITE NOISE EXCITATION 61

1. Introduction

Ships are designed and built for transportation upon the sea. Any ship must possess some basic characteristics to float in a stable upright position, move with sufficient speed, maneuver in restricted routes, and withstand the reasonable loads. With the basic knowledge of hydrostatics and hydrodynamics, prediction of the ship performance in calm water is available for naval architects, and has been the basis for new ship designs for a long time. However, the success of a ship design is ultimately determined by its performance in a seaway. The real sea is rarely calm, and the ship performance is always degraded due to wave effects. Ship seakeeping research aims to limit the wave-induced ship motions and reduce the performance degradation.

There are several sequential steps involved in seakeeping performance research. Lloyd(1991) gives an overall description about these steps, including:

1. study ship motion behavior in irregular sea state;
2. estimate the dynamic effects caused by the motions;
3. determine the maximum permissible motion levels;
4. find the quantitative index of seakeeping performance measurement;
5. develop strategies in design to achieve acceptable performance.

Obviously ship motion study is the initial point for ship seakeeping performance research. Among the six degrees of freedom of ship motions, heave is the motion vertically up and down, and pitch is the angular motion about a horizontal transverse axis. These motions are always coupled in reality. Identification of coupled heave and pitch motions in random waves is the concern of this research.

Ship motions are usually investigated in four ways: theoretical analysis, model experiments, empirical formulae, and ship trials analysis. Theoretical analysis involves the methods such as strip theory, spectral theory and computational fluid dynamics (CFD). Model experiments method is to scale up the experiment results given the corresponding model law. Empirical formulae or database method is to draw conclusions based upon statistical observations. Above three methods are mainly used in ship design stage for motion predictions. After ship construction, however, ship trials analysis is the only way to explore the actual motion behavior and verify all motion predictions. Because of the randomness involved in ship motions, direct comparison between motion records and predictions is usually impossible. Some statistical methods have to be incorporated for motion identification from the ship motion records. In this research a particular method for identification of coupled heave and pitch motion from the random motion history is developed and validated through the model experiments and numerical simulations.

Various system identification techniques start with the assumption that a ship in seaway is an input/output system with the waves as input and ship motions as output. Both input

and output are irregular. The random ship motion responses could be measured and recorded in real time, but a complete knowledge of wave behavior in seaway is usually not available. The conventional identification techniques can not achieve the goal in this case. The Random Decrement technique is thus employed for motion data processing. Under certain conditions, the resulted Random Decrement signatures would agree well with system free response signatures. Application of Random Decrement technique makes it possible to identify ship motions without the complete wave input knowledge. This technique was empirically developed in the late 1960's by Henry Cole(1971) for structure vibration identification. The mathematical interpretation was formulated by Vandiver et al.(1982). The single-degree Random Decrement technique was extended to multiple-degree cases by Ibrahim(1977). Haddara and Wu(1993) first applied the Random Decrement technique into ship rolling identification. In this research two-degree Random Decrement technique is adopted to process the coupled heave and pitch motion data.

Since the Random Decrement signature corresponds to free response signature under certain conditions, the Random Decrement equations are assumed to have the same form as that of ship motion free response equations. In this research the coupled heave and pitch Random Decrement signatures obtained from the random motion time series are used to identify Random Decrement equations. In conventional system identification techniques, the unknown parameters in the assumed motion equations are adjusted to match the sample data. For complex coupled motion systems, too many unknown

parameters in motion model would make it very difficult, even impossible, to achieve the acceptable identification results. The Neural Networks technique provides a means for identification of complex systems instead of the conventional methods. Various Neural Networks structures and algorithms are explicitly described in Hush and Horne(1993). The Multilayer Perceptron networks have been used in ship motion identification by Haddara and Hinchey(1995), Haddara and Wang(1996). In this research the modified algorithm of the Multilayer Perceptron networks is applied to identification of coupled heave and pitch motions.

The identified Random Decrement equations have to be verified and analyzed for their validation. First of all, the actual Random Decrement signatures should satisfy the identified equations. This generalization is verified by comparison between the actual Random Decrement signatures and the predicted signatures. Secondly, the identified equations have to be analyzed in some ways to show its relation with system free response equations. If the free response signatures are available, they will be compared with the predicted signatures. Only the Random Decrement equations that agree with system free response equations could be used for further seakeeping research.

This developed method is applied to several motion identifications. One group of the motion data is measured from ship model experiments in JONSWAP waves. The other motion data are generated from the numerical simulations for both JONSWAP wave and White Noise excitations. The presented results show that the validation of motion identification is mainly dependent on the nature of the Random Decrement signatures and

the quality of the Neural Networks training. The JONSWAP wave input could not ensure the agreement between the identified Random Decrement equations and the free response equations for coupled heave and pitch motions. Only White Noise or broad-band spectrum excitations yield the required agreement.

2. Methods and Procedures

System identification process usually consists of several sequential steps including data acquisition, data processing, system model formulation, system identification and results verification. There are various methods for every individual step, and the choice of the particular method is determined by the nature of the problem.

In this research, irregular ship motion data were obtained from the ship model experiments and numerical simulations. Records of the coupled heave and pitch motion histories were processed using two-degree Random Decrement technique. The motion system was represented by simultaneous differential equations. Multilayer Perceptron neural networks were adopted for system identification. The identified equations were verified using actual Random Decrement signatures and free response signatures.

2.1 Motion Data Acquisition

Motion identification method is practically applied to full scale measurements. For research convenience, some motion data obtained from model experiments and numerical simulations are also required because the environmental conditions could be controlled. In this research the heave and pitch motion data of a ship model 'R-Class Icebreaker' were obtained to develop and validate a particular identification method. The model hydrostatic particulars and body plan are presented in Table i and Figure 1. One group of motion data was measured from wave tank experiments, and the other groups were generated from numerical simulations.

Table i: Hydrostatic Particulars for Model 'R-Class Icebreaker'

Length between perpendiculars (LPP), m	2.1985
Length of waterline (LWL), m	2.3250
Waterline beam at midships, m	0.4840
Waterline beam at maximum section, m	0.4840
Maximum waterline beam, m	0.4845
Draft at midships, m	0.1735
Draft at maximum section, m	0.1745
Draft at aft perpendicular, m	0.1790
Draft at forward perpendicular, m	0.1675
Equivalent level keel draft, m	0.1735
Maximum section forward at midships, m	-0.1850
Parallel middle body, from aft of midships to forward of midships, m	+0.1850 -0.1850
Area of maximum station, m^2	0.1545
Center of buoyancy forward of midships, m	-0.0080
Center of buoyancy above keel, m	+0.0970
Wetted surface area, m^2	1.1335
Volume of displacement, m^3	0.1190
Displacement of fresh water, kg	121.6
Center of floatation forward of midships, m	-0.0175
Center of floatation above keel, m	+0.1735
Area of waterline plane, m^2	0.899
Transverse metacentric radius, m	0.122
Longitudinal metacentric radius, m	2.4

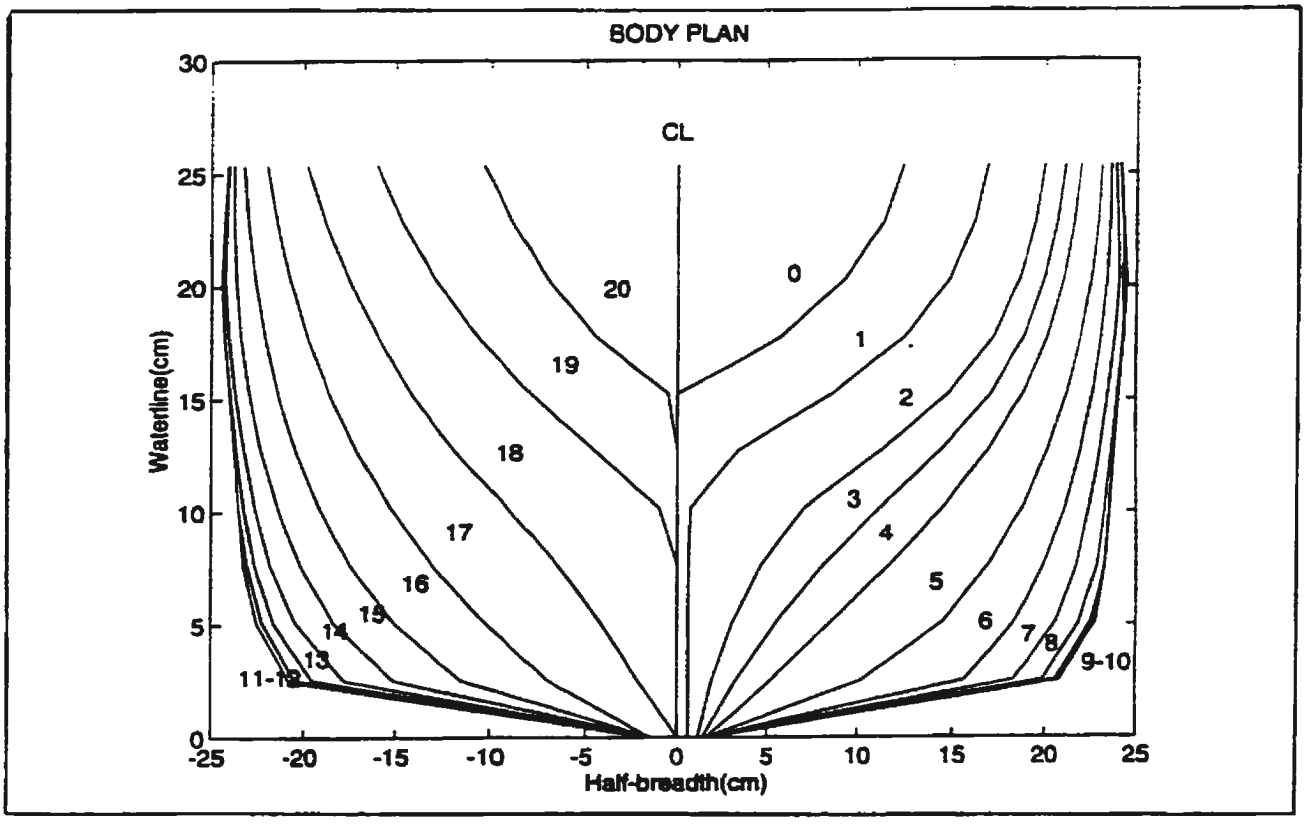

Figure 1: Body Plan of 'R-Class Icebreaker' Ship Model

2.1.1 Ship Model Experiments

A group of motion data was directly measured from model experiments conducted in the wave tank at Memorial University of Newfoundland. The whole facility consists of a large wave tank, an instrumented towing carriage, and a fully equipped control room containing a complete range of data acquisition and analysis equipment.

The wave tank has inside dimensions of 58.27m in length, 4.57m in width, and 3.04m in depth. At one end is a hydraulically operated, piston type wave generator. The waveboard is fabricated from aluminum with a watertight Teflon seal around its periphery. At the other end is a parabolic beach consisting of an aluminum frame covered by wooden slats. This construction is intended to absorb and dissipate the energy contained in the incident

wave and maintain a minimum reflection coefficient. Waves are created in the tank by the translatory motion of the waveboard over its 0.5m stroke. Electronic control for the waveboard is provided from the control room. Control signals for irregular wave spectra are generated by computer and the resultant time series are transferred to a microcomputer controlled digital to analog converter, which allows reproduction of any theoretical spectrum.

The towing carriage over the wave tank is equipped with a dynamometer that can measure horizontal forces of ± 20 kg, vertical movements over a 0.4m range, and rotations within a ± 30 degree arc. Wave probes are employed to monitor the time history of the wave profile. Further data acquisition and analysis are performed in the control room. Data from the dynamometer and wave probes are recorded in analog format on one or more multi-channel instrumentation recorders, and simultaneously digitized with a multi-channel analog to digital converter and a computer.

During 'R-Class Icebreaker' model experiments, the ship model was positioned along the center line of the wave tank, heading towards the wave generator. The model was allowed only to move in vertical plane, heaving and pitching. The dynamometer was attached to the ship model at the cross point of midship and center line. The coupled heave motion displacement and angular pitch displacement were collected simultaneously by the dynamometer. A wave probe was located beside the ship model about 0.5m apart.

The JONSWAP (Joint North Sea Wave Project) spectrum wave was generated in the wave tank as ship motion excitation. This spectrum is always used for coastal waters where the fetch may be limited. It is defined by wave energy density $S(m^2/Hz)$ as the function of wave component frequency f(Hz). In this research the following function was employed for generation of required wave time series,

$$S(f)=\frac{5H_s{}^2 f_m{}^4}{16f^5\gamma^{\frac{1}{3}}}\exp(-\frac{5f_m{}^4}{4f^4})\gamma^{\exp\left[\frac{(f-f_m)^2}{2\sigma^2 f_m{}^2}\right]} \qquad (1)$$

where the parameters are wave significant height H_s, peak frequency f_m, peak enhancement factor γ, and shape parameter σ. A particular JONSWAP spectrum is shown in Figure 2.

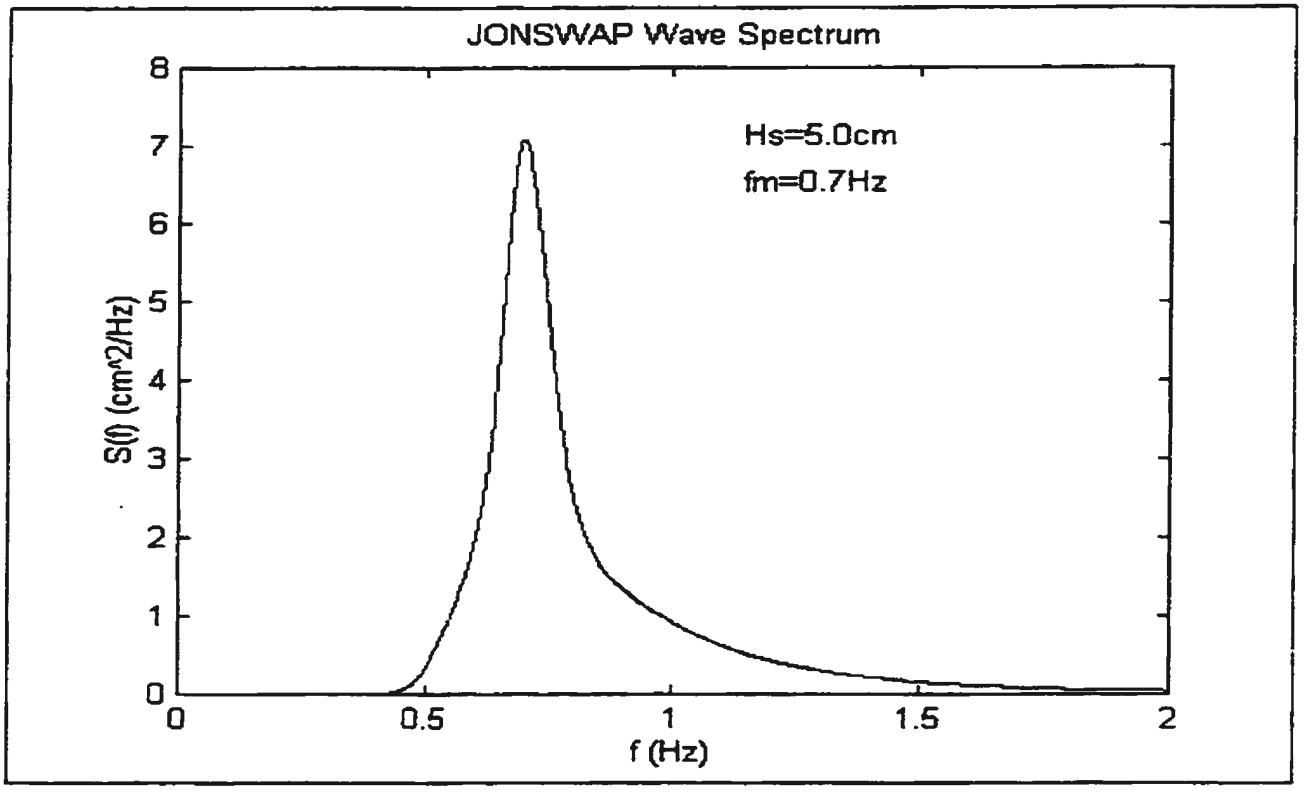

Figure 2: JONSWAP Wave Spectrum

In this research two groups of JONSWAP waves were generated for ship model excitation. In each group there were three different wave series resulted from the same spectrum. The wave spectrum used in the first group is that shown in Figure 2. In addition to experiments under JONSWAP wave, the heave and pitch free response tests were also performed by giving ship model a certain initial displacement. The various experiments are tabulated in Table ii. Motion data were collected for 400 seconds with a time interval of 0.05 second. There were 8001 data points in every record. The collected heave data was the heave displacement of the cross point of midship and center line, where the dynamometer was attached.

Table ii: Ship Model Experiments Category

	Wave Spectrum Parameters			
Time Series	H_s (cm)	f_m (Hz)	γ	σ
J7H5	5.0	0.7	3.3	0.07 ($f < f_m$) 0.09 ($f > f_m$)
J7H5a	5.0	0.7	3.3	0.07 ($f < f_m$) 0.09 ($f > f_m$)
J7H5b	5.0	0.7	3.3	0.07 ($f < f_m$) 0.09 ($f > f_m$)
J7H75	7.5	0.7	3.3	0.07 ($f < f_m$) 0.09 ($f > f_m$)
J7H75a	7.5	0.7	3.3	0.07 ($f < f_m$) 0.09 ($f > f_m$)
J7H75b	7.5	0.7	3.3	0.07 ($f < f_m$) 0.09 ($f > f_m$)
Free Response	Calm Water			

2.1.2 Motion Simulation

Besides ship model experiments, some numerical simulations were also employed in this research to explore what happened behind the experiment results. The interrelationship between the involved parameters could be displayed through analysis of the various simulation results.

Any kind of simulation is based on a particular mathematical model that represents the original system theoretically. For ship heave and pitch motion, strip theory is usually employed to estimate the parameters in the dynamic motion equations. From the calculations detailed in Appendix A, which are based on the algorithm from

Bhattacharyya (1979), the dynamic equations for simulation of 'R-Class Icebreaker' heave and pitch motions are expressed as (2),

$$\begin{aligned} Z'' + 2.824Z' + 34.092Z + 0.158\theta' + 0.238\theta &= 0.4126F(t) - 0.0273M(t) \\ \theta'' + 0.580Z' + 0.629Z + 2.632\theta' + 30.780\theta &= -0.0273F(t) + 1.560M(t) \end{aligned} \qquad (2)$$

where Z denotes heave displacement of ship model CG (center of gravity), θ denotes pitch angular displacement, and symbols Z'',θ'' and Z',θ' represent second-order and first-order differentiation of heave and pitch displacement with respect to time respectively. The random excitation force F(t) and moment M(t) for the ship model are dependent on wave spectrum and model hull geometry. During simulations two sets of excitation forces were generated, one set from JONSWAP wave environment, the other set from a white noise excitation spectrum.

For the JONSWAP wave case, wave time history was generated by adding a large number of component sine waves. Every component sine wave was derived from the specified spectrum and expressed as equations (3), where ε_n is a random angle. The random wave series were obtained by adding a large number of individual component waves as shown in equation (4). In this research there were 800 component waves involved. For details about wave synthesis method, reference should be made to Lloyd (1989). For every component sine wave, the corresponding excitation forces $F_n(t)$ and $M_n(t)$ were calculated using strip theory. The calculations based on Bhattacharyya (1978) are detailed in Appendix B. The ratios between force amplitude and corresponding wave amplitude, and

the phase differences between the forces and waves were expressed as functions of the wave frequency. These excitation transform functions, combined with the wave components, generated the final random forces F(t) and M(t) expressed as equations (5).

$$\zeta_{n0} = \sqrt{2S(f_n)\delta f} \qquad (3)$$
$$\zeta_n(t) = \zeta_{n0}\cos(2\pi f_n t + \varepsilon_n)$$

$$\zeta(t) = \sum_{n=1}^{800} \zeta_{n0}\cos(2\pi f_n t + \varepsilon_n) \qquad (4)$$

$$F(t) = \sum_{n=1}^{800} r_{1n}\zeta_{n0}\cos(2\pi f_n t + \varepsilon_n + phase_{1n}) \qquad (5)$$
$$M(t) = \sum_{n=1}^{800} r_{2n}\zeta_{n0}\cos(2\pi f_n t + \varepsilon_n + phase_{2n})$$

For the white noise excitation case, the generation of the forces was simplified by direct employment of the white noise spectrum for excitation forces. White noise is defined as stationary random process whose power spectral density is constant, that is, independent of frequency. Physically white noise is not possible because this demands infinite power. In this research the broad band spectrum shown in Figure 3 was used to approximate the white noise excitation situation. The forces F(t) and M(t) were generated as(6), where the phase differences were obtained from the excitation transform functions presented in Appendix B.

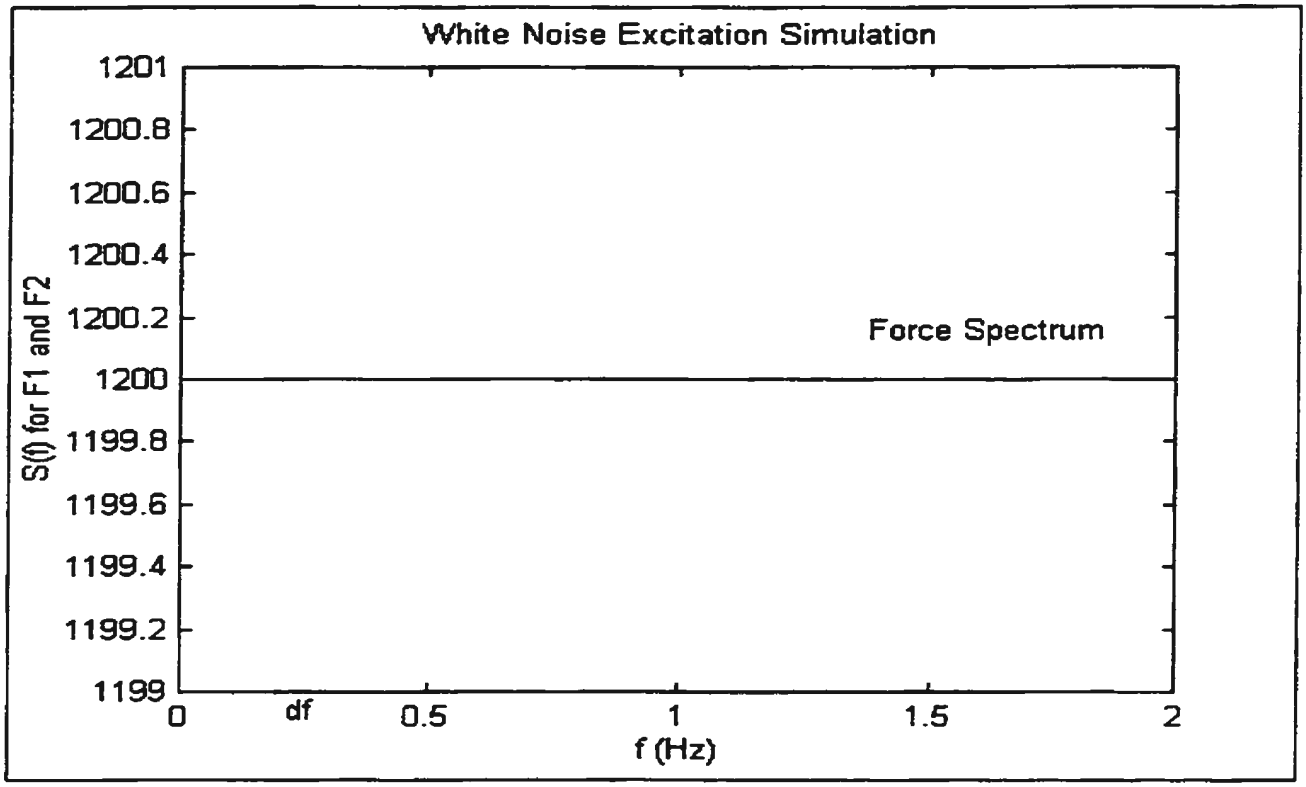

Figure 3: White Noise Excitation Forces Spectrum

$$F(t) = \sum_{n=1}^{800} \sqrt{2S_1 \delta f}\, \cos(2\pi f_n t + \varepsilon_n + phase_{1n}) \qquad (6)$$

$$M(t) = \sum_{n=1}^{800} \sqrt{2S_2 \delta f}\, \cos(2\pi f_n t + \varepsilon_n + phase_{2n})$$

After the excitation forces were calculated, the simulated motion time series were obtained from the numerical solutions to the equation (2). A fourth-order Runge-Kutta method was employed in solving the simultaneous differential equations. The algorithm is as follows.

$$
\begin{aligned}
Z(t+\Delta t) &= Z(t) + (K_1 + 2K_2 + 2K_3 + K_4)/6 \\
Z'(t+\Delta t) &= Z'(t) + (L_1 + 2L_2 + 2L_3 + L_4)/6 \\
\theta(t+\Delta t) &= \theta(t) + (M_1 + 2M_2 + 2M_3 + M_4)/6 \\
\theta'(t+\Delta t) &= \theta'(t) + (N_1 + 2N_2 + 2N_3 + N_4)/6
\end{aligned}
\tag{7}
$$

$$
\begin{aligned}
K_1 &= \Delta t \times \{Z'(t)\} \\
L_1 &= \Delta t \times \{F_1(t) - 2.824Z'(t) - 34.092Z(t) - 0.158\theta'(t) - 0.238\theta(t)\} \\
M_1 &= \Delta t \times \{\theta'(t)\} \\
N_1 &= \Delta t \times \{F_2(t) - 0.580Z'(t) - 0.629Z(t) - 2.632\theta'(t) - 30.780\theta(t)\}
\end{aligned}
$$

$$
\begin{aligned}
K_2 &= \Delta t \times \{Z'(t) + 0.5L_1\} \\
L_2 &= \Delta t \times \left\{ \begin{array}{l} [F_1(t) + F_1(t+\Delta t)]/2 - 2.824[Z'(t) + 0.5L_1] - 34.092[Z(t) + 0.5K_1] \\ -0.158[\theta'(t) + 0.5N_1] - 0.238[\theta(t) + 0.5M_1] \end{array} \right\} \\
M_2 &= \Delta t \times \{\theta'(t) + 0.5N_1\} \\
N_2 &= \Delta t \times \left\{ \begin{array}{l} [F_2(t) + F_2(t+\Delta t)]/2 - 0.580[Z'(t) + 0.5L_1] - 0.629[Z(t) + 0.5K_1] \\ -2.632[\theta'(t) + 0.5N_1] - 30.780[\theta(t) + 0.5M_1] \end{array} \right\}
\end{aligned}
$$

$$
\begin{aligned}
K_3 &= \Delta t \times \{Z'(t) + 0.5L_2\} \\
L_3 &= \Delta t \times \left\{ \begin{array}{l} [F_1(t) + F_1(t+\Delta t)]/2 - 2.824[Z'(t) + 0.5L_2] - 34.092[Z(t) + 0.5K_2] \\ -0.158[\theta'(t) + 0.5N_2] - 0.238[\theta(t) + 0.5M_2] \end{array} \right\} \\
M_3 &= \Delta t \times \{\theta'(t) + 0.5N_2\} \\
N_3 &= \Delta t \times \left\{ \begin{array}{l} [F_2(t) + F_2(t+\Delta t)]/2 - 0.580[Z'(t) + 0.5L_2] - 0.629[Z(t) + 0.5K_2] \\ -2.632[\theta'(t) + 0.5N_2] - 30.780[\theta(t) + 0.5M_2] \end{array} \right\}
\end{aligned}
$$

$$K_4 = \Delta t \times \{Z'(t) + L_3\}$$

$$L_4 = \Delta t \times \begin{Bmatrix} F_1(t+\Delta t) - 2.824[Z'(t) + L_3] - 34.092[Z(t) + K_3] \\ -0.158[\theta'(t) + N_3] - 0.238[\theta(t) + M_3] \end{Bmatrix}$$

$$M_4 = \Delta t \times \{\theta'(t) + 0.5N_3\}$$

$$N_4 = \Delta t \times \begin{Bmatrix} F_2(t+\Delta t) - 0.580[Z'(t) + L_3] - 0.629[Z(t) + K_3] \\ -2.632[\theta'(t) + N_3] - 30.780[\theta(t) + M_3] \end{Bmatrix}$$

The time interval Δt was taken as 0.05 second with a total of 8001 data points in every simulated time series.

Different simulation series were obtained by varying the damping levels in the mathematical model. Various results were compared and analyzed.

2.2 Random Decrement Technique

The motion data of 'R-Class Icebreaker', whether from model experiments or from motion simulations, are records of random time series. Some statistical methods are needed for data processing in the identification process. In this research the two-degree Random Decrement technique was employed for heave and pitch motion data processing.

The Random Decrement technique was empirically developed in the late 1960's by Cole(1971), and has been widely used in the aerospace industry for the analysis of experimentally generated vibration data. A single-degree random decrement signature is simply the trace formed by a waveform averaging a number of specially selected segments from a measured motion time history. Each of the selected segments shares the common attribute of the same initial conditions. The most popular choice is to only

specify the initial motion displacement. From empirical induction, the basic conclusion has been widely accepted — if a linear system is excited by a stationary, Gaussian random process, the Random Decrement signature of the output is similar to the free response signature.

Although it is difficult to derive the general mathematical conclusions, Vandiver et al.(1982) provided a mathematical interpretation through the analysis of a specific case. For a linear, time-invariant system excited by a zero-mean, stationary, Gaussian random process, the response will also be a zero-mean, stationary, Gaussian random process. Its Random Decrement signature $D_{X0}(\tau)$ is simply the product of the correlation function and the trigger level X_0 as expressed in the equation (8).

$$D_{x0}(\tau) = \frac{R_x(\tau)}{R_x(0)} X_0 \qquad (8)$$

Based upon the above expression, there are several conclusions regarding the response Random Decrement signature $D_{X0}(\tau)$.

- If the input is white noise, the Random Decrement signature of the output will exactly represent the transient decay of the system from the specified trigger level X_0.
- If the excitation is not white noise, but sufficiently broad-band, the above conclusion will apply well.

- For a band limited excitation spectrum, a lightly damped system often yields the results which to sufficient accuracy are equivalent to the response of a white noise input.

For more complicated systems, there have been no general mathematical conclusions in the published literature. Obviously the Random Decrement technique is still an empirical technique that needs careful verification for every application case. Haddara and Wu(1993) presented such an example for the ship rolling identification, which involved a light damping system under the band limited excitations. The results were compatible with the conclusions in Vandiver et al.(1982).

The single-degree Random Decrement technique has been extended to multiple-degree cases by Ibrahim(1977) without any mathematical reasoning. In this research the two-degree algorithm was employed to obtain coupled heave and pitch Random Decrement signatures from the heave and pitch random time series $X_3(t)$ and $X_5(t)$. The heave signal $X_3(t)$ was chosen as leading signal. The heave Random Decrement signature $Z(\tau)$ was computed according to the following equation,

$$Z(\tau)=\frac{1}{2N}\left[\sum_{i=1}^{N} X_3(t_i+\tau)+\sum_{j=1}^{N} X_3(t_j+\tau)\right] \qquad (9)$$

with the following conditions:

$$t = t_i \quad \text{when } X_3(t) = Z_0 \text{ and } X_3' > 0$$

$$t = t_j \quad \text{when } X_3(t) = Z_0 \text{ and } X_3' < 0$$

where Z_o is the specified trigger value. The successive segments should not overlap to ensure their independence. The corresponding pitch Random Decrement signature $\theta(\tau)$ was computed by averaging the segments from $X_5(t)$ with the same starting point and time intervals as that of the leading signal $X_3(t)$. The equation is shown below,

$$\theta(\tau) = \frac{1}{2N}\left[\sum_{i=1}^{N} X_5(t_i + \tau) + \sum_{j=1}^{N} X_5(t_j + \tau)\right] \qquad (10)$$

with the same conditions:

$$t = t_i \quad \text{when } X_3(t) = Z_0 \text{ and } X_3' > 0$$

$$t = t_j \quad \text{when } X_3(t) = Z_0 \text{ and } X_3' < 0$$

In this research there were 200 data points in every Random Decrement signature with the time interval of 0.05 second. The illustration of the two-degree Random Decrement technique is shown in Figure 4. The first two segments start from the points t_1 and t_2 respectively, which both satisfy the condition $X_3(t)=Z_0$.

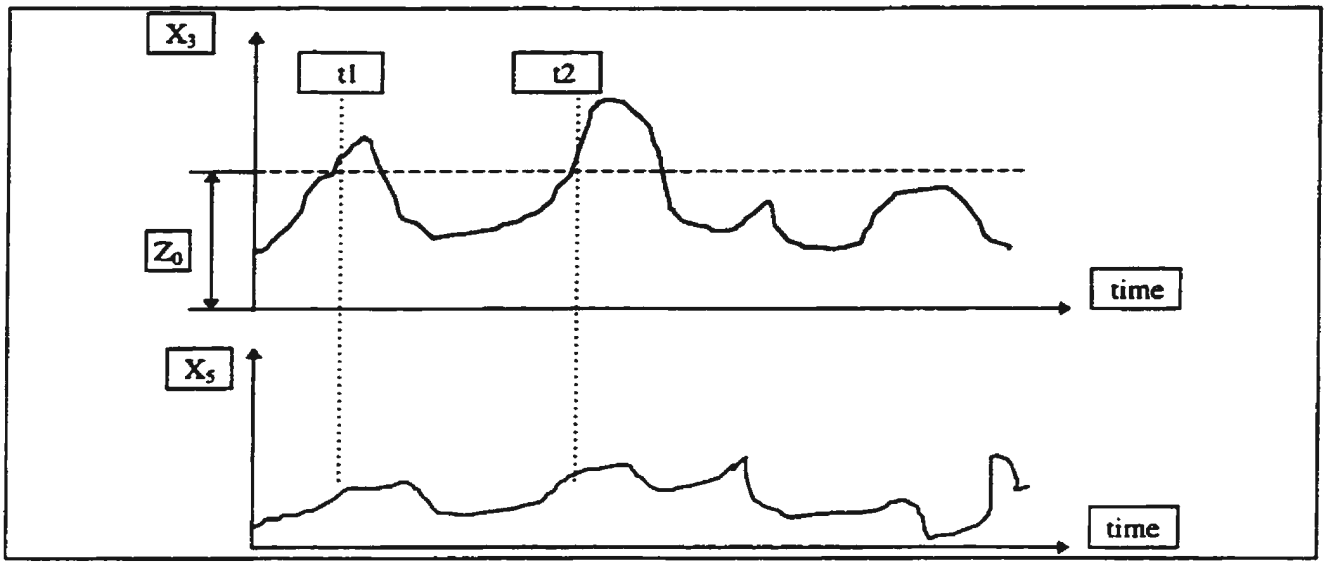

Figure 4: Illustration of Two-Degree Random Decrement Technique

From Ibrahim(1977), the two-degree Random Decrement signatures were claimed to agree with the system free response signatures in most cases. It thus provides a possible means to identify the free response equations from the Random Decrement signatures.

For single-degree Random Decrement signature, Vandiver et al.(1982) presented the proportional relationship between Random Decrement signature and autocorrelation function. In this case, the autocorrelation function could be used instead of the Random Decrement signature and usually is more accurate than the Random Decrement signature. However, for multiple-degree Random Decrement signatures, such relationship is not retained due to the phase difference between the individual signals in Random Decrement signatures. Only for leading signal could some comparisons be made between Random Decrement signature and autocorrelation function.

2.3 Formulation of Random Decrement Equations

Among six-degree ship motions, heaving and pitching are always coupled in the vertical plane. From Lloyd(1989) the coupled linear heave and pitch motions of a particular ship in the wave could be described by the following simultaneous ordinary differential equations,

$$\begin{aligned}(m+a_{33})X_3'' + b_{33}X_3' + c_{33}X_3 + a_{35}X_5'' + b_{35}X_5' + c_{35}X_5 &= F_3(t) \\ a_{53}X_3'' + b_{53}X_3' + c_{53}X_3 + (I_{55}+a_{55})X_5'' + b_{55}X_5' + c_{55}X_5 &= F_5(t)\end{aligned} \qquad (11)$$

where X_3 indicates linear heave displacement of ship's CG (center of gravity); X_5 indicates angular pitch displacement; m is the ship mass and I_{55} is the mass moment of the inertia of the ship about the transverse axis passing through the CG; the a, b, c and F are the coefficients or values related to the added masses, damping, restorations and excitations respectively. Using matrix notation, equation (11) could be rewritten as follows,

$$\begin{pmatrix} X_3'' \\ X_5'' \end{pmatrix} + \begin{pmatrix} B_{33} & B_{35} \\ B_{53} & B_{55} \end{pmatrix} \begin{pmatrix} X_3' \\ X_5' \end{pmatrix} + \begin{pmatrix} C_{33} & C_{35} \\ C_{53} & C_{55} \end{pmatrix} \begin{pmatrix} X_3 \\ X_5 \end{pmatrix} = \begin{pmatrix} G_3(t) \\ G_5(t) \end{pmatrix} \qquad (12)$$

where $\begin{pmatrix} B_{33} & B_{35} \\ B_{53} & B_{55} \end{pmatrix} = \begin{pmatrix} m+a_{33} & a_{35} \\ a_{53} & I_{55}+a_{55} \end{pmatrix}^{-1} \begin{pmatrix} b_{33} & b_{35} \\ b_{53} & b_{55} \end{pmatrix}$,

$$\begin{pmatrix} C_{33} & C_{35} \\ C_{53} & C_{55} \end{pmatrix} = \begin{pmatrix} m+a_{33} & a_{35} \\ a_{53} & I_{55}+a_{55} \end{pmatrix}^{-1} \begin{pmatrix} c_{33} & c_{35} \\ c_{53} & c_{55} \end{pmatrix},$$

and $\begin{pmatrix} G_3(t) \\ G_5(t) \end{pmatrix} = \begin{pmatrix} m+a_{33} & a_{35} \\ a_{53} & I_{55}+a_{55} \end{pmatrix}^{-1} \begin{pmatrix} F_3(t) \\ F_5(t) \end{pmatrix}$.

For free response situation, the excitation forces $F_3(t)$, $F_5(t)$ and $G_3(t)$, $G_5(t)$ are all zero. The free response equations could be converted from matrix form to the following,

$$X_3'' + B_{33}X_3' + C_{33}X_3 + B_{35}X_5' + C_{35}X_5 = 0$$
$$X_5'' + B_{53}X_3' + C_{53}X_3 + B_{55}X_5' + C_{55}X_5 = 0 \qquad (13)$$

The above free response equations represent the coupled heave and pitch motion system. If the unknown parameters B and C are determined, such motion system is identified. However, the free response signatures are usually not available for full scale ship motions. Thus the free response equations can not be identified directly. Instead, the Random Decrement signatures were used in this research to identify the motion system.

The heave and pitch Random Decrement signatures $Z(\tau)$ and $\theta(\tau)$ were obtained from the motion time series $X_3(t)$ and $X_5(t)$ as expressed in equations (9) and (10). If the excitation forces are Gaussian, white noise random processes with means of zero, it is proved by Haddara(1997) that the corresponding Random Decrement equations are exactly similar to the free response equations (13). For other excitation cases, it is assumed that the Random Decrement equations have the same form. Thus the general Random Decrement equations are expressed as (14),

$$Z'' + A_1Z' + B_1Z + C_1\theta' + D_1\theta = 0$$
$$\theta'' + A_2Z' + B_2Z + C_2\theta' + D_2\theta = 0 \qquad (14)$$

where A, B, C and D are unknown parameters. The Random Decrement equations could be identified from the Random Decrement signatures. For a particular excitation case, if the Random Decrement signature does agree well with system free response signature, the identified Random Decrement equations will represent the free response equations. This is the aim of the method.

2.4 Neural Network Technique for Motion Identification

After formulation of the Random Decrement equations, the identification of heave and pitch motions could be achieved by estimating the unknown parameters A, B, C and D in (14) from the Random Decrement signature $Z(\tau)$ and $\theta(\tau)$. The conventional system identification techniques are not efficient for such a problem with eight unknown parameters. The Neural Networks technique was employed in this research instead of conventional methods.

Neural Networks technique simulates the human brain functions to learn some rules from the training process. In practical application, one kind of rules is of functional relation between different data groups. It is thus possible to approximate the unknown functions by training the Neural Network from the input and output samples. The various Neural Network forms and algorithms have been explicitly described by Hush and Horne(1993). The Multilayer Perceptron Network technique was used in this research with some modifications.

Because the Neural Network technique was intended for identification of unknown functions, the heave and pitch Random Decrement equation (14) was converted to the following form,

$$Z'' + \omega_3{}^2 Z + G_1(Z', Z, \theta', \theta) = 0$$
$$\theta'' + \omega_5{}^2 \theta + G_2(Z', Z, \theta', \theta) = 0 \qquad (15)$$

where ω_3 and ω_5 are damped frequencies of heave and pitch respectively. The unknown functions G_1 and G_2 consist of the damping terms and part of the restoring terms. The damped frequencies ω_3 and ω_5 were estimated directly from the Random Decrement signature $Z(\tau)$ and $\theta(\tau)$. The functions G_1 and G_2 were identified using the Multilayer Perceptron Network shown in Figure 5.

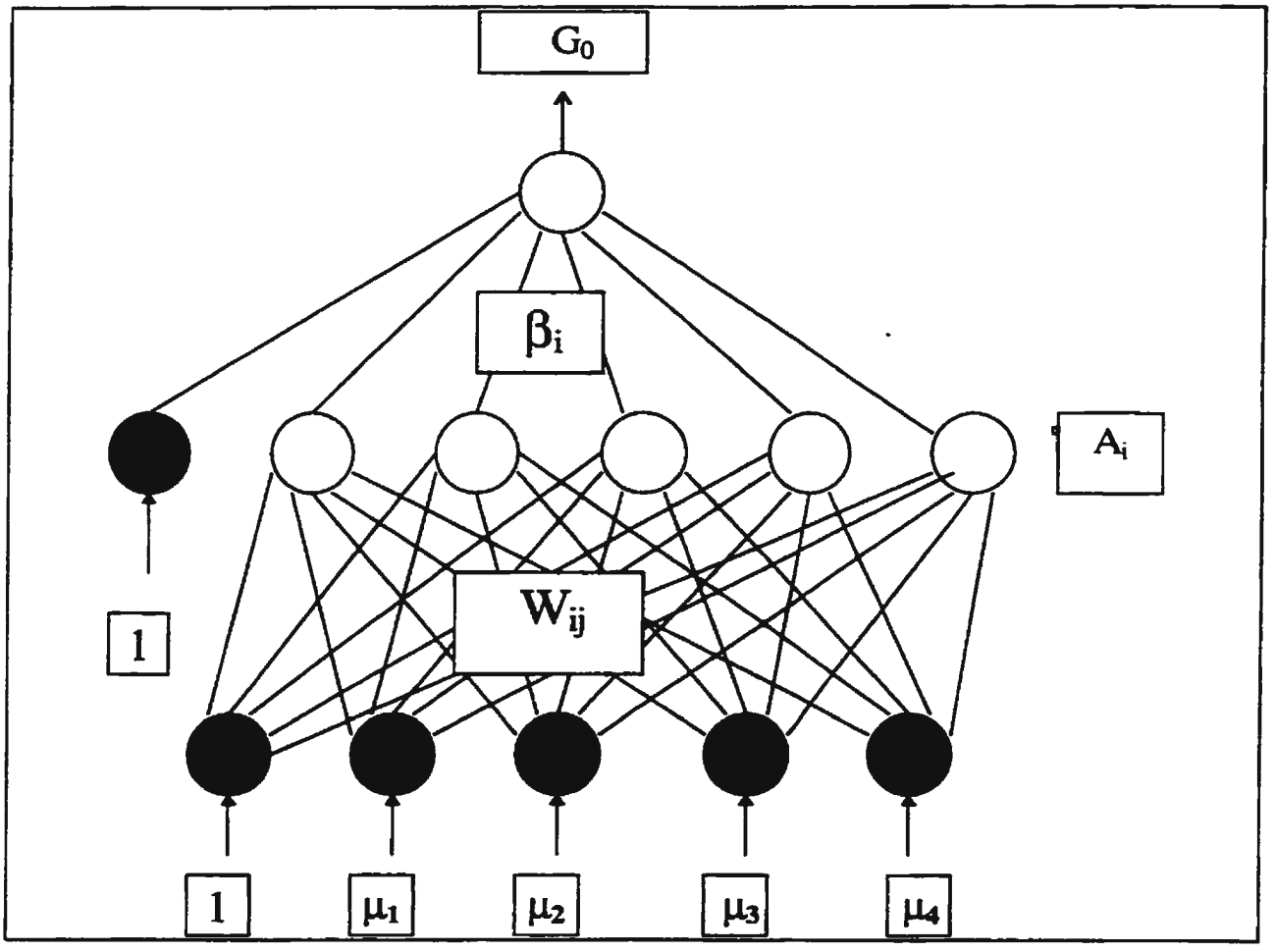

Figure 5: Multilayer Perceptron Neural Network

The inputs are μ_1, μ_2, μ_3 and μ_4 with the output G_0. There are six neurons in the hidden layer. One set of weight values W_{ij} and β_i uniquely determines the functional relation between the output and inputs, which is expressed by the equations (16) and (17).

The outputs of six hidden layer neurons A_i (i=0,1,2,3,4,5) are,

$$\begin{cases} A_0 = 1 \\ A_i = \left\{1 + \exp\left[-(1W_{i0} + \mu_1 W_{i1} + \mu_2 W_{i2} + \mu_3 W_{i3} + \mu_4 W_{i4})\right]\right\}^{-1}, (i = 1,2,3,4,5) \end{cases} \quad (16)$$

The final output of the Neural Network G_0 is,

$$G_0 = \sum_{i=0}^{5} (\beta_i \times A_i) \qquad (17)$$

Given a group of input sample data and the required output data G, the weight values W_{ij} and β_i are adjusted through an iterative training process to minimize the errors between the required data G and the output data G_0. The final weight values should satisfy the following conditions,

$$\frac{\partial\left[(G-G_0)^2\right]}{\partial W_{ij}} = 0 \qquad (18)$$

$$\frac{\partial\left[(G-G_0)^2\right]}{\partial \beta_i} = 0$$

This set of weight values is the identification result for the unknown function.

In this research the inputs sample data were $Z'(\tau)$, $Z(\tau)$, $\theta'(\tau)$ and $\theta(\tau)$, where $Z(\tau)$,$\theta(\tau)$ were from Random Decrement signature of ship's CG (center of gravity), and $Z'(\tau)$,$\theta'(\tau)$ were obtained by numerical differentiation of $Z(\tau)$ and $\theta(\tau)$ with respect to time t. The required function outputs G_1 and G_2 , however, were not available directly because the accuracy of numerical second-order differentiation $Z''(\tau)$,$\theta''(\tau)$ was not acceptable. Thus the conventional error definition $(G_0 - G_1)^2$ and $(G_0 - G_2)^2$ in (18) was not applicable. The modified error was computed as below,

$$E_1 = \sum_{\tau=1}^{200} \left[Z(\tau) - Z_0(\tau) \right]^2 \qquad (19)$$
$$E_2 = \sum_{\tau=1}^{200} \left[\theta(\tau) - \theta_0(\tau) \right]^2$$

where $Z_0(\tau)$ and $\theta_0(\tau)$ were numerical solutions to the following equations,

$$Z_0'' + \omega_3^2 Z_0 + G_0(Z', Z, \theta', \theta) = 0 \qquad (20)$$
$$\theta_0'' + \omega_5^2 \theta_0 + G_0(Z', Z, \theta', \theta) = 0$$

The final weight values should minimize the error E_1 and E_2. The iteration algorithm for searching the optimum weight values is given by

$$W_{ij}(n+1) = W_{ij}(n) - \gamma \frac{\partial E}{\partial W_{ij}(n)} \qquad (21)$$
$$\beta_i(n+1) = \beta_i(n) - \gamma \frac{\partial E}{\partial \beta_i(n)}$$

where γ is a rate value to control searching rate and stability. The initial values of weight W_{ij} and β_i were chosen arbitrarily. The partial values $\frac{\partial E}{\partial W_{ij}(n)}, \frac{\partial E}{\partial \beta_i(n)}$ could not be computed using the analytical algorithm described in Hush and Horne(1993). Instead, the following numerical algorithm was employed,

$$\frac{\partial E}{\partial W_{ij}(n)} = \frac{E\left[W_{ij}(n) + \Delta W\right] - E\left[W_{ij}(n) - \Delta W\right]}{2\Delta W} \qquad (22)$$
$$\frac{\partial E}{\partial \beta_i(n)} = \frac{E\left[\beta_i(n) + \Delta\beta\right] - E\left[\beta_i(n) - \Delta\beta\right]}{2\Delta\beta}$$

The searching process was terminated when the following conditions were satisfied.

$$\frac{\partial E}{\partial W_{ij}} \cong 0 \qquad (23)$$
$$\frac{\partial E}{\partial \beta_i} \cong 0$$
$$E \cong 0$$

The weight values W_{ij} and β_i constitute the identification result for the Random Decrement equations.

2.5 Verification and Analysis of Identified Equations

The validation of the identification results is dependent on the nature of the Random Decrement signatures and the quality of the Neural Networks training. The agreement between the Random Decrement signatures and the free response signatures is the prerequisite to the validation. For training process, too many sample data with a relatively small network will reduce the accuracy of function approximation. Too big network structure with a large number of neurons and weights will not achieve the required generalization. In that case the identified function is possibly not the true function even though the training result is perfect.

In this research the generalization of the identified equations was verified by comparing the actual heave and pitch Random Decrement signatures with the predictions from the identified equations. Given some specified initial values, the solutions to the identified

Random Decrement equations were obtained as predicted Random Decrement signatures. The solution algorithm was based on the fourth-order Runge-Kutta method.

Since Random Decrement technique is an empirical technique without analytical conclusions for its application, it is necessary to verify the agreement between the identified Random Decrement equations and free response equations for every application case. Only the Random Decrement equations that represent the free response equations could be used for further seakeeping study. In this research the agreement was verified by the comparison between the free response signatures and the predictions from the identified Random Decrement equations. For model experiments, the free responses were recorded directly from the measurements. For motion simulations, the free responses were derived from the mathematical model using the fourth-order Runge-Kutta method.

3. Results and Discussion

In this research the identification method was applied to ship model motion data obtained from the wave tank experiments. Also the JONSWAP wave and white noise excitation cases were tested separately by simulation method. All results are presented and discussed in the following sections.

3.1 Ship Model Experiment Results

During wave tank experiments, 'R-Class Icebreaker' ship model was tested in two groups of JONSWAP waves for random motion data and excited in calm water for free response signatures. The motion data files were tabulated in the following Table iii with the corresponding experimental conditions.

Table iii : Model Experiments Motion Data Files

Motion Data	Wave Series	Wave Direction	JONSWAP Parameters
RHP21	J7H5	Heading	$H_s = 5.0$cm, $f_m = 0.7$ Hz
RHP22	J7H5a	Heading	$H_s = 5.0$cm, $f_m = 0.7$ Hz
RHP23	J7H5b	Heading	$H_s = 5.0$cm, $f_m = 0.7$ Hz
RHP41	J7H75	Heading	$H_s = 7.5$cm, $f_m = 0.7$ Hz
RHP42	J7H75a	Heading	$H_s = 7.5$cm, $f_m = 0.7$ Hz
RHP43	J7H75b	Heading	$H_s = 7.5$cm, $f_m = 0.7$ Hz
RPH11	Calm Water for Free Response		
RPH12	Calm Water for Free Response		
RPH13	Calm Water for Free Response		

The recorded motion data are motion displacements of the cross point of model midship and center line. They had to be converted to the heave displacement of the CG (center of

gravity) and pitch angular displacement. In this research both heave and pitch time series are assumed to be zero-mean, stationary random processes. The experiment results presented in Table iv supported such assumption. Since the axis system for experimental measurement was not set on the equilibrium CG point, the motion measurements were not real displacement values. From definition the real displacements of the stationary state should be zero. In Table iv the mean values of every random process agreed well with the measurements of the stationary state, thus the real mean values are all zero. The real motion series were obtained by subtracting the mean values from the experimental measurements.

Table iv: Mean Value Analyses

Random Process	**Heave Mean Value (Stationary Measurement) (cm)**	**Pitch Mean Value (Stationary Measurement) (deg)**
RHP21	18.60 (18.62)	0.43 (0.41)
RHP22	20.01 (20.03)	0.43 (0.42)
RHP23	19.99 (20.03)	0.43 (0.42)
RHP41	19.97 (20.00)	0.44 (0.42)
RHP42	19.95 (19.99)	0.45 (0.44)
RHP43	19.94 (19.97)	0.45 (0.43)

3.1.1 Random Decrement Signature

The zero-mean motion series of the ship's CG were processed to obtain the heave and pitch Random Decrement signatures. For different trigger value, there was different Random Decrement signature. The Random Decrement signatures from group one motion data (RHP21, RHP22, RHP23) and group two motion data (RHP41, RHP42, RHP43) are presented separately in Figure 6 to Figure 9 with the same heave trigger value 0.7cm. Two groups of Random Decrement signatures were also compared in Figure 10.

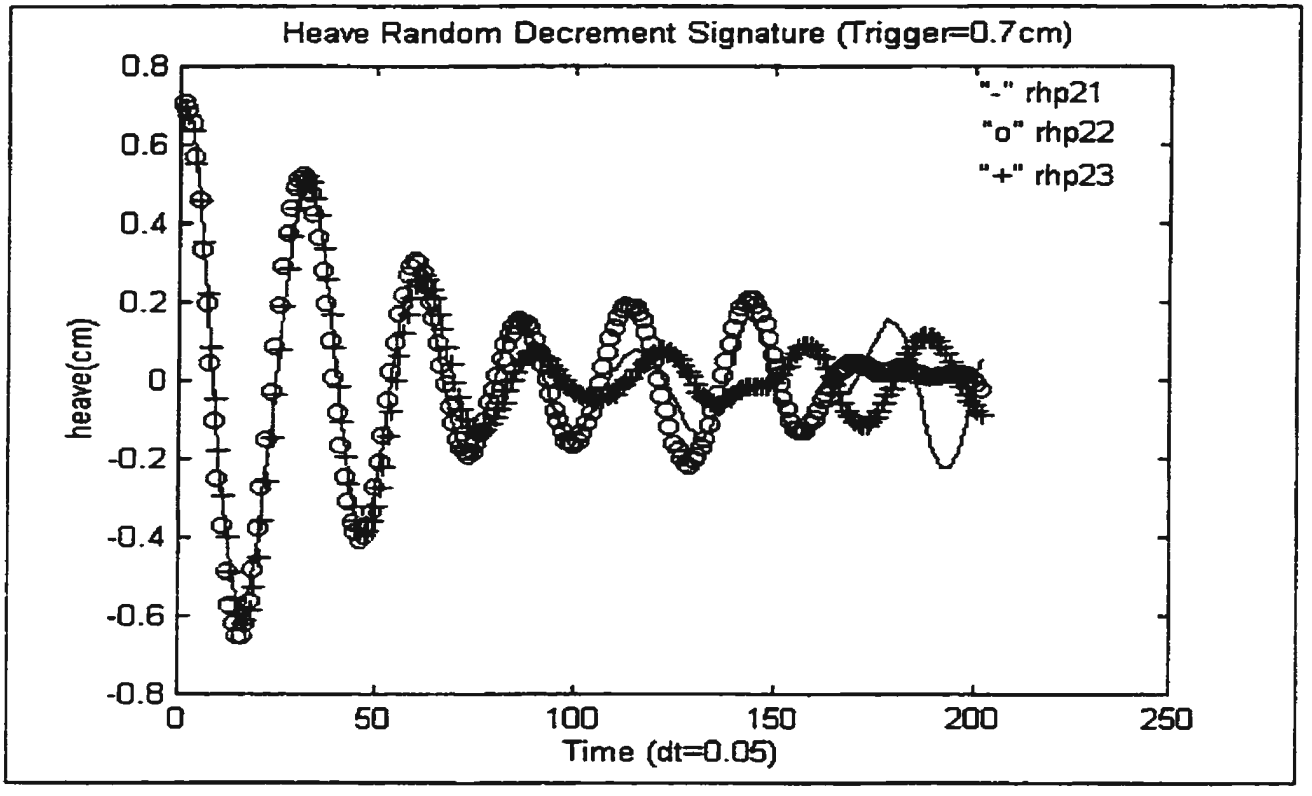

Figure 6: Heave Random Decrement Signature of Group One -- RHP21, RHP22 and RHP23

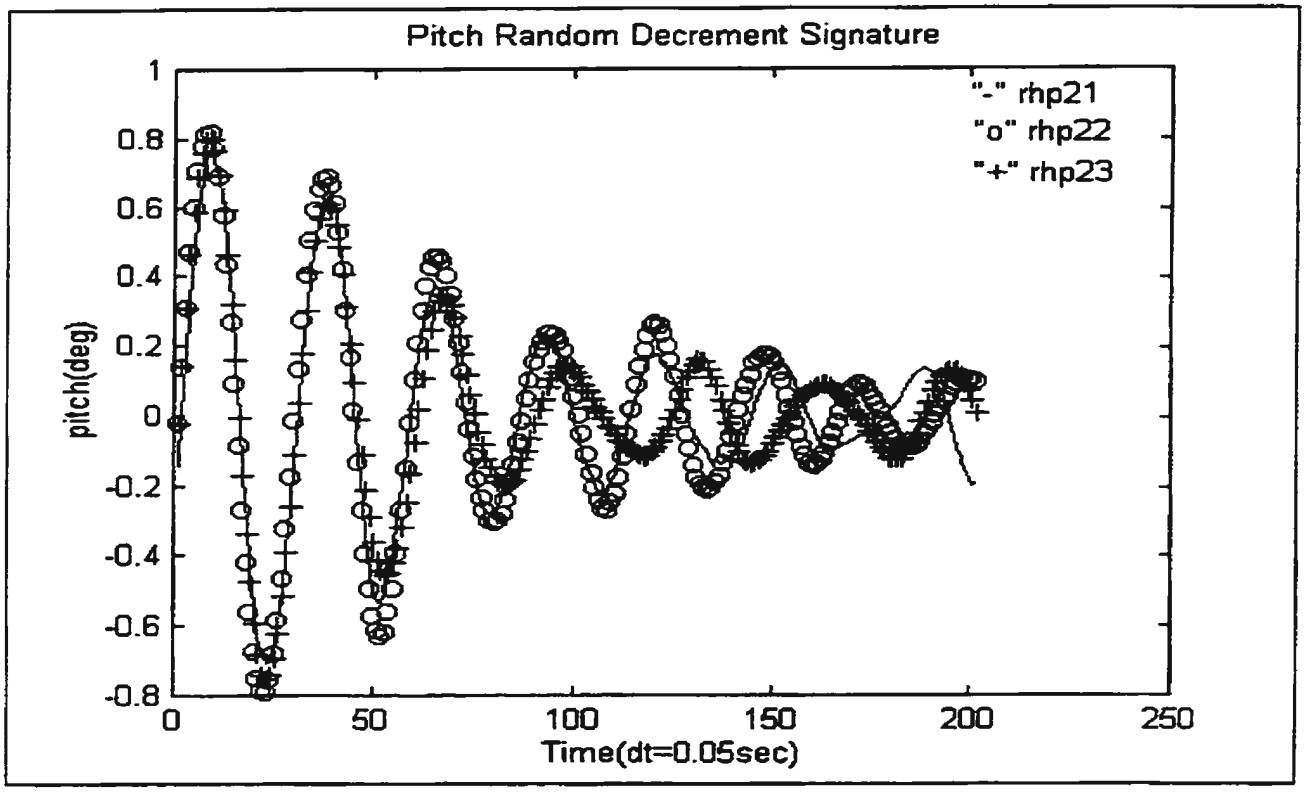

Figure 7: Pitch Random Decrement Signature of Group One -- RHP21, RHP22 and RHP23

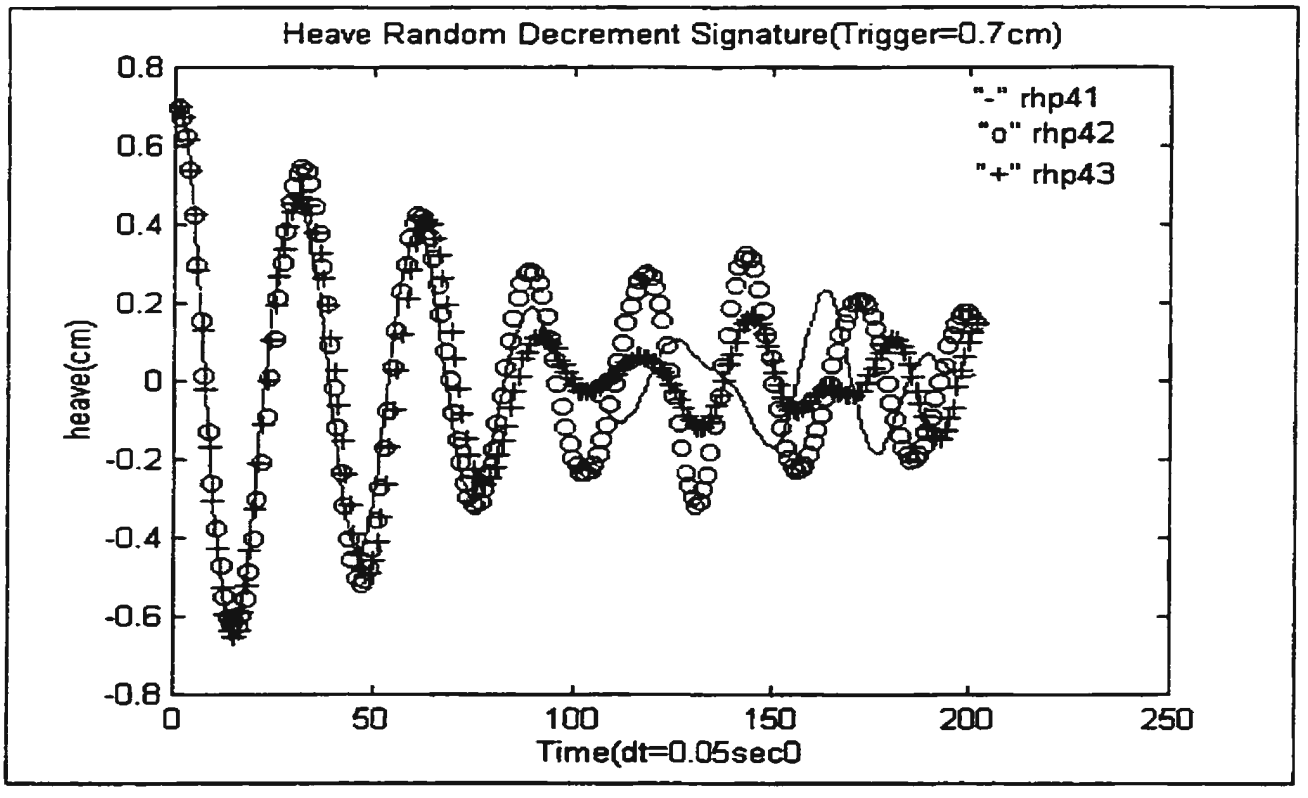

Figure 8: Heave Random Decrement Signature of Group Two -- RHP41, RHP42 and RHP43

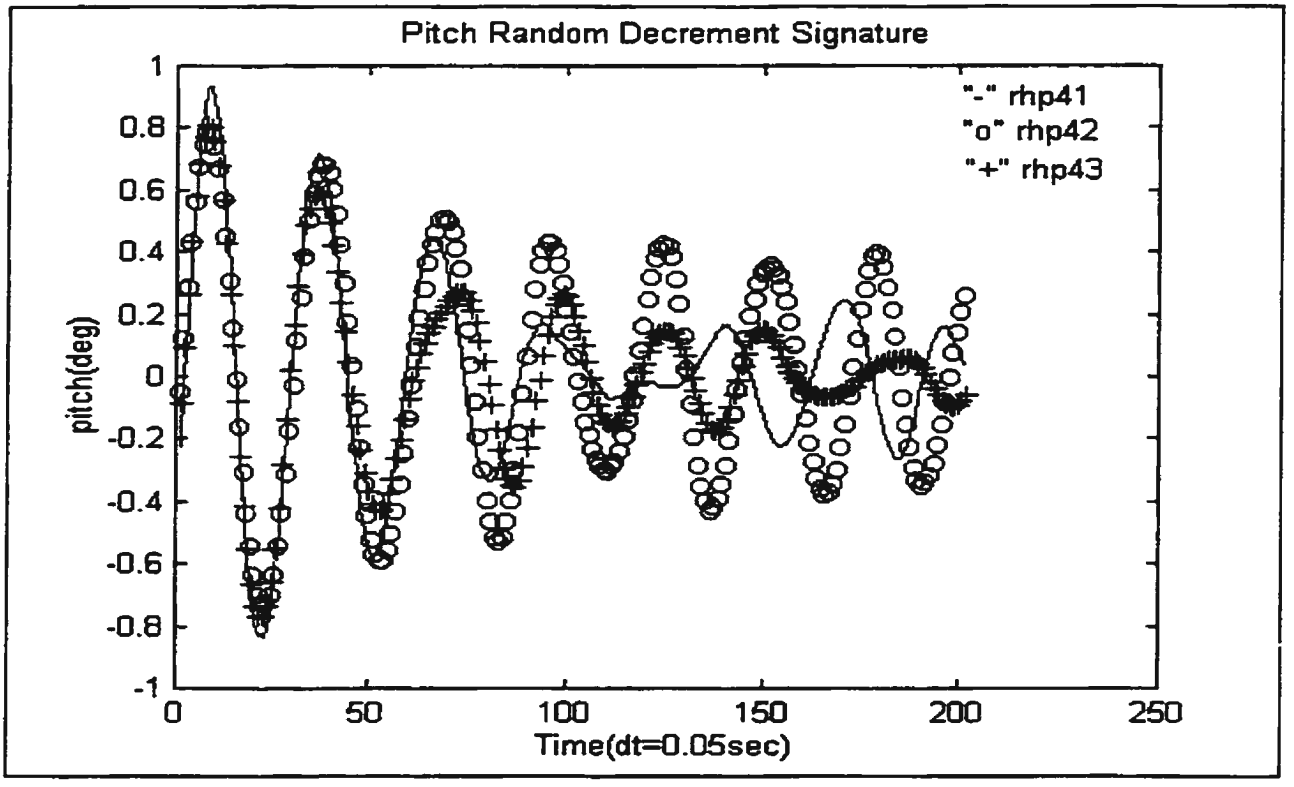

Figure 9: Pitch Random Decrement Signature of Group Two -- RHP41, RHP42 and RHP43

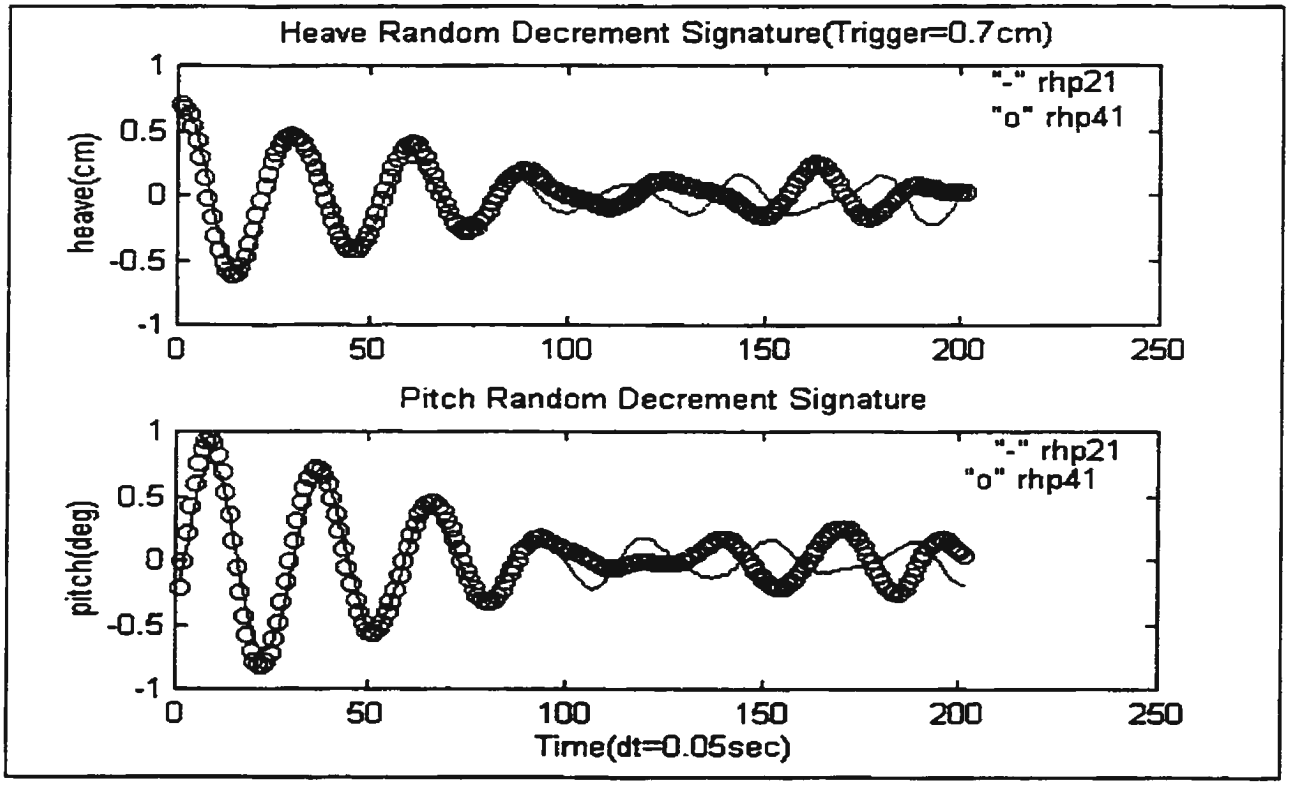

Figure 10: Random Decrement Signature of Group One & Group Two

The obtained two-degree Random Decrement signatures had the decay form similar to that of the free response signatures. There was a phase difference between the coupled heave and pitch signals. Under same wave spectrum, the Random Decrement signatures from the different time series (RHP21, RHP22, RHP23 or RHP41, RHP42, RHP43) agreed well except the latter part. Even different spectrum significant height did not influence this agreement (RHP21 & RHP41). The observation of the obtained results suggested that the heave and pitch Random Decrement signatures are independent of the particular wave time series under the same wave spectrum.

The latter part of the Random Decrement signatures was apparently interfered by some noise. One cause of the noise is the experiment facility. The used wave tank is too narrow to prevent from tank wall interference and wave reflection. The seakeeping basin is expected to generate better motion data. The other cause is the limited length of the motion time series. Since the Random Decrement signature was obtained by averaging the selected data segments, too short motion time series could not provide enough segments with the specified initial value. In this experiment, there were 8001 data points in every motion history while the required segment length was 200 data points. Thus only about 30 segments could be selected for either positive velocity specification or negative velocity specification. The Random Decrement signature was finally formed by averaging about 60 segments. It is insufficient for practical application.

3.1.2 Neural Network Identification

The coupled heave and pitch Random Decrement signature obtained from the motion time series RHP21 was used for identification of the Random Decrement equations. The damped frequencies ω_3 and ω_5 were estimated from the first 100 data points that were free of apparent noise interference. The Neural Network shown in **Figure 5** was employed to identify the unknown functions G_1 and G_2 respectively. After training in iterative process, the Neural Network outputs were close enough to training signature as shown in Figure 11. The final weight values were tabulated in Table v.

Table v: Identification Results for Random Decrement Equations

Weight Values for Identified Function $G_1(Z', Z, \theta', \theta)$						
β_1 , i=0,1,2,3,4,5	-9.270	7.066	2.468	1.928	2.644	2.826
W_{1i} , i=0,1,2,3,4	-2.904	3.569	-2.808	-1.110	4.294	
W_{2i} , i=0,1,2,3,4	8.798	2.975	-4.297	-3.093	1.684	
W_{3i} , i=0,1,2,3,4	2.640	-0.992	-4.205	0.611	1.268	
W_{4i} , i=0,1,2,3,4	1.356	-2.616	-6.127	1.393	-0.494	
W_{5i} , i=0,1,2,3,4	6.225	2.172	-1.187	7.123	3.070	
Weight Values for Identified Function $G_2(Z', Z, \theta', \theta)$						
β_1 , i=0,1,2,3,4,5	-1.624	-9.906	-2.654	8.020	5.926	1.169
W_{1i} , i=0,1,2,3,4	4.789	10.884	1.962	3.321	-1.061	
W_{2i} , i=0,1,2,3,4	0.706	5.386	3.508	2.989	5.304	
W_{3i} , i=0,1,2,3,4	2.979	7.671	-6.729	2.245	10.837	
W_{4i} , i=0,1,2,3,4	1.627	10.525	1.572	5.983	1.348	
W_{5i} , i=0,1,2,3,4	0.865	6.329	2.392	4.325	2.868	
Damped Frequencies for Heave and Pitch Random Decrement Signature						
Heave frequency ω_3	4.48799 (rad / sec)					
Pitch Frequency ω_5	4.59745 (rad / sec)					

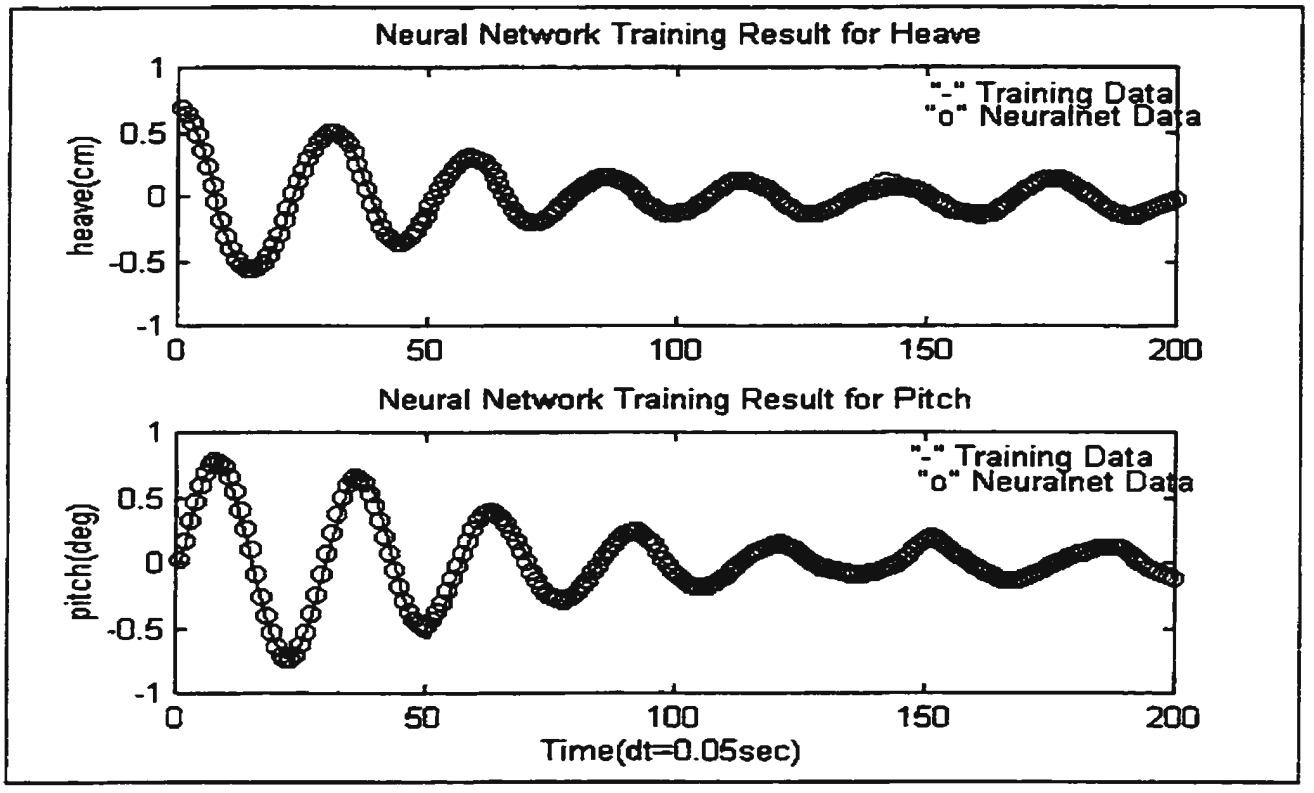

Figure 11: Neural Network Training Results

Finally the identified heave and pitch Random Decrement equations for 'R-Class Icebreaker' model were expressed as the following simultaneous equation system,

$$\begin{aligned} Z'' + 4.48799^2 Z + G_1(Z', Z, \theta', \theta) = 0 \\ \theta'' + 4.59745^2 \theta + G_2(Z', Z, \theta', \theta) = 0 \end{aligned} \qquad (24)$$

where the functions G_1 and G_2 were uniquely determined by the weight values listed in Table v.

3.1.3 Verification of Identification Results

The solutions to the identified Random Decrement equations could be obtained using the fourth-order Runge-Kutta method if the initial conditions were specified. They were obtained as the predicted Random Decrement signature. With the same initial conditions,

the actual Random Decrement signatures could be formed from the recorded heave and pitch motion time series. The predicted and the actual Random Decrement signatures should be compatible with each other to ensure the generalization of the identification result. In this research various trigger values were specified, and the actual Random Decrement signatures were obtained from motion record RHP21. The predicted signatures were compared with the actual Random Decrement signature in the Figure 12 to Figure 17.

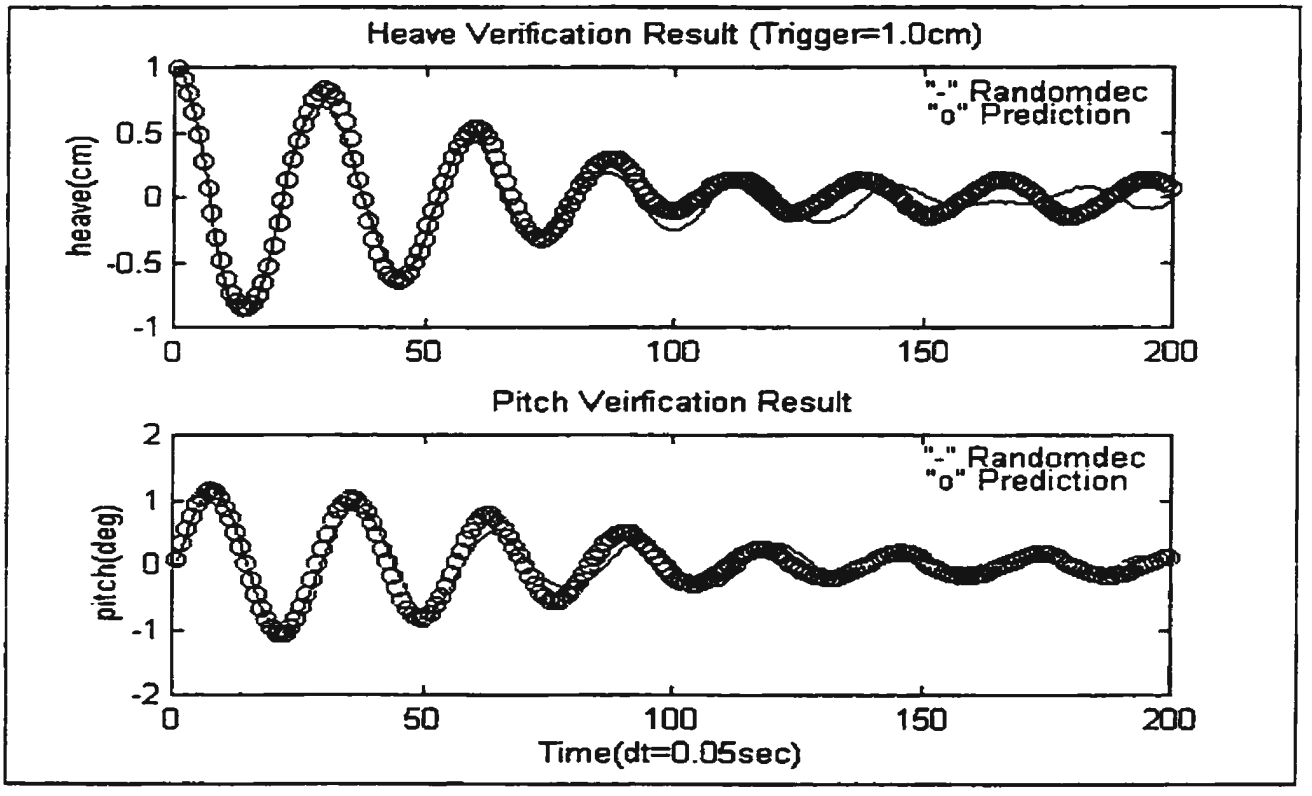

Figure 12: Verification Results for Heave Trigger 1.0cm

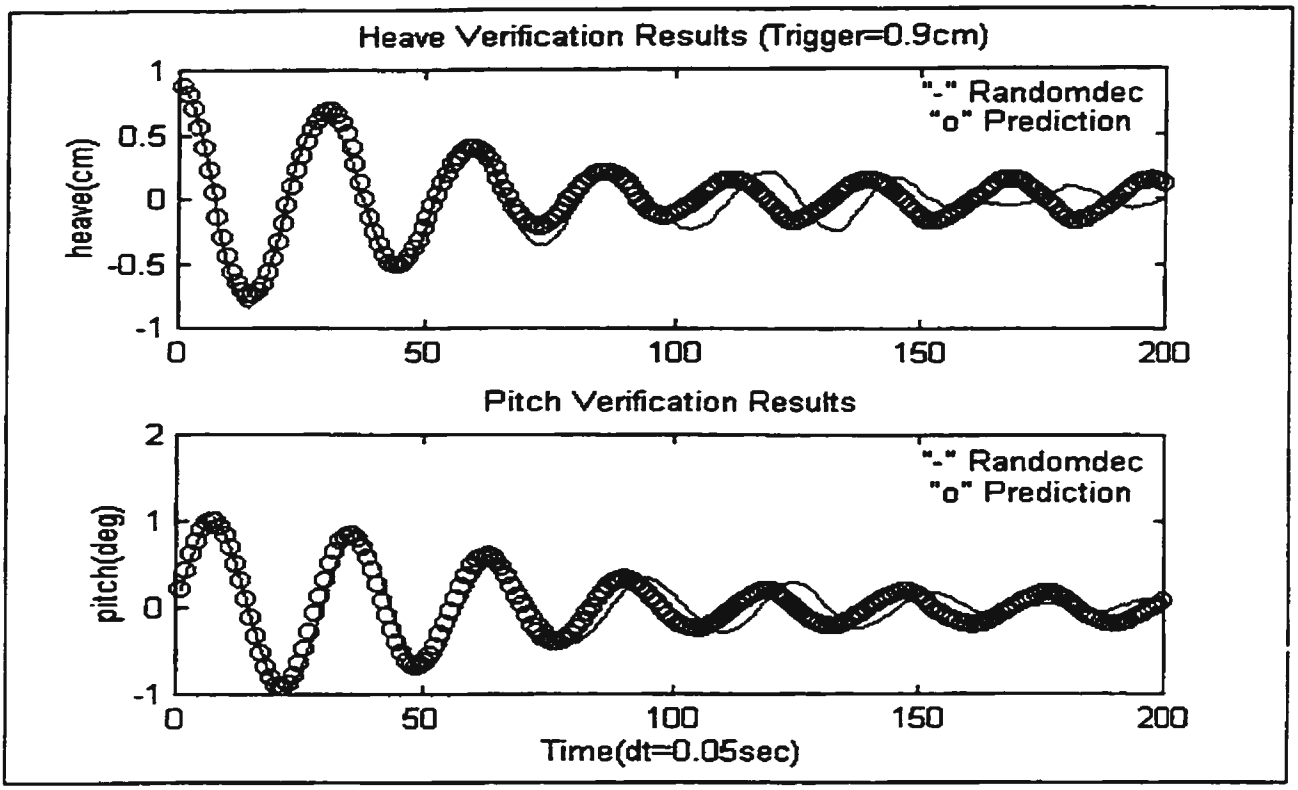

Figure 13: Verification Results for Heave Trigger 0.9cm

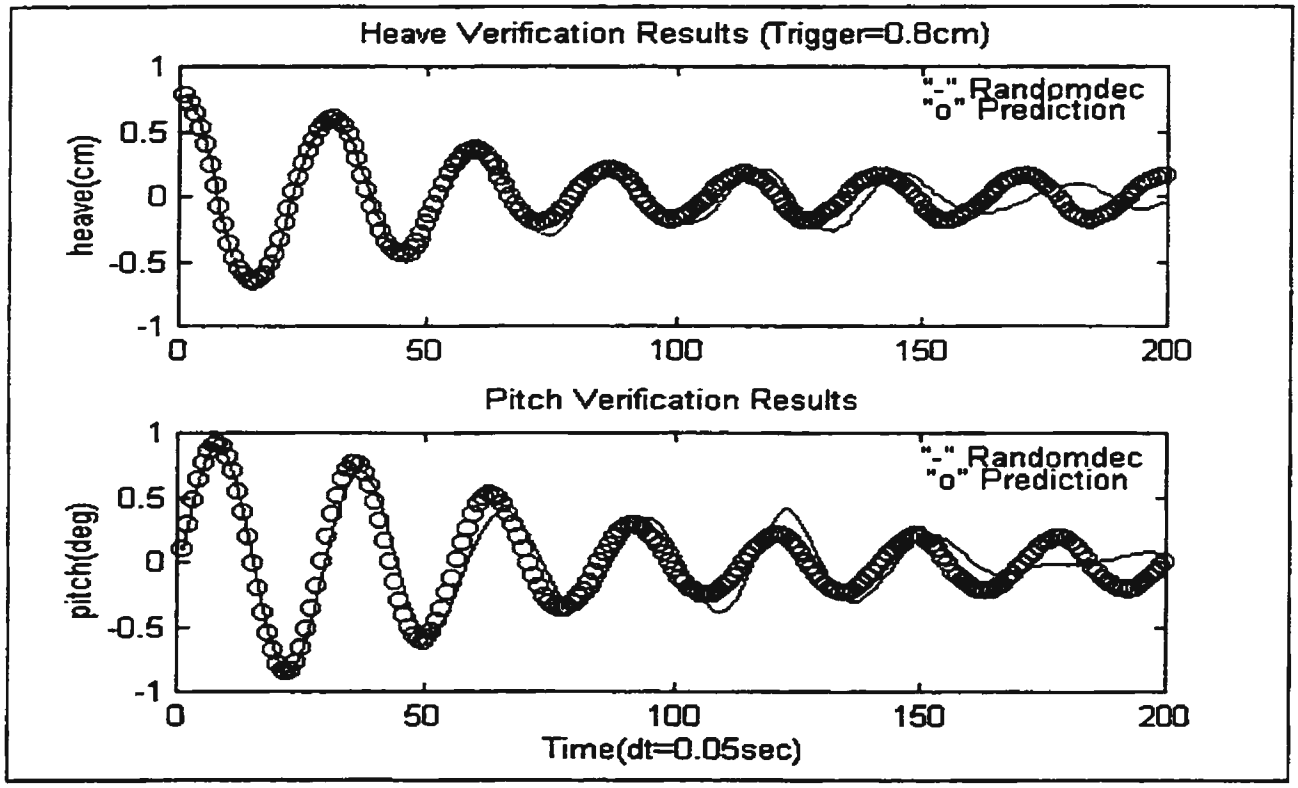

Figure 14: Verification Result for Heave Trigger 0.8cm

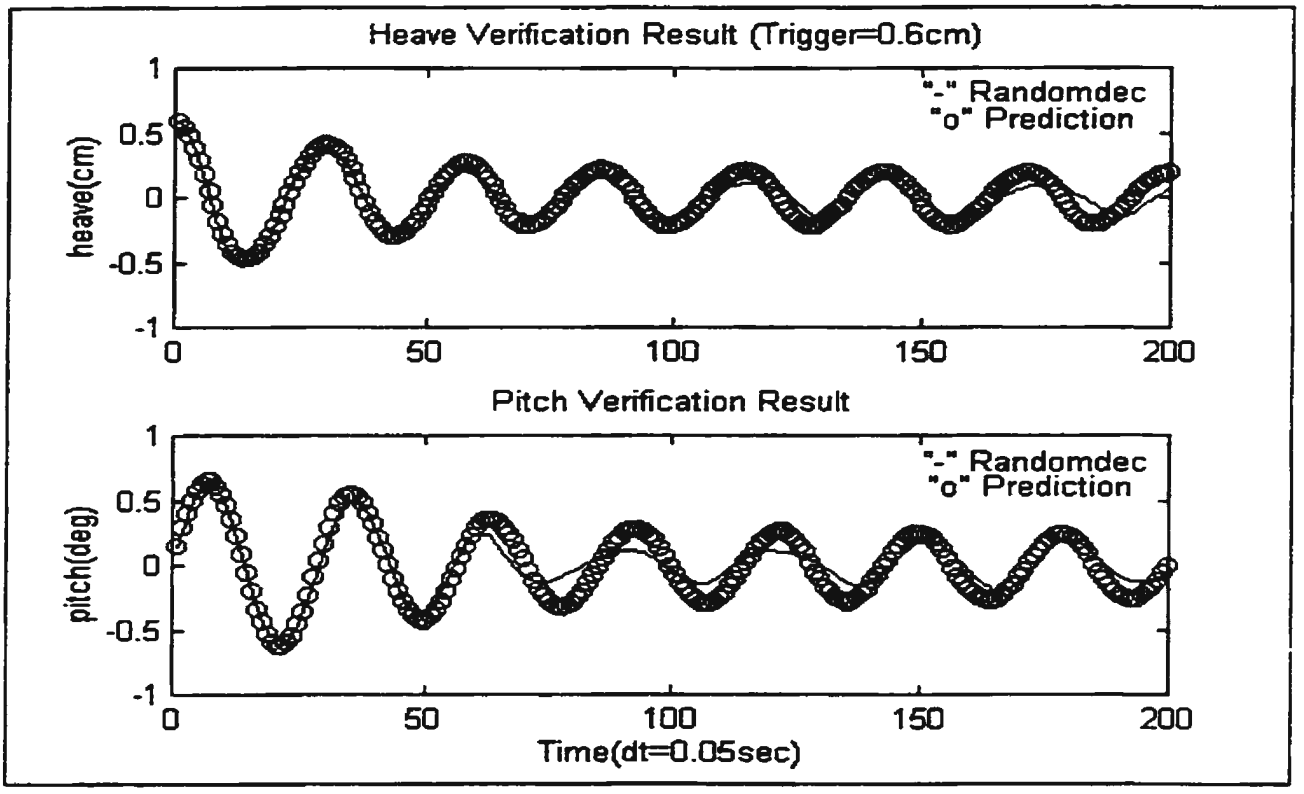

Figure 15: Verification Results for Heave Trigger 0.6cm

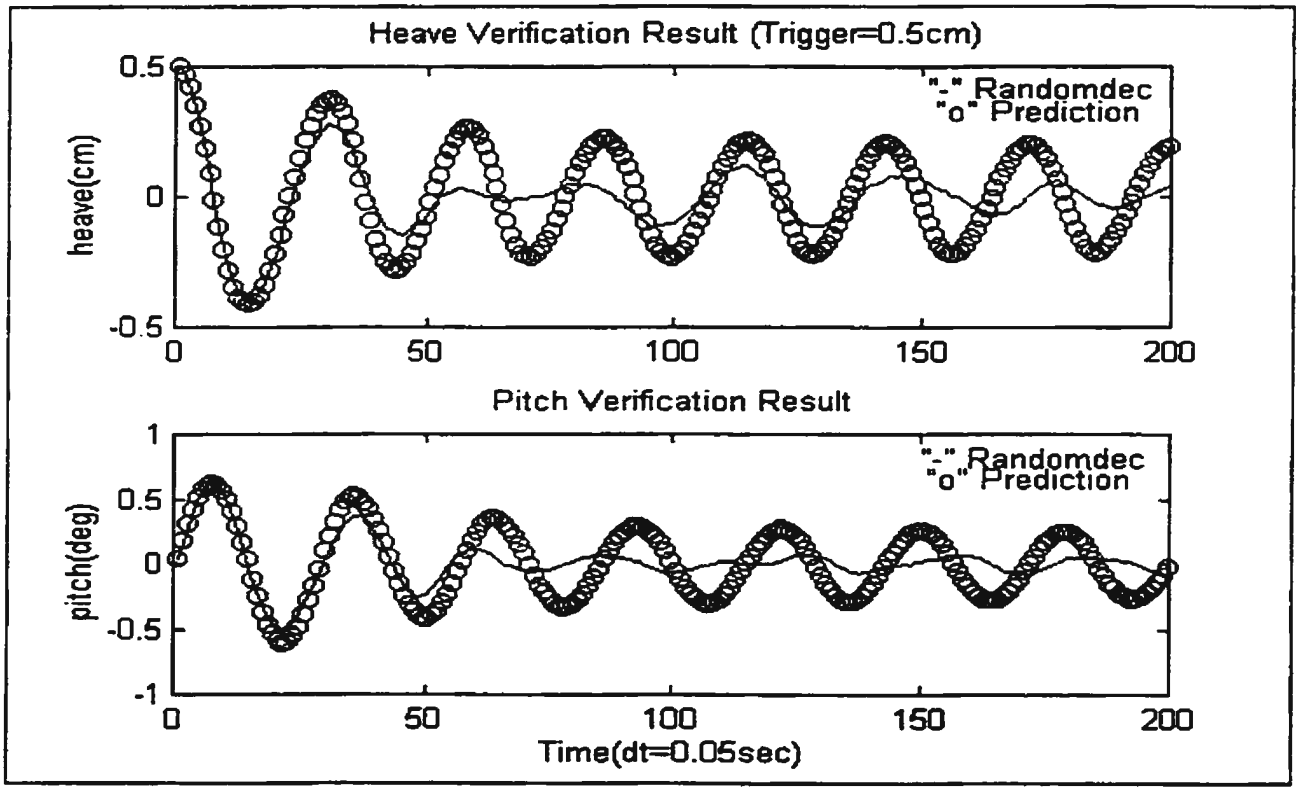

Figure 16: Verification Results for Heave Trigger 0.5cm

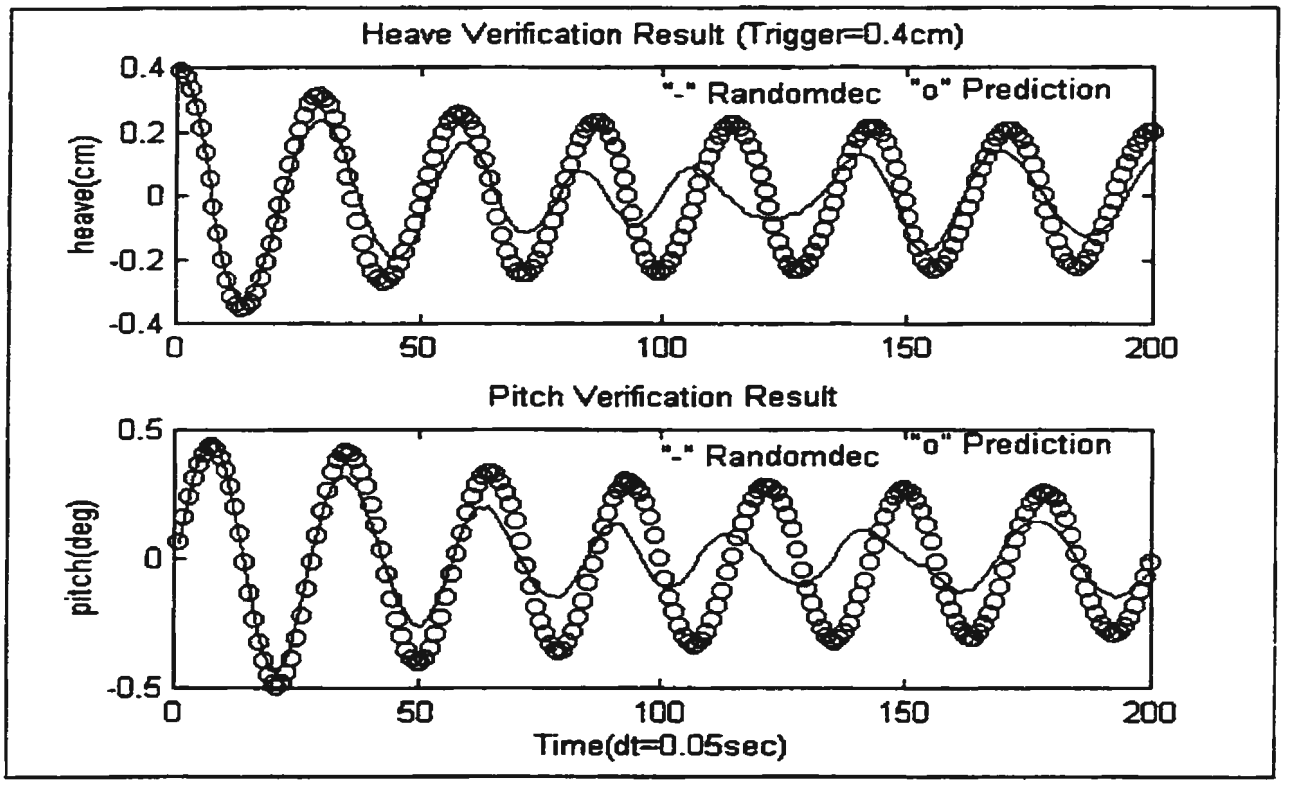

Figure 17: Verification Results for Heave Trigger 0.4cm

For heave trigger value 1.0cm, 0.9cm, 0.8cm, 0.6cm, the predicted and actual Random Decrement signature agreed well particularly for the first 100 data points. For heave trigger value 0.5cm and 0.4cm, the expected agreement was not achieved after the first 50 data points. It was due to the noise interference that had much more influence for smaller value Random Decrement signatures. Also the predicted signatures contained some noise transferred from the training data. Even with some noise interference, the above verifications proved the generalization of the identified Random Decrement equations.

Only the Random Decrement equations that represent the system free response equations could be used for further seakeeping research. In that case the free response signature should be one of the solutions to the identified Random Decrement equations. During 'R-

Class Icebreaker' model experiments, the free response signatures were obtained by exciting the ship model in calm water. The coupled heave and pitch free response signatures are shown in Figure 18 to Figure 20. The initial irregular parts represented the manual excitation process, while the other excitations in the latter part were caused by the noise due to tank wall interference and wave reflection. The best part of free response RPH11, which ranges from point 50 to point 250 in Figure 18, was selected to compare with the prediction of the identified Random Decrement equations. The comparison result is shown in Figure 21.

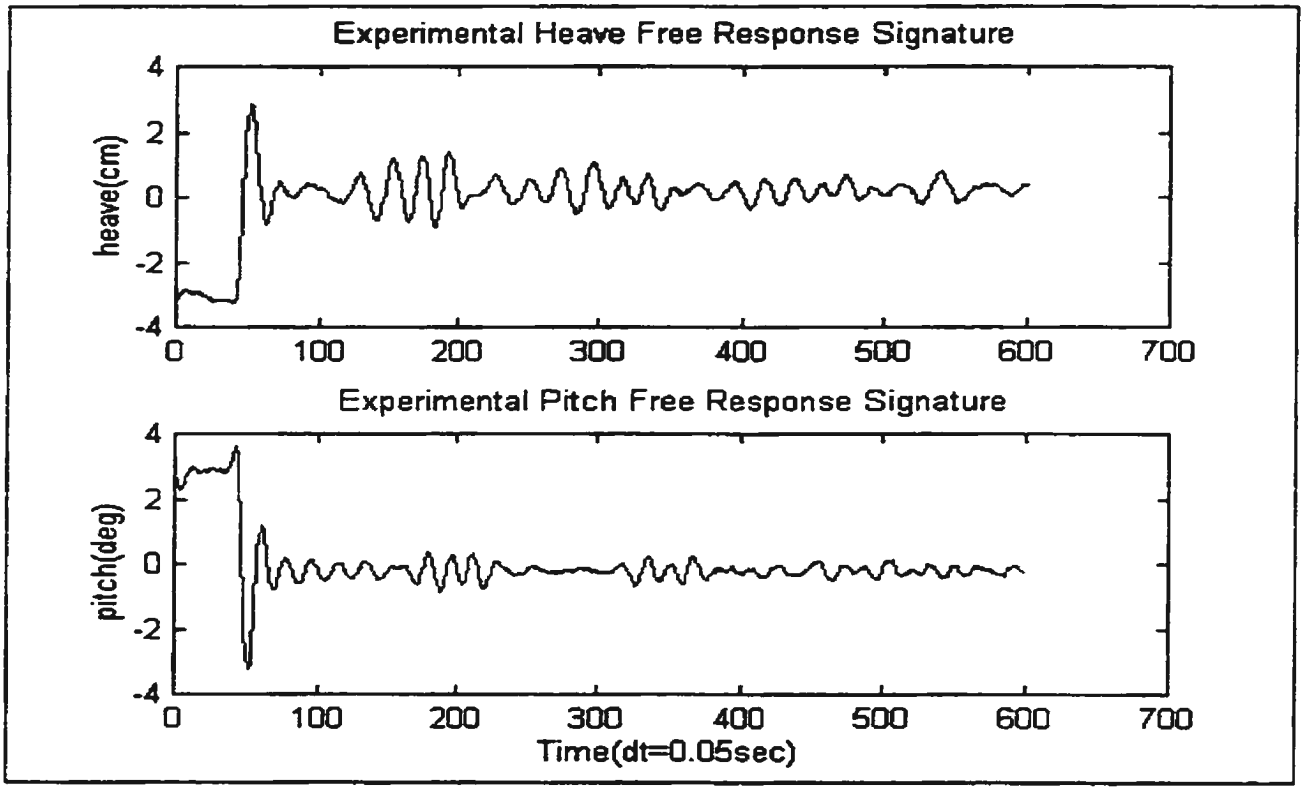

Figure 18: Experimental Heave & Pitch Free Response Signature RPH11

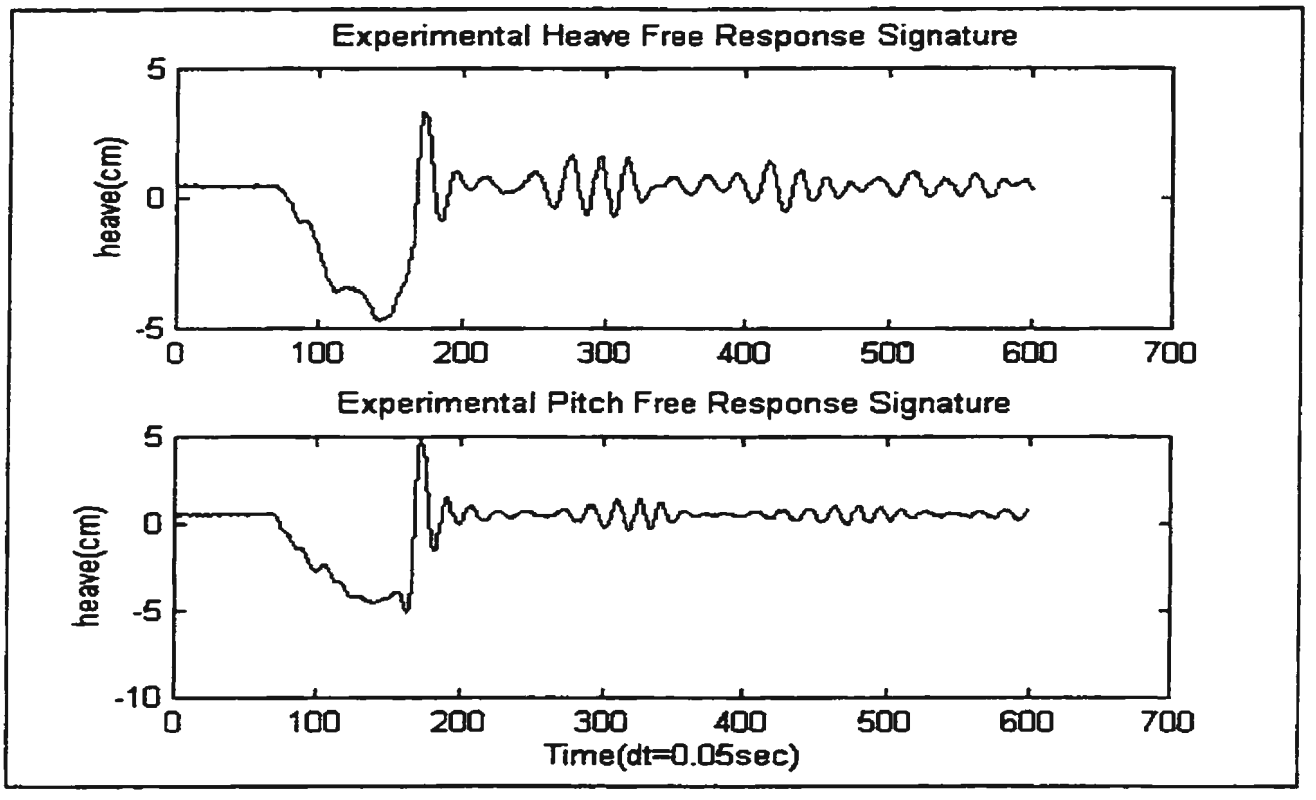

Figure 19: Experimental Heave & Pitch Free Response Signature RPH12

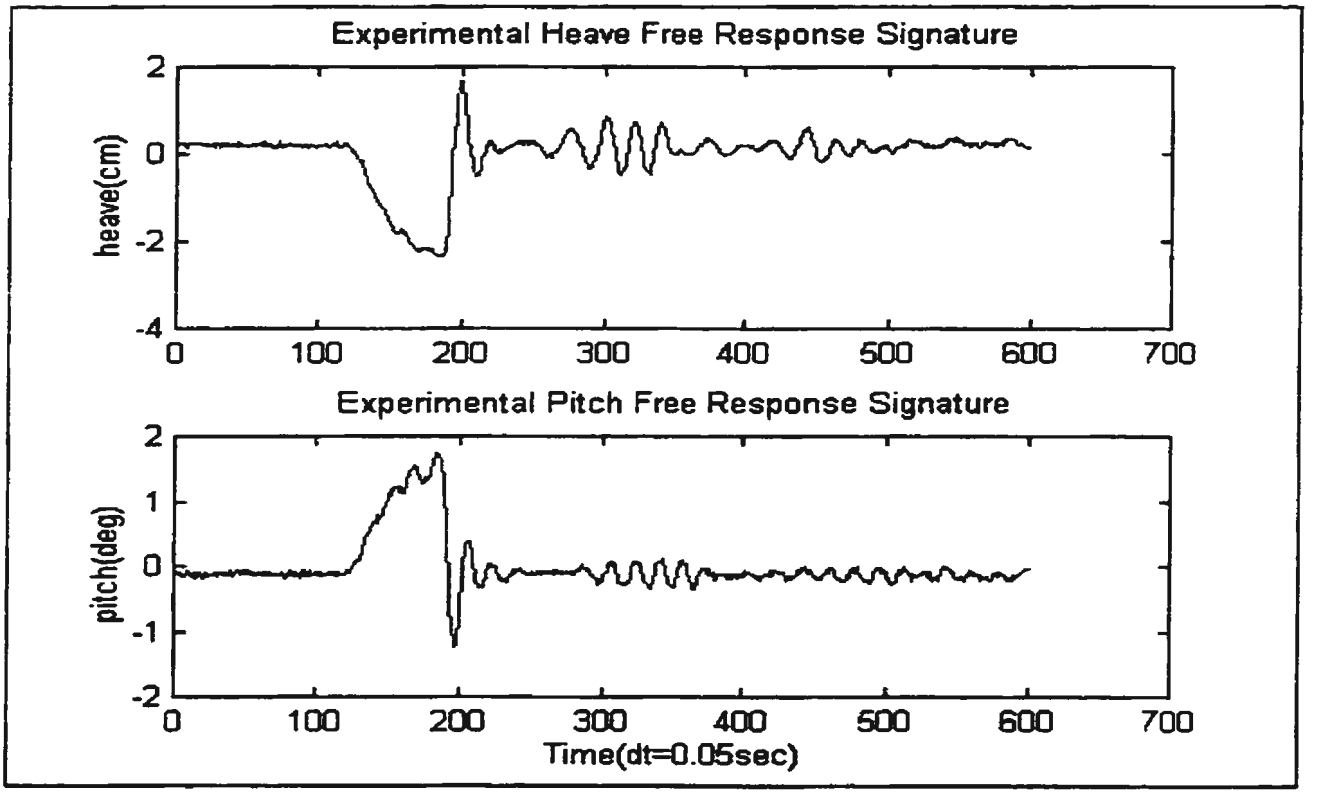

Figure 20: Experimental Heave & Pitch Free Response Signature RPH13

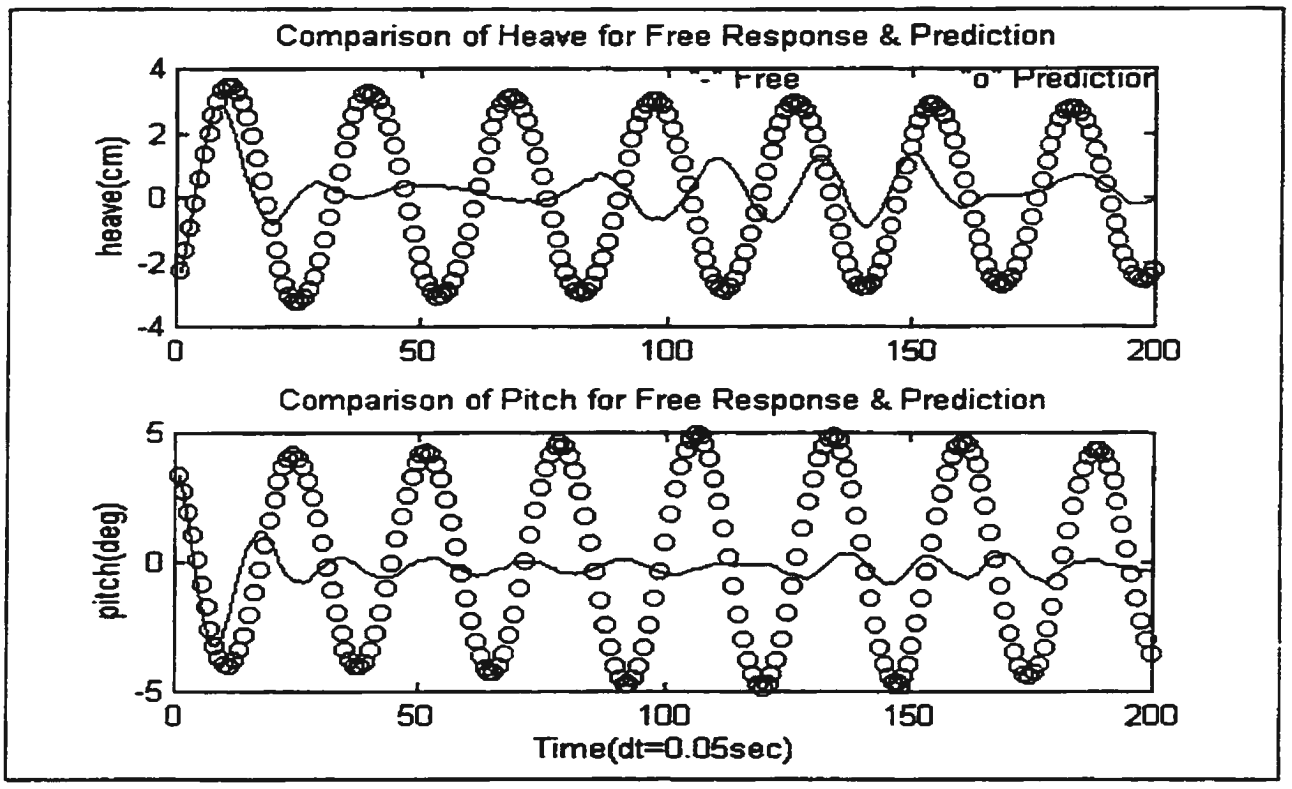

Figure 21: Comparison Between Experimental Free Response and Random Decrement Prediction

From Figure 21 it is obvious that the experimental heave and pitch free response signature was not the solution to the identified Random Decrement equations. The free response signature showed heavy damping nature while the identified Random Decrement equations represented a light damping motion system. This disagreement could not be explored from the 'R-Class Icebreaker' experimental data, nor explained by the theory of empirical Random Decrement technique. The only possible way to analyze this disagreement is motion simulations.

3.2 Ship Model Simulation Results (JONSWAP Wave)

In ship model experiments, only one model form 'R-Class Icebreaker' was tested for the application of the developed identification method. The general conclusions to the validation of this identification method could not be based solely on the experiment results of one model. The convenient way to test different ship models under various environmental conditions is numerical simulation with the variable parameters in the mathematical model. In this research, the mathematical model for heave and pitch motions of 'R-Class Icebreaker' was derived from the strip theory as shown in Appendix A. The excitation forces under the JONSWAP wave were generated from the combination of the wave synthesis and the excitation transform functions presented in Appendix B. The interrelation between the system parameters and the identification results was explored by variation of the damping parameters in the mathematical model.

3.2.1 System Analysis for Various Damping Parameters

The mathematical model for "R-Class Icebreaker' motion simulations was derived in Appendix A as the following equation,

$$\begin{aligned} Z'' + 2.824Z' + 34.092Z + 0.158\theta' + 0.238\theta &= 0.4126F(t) - 0.0273M(t) \\ \theta'' + 0.580Z' + 0.629Z + 2.632\theta' + 30.780\theta &= -0.0273F(t) + 1.560M(t) \end{aligned} \qquad (25)$$

The random excitation forces F(t) and M(t) under JONSWAP wave were generated from the wave spectrum shown in **Figure 2** and the excitation transform functions presented in Appendix B. The numerical solutions to equation (25) was obtained as the simulated

motion time series, from which the specified segments were selected to form the heave and pitch Random Decrement signature. Corresponding to the initial conditions of the Random Decrement signature, the heave and pitch free response signature was obtained from the system free response equations as below,

$$\begin{aligned} Z'' + 2.824Z' + 34.092Z + 0.158\theta' + 0.238\theta = 0 \\ \theta'' + 0.580Z' + 0.629Z + 2.632\theta' + 30.780\theta = 0 \end{aligned} \qquad (26)$$

The agreement between the Random Decrement signature and the free response signature is the prerequisite to the validation of the identification results. Their comparison results are shown in Figure 22 and Figure 23.

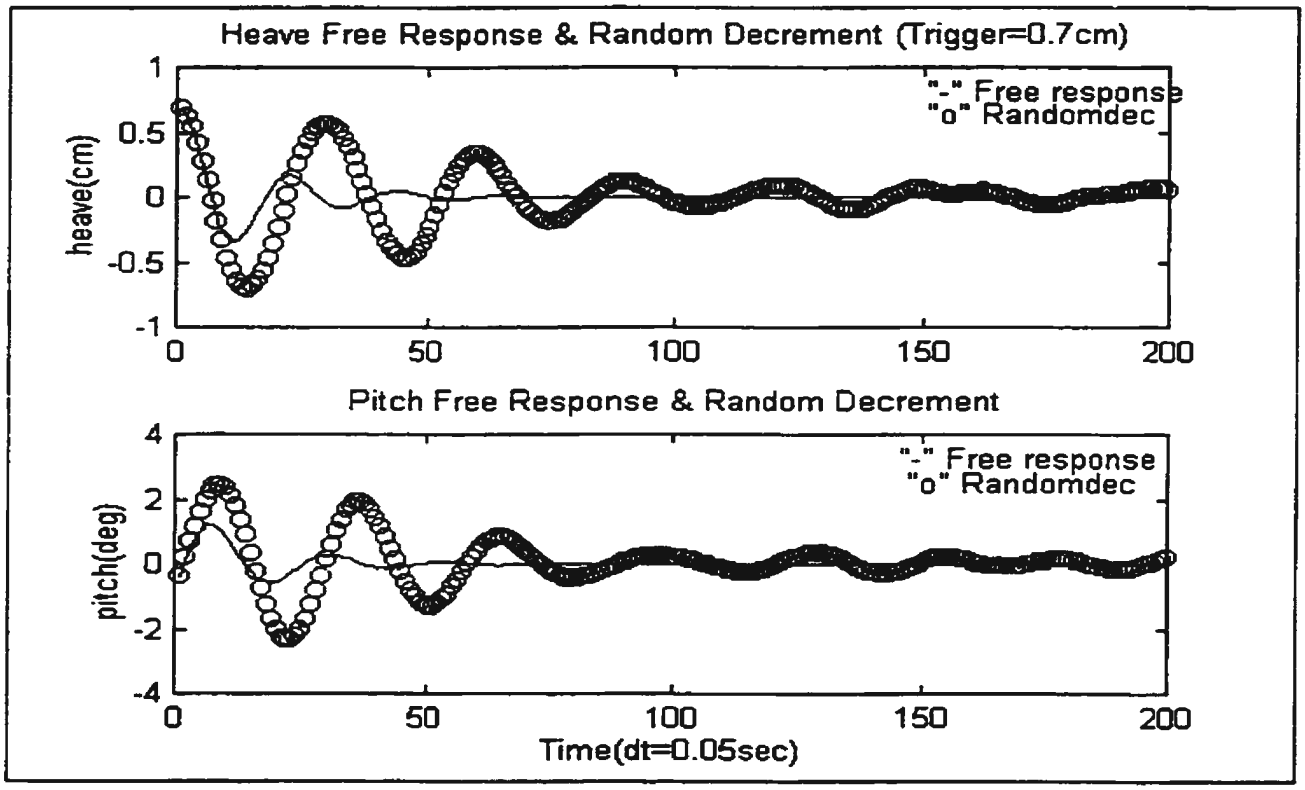

Figure 22: Comparison Between Free Response & Random Decrement Signature (Heave Trigger 0.7 cm)

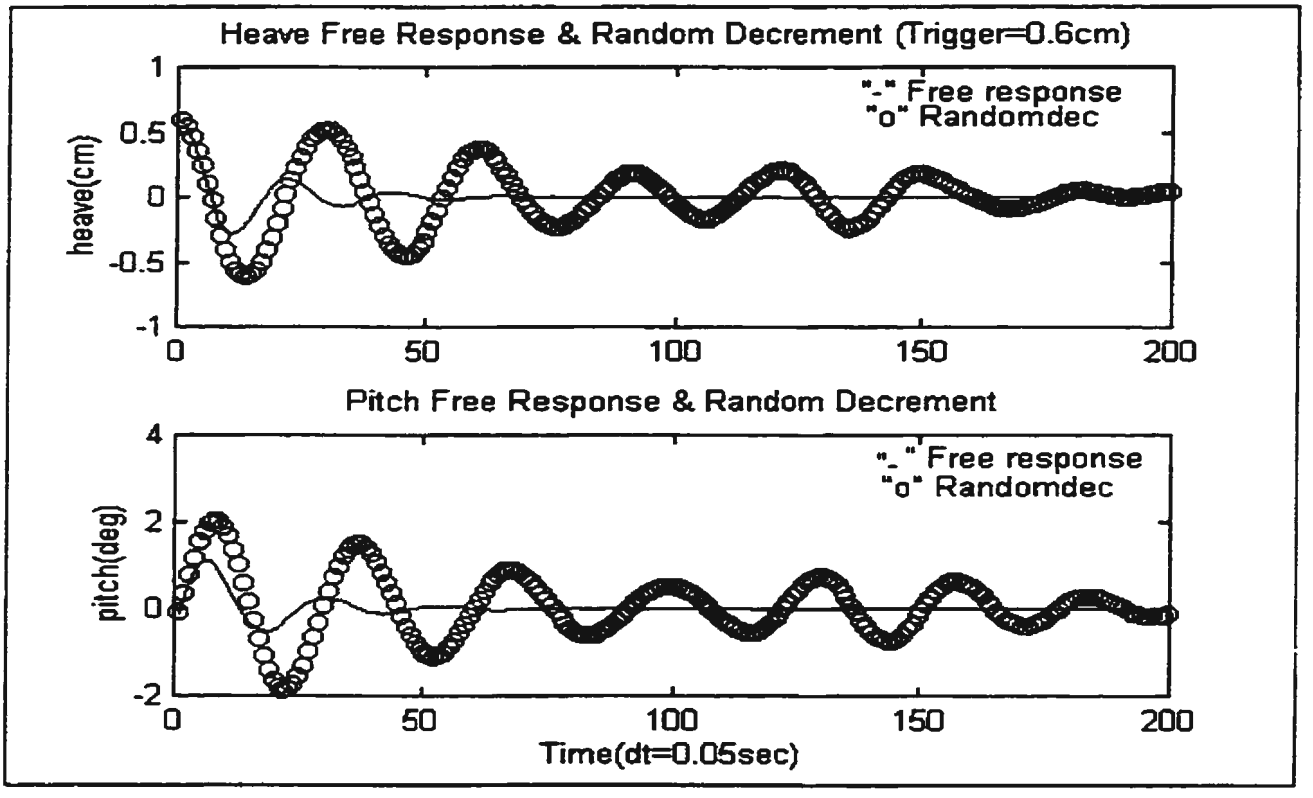

Figure 23: Comparison Between Free Response & Random Decrement Signature (Heave Trigger 0.6 cm)

From above comparison results, the heave and pitch Random Decrement signatures were not compatible with the free response signatures for the 'R-Class Icebreaker' model under JONSWAP waves. The free response signatures showed heavy damping nature while the Random Decrement signatures represented the light damping system. This simulation result is similar to the experimental result.

To simulate other motion systems with different damping parameters, the damping coefficient ζ was incorporated into the mathematical model (27), which was based on the 'R-Class Icebreaker' simulation model (25),

$$Z'' + 2\zeta\sqrt{34.092}Z' + 34.092Z + 0.158\theta' + 0.238\theta = 0.4126F(t) - 0.0273M(t) \quad (27)$$
$$\theta'' + 0.580Z' + 0.629Z + 2\zeta\sqrt{30.780}\theta' + 30.780\theta = -0.0273F(t) + 1.56M(t)$$

The ζ value for the 'R-Class Icebreaker' is greater than 0.2 according to equations (25). The comparison results between the free response signature and the Random Decrement signature for the motion model with ζ value of 0.2, 0.16, 0.12, 0.08, 0.04, 0.02 are shown in Figure 24 to Figure 29. The results showed that the lighter damping systems under JONSWAP waves could achieve the better agreement between free response signature and the Random Decrement signature. The motion system (ζ=0.02) was further used in the following sections to validate the developed identification method.

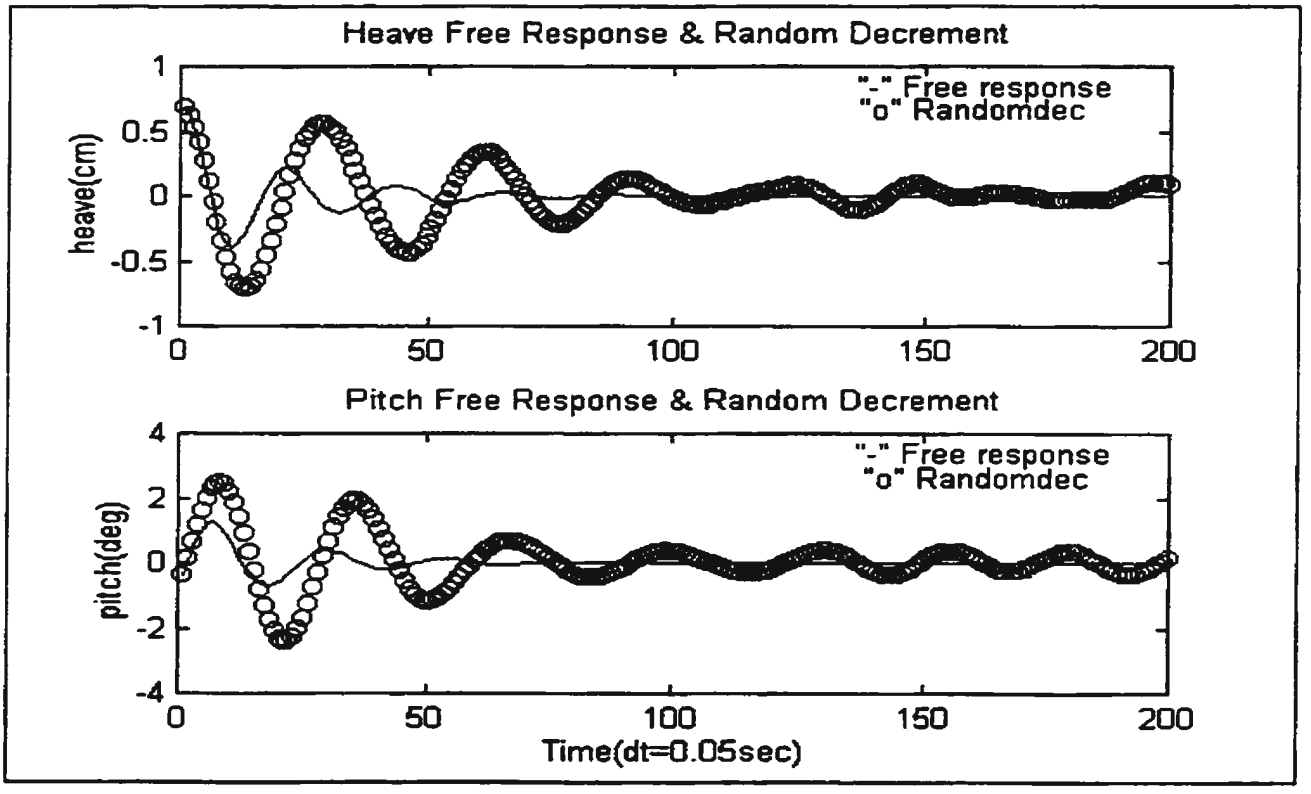

Figure 24: Comparison Between Free Response & Random Decrement Signature for ζ=0.20

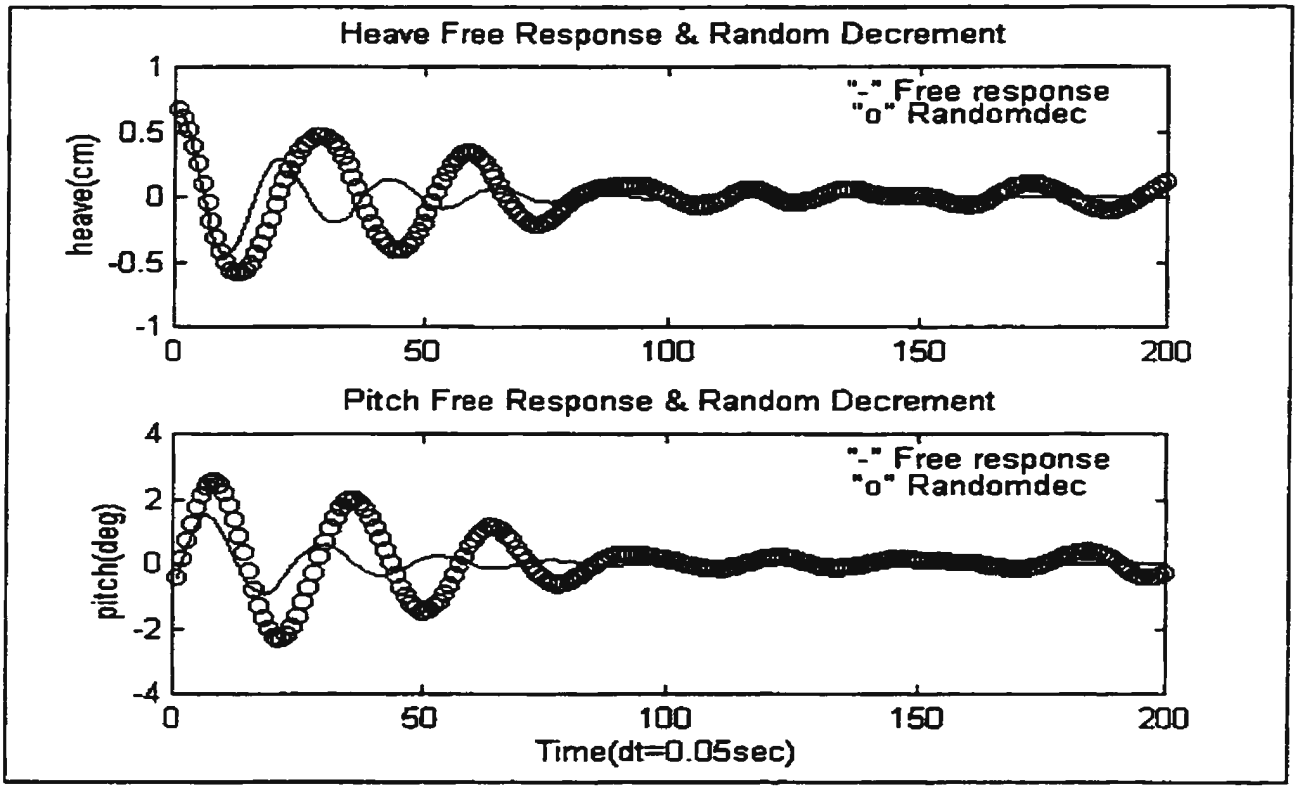

Figure 25: Comparison Between Free Response & Random Decrement signature for ζ=0.16

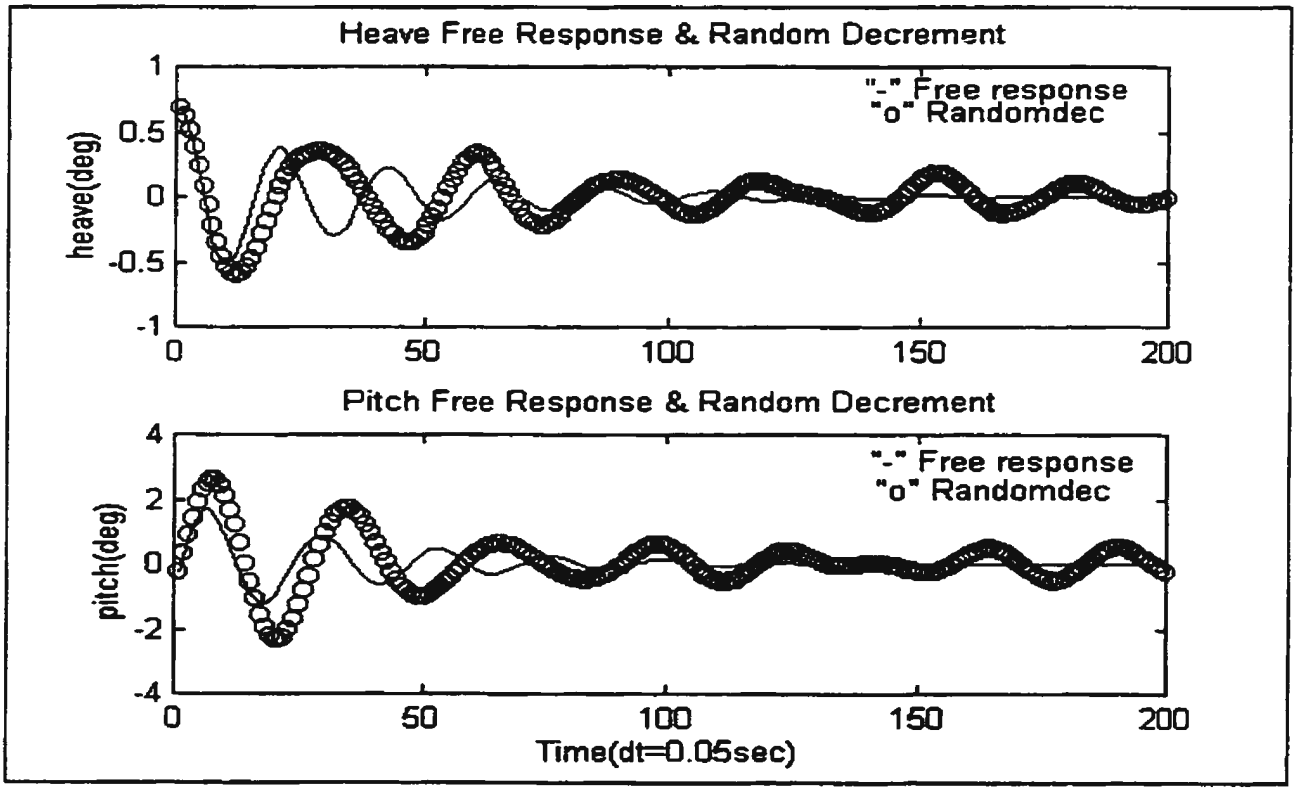

Figure 26: Comparison Between Free Response & Random Decrement Signature for ζ=0.12

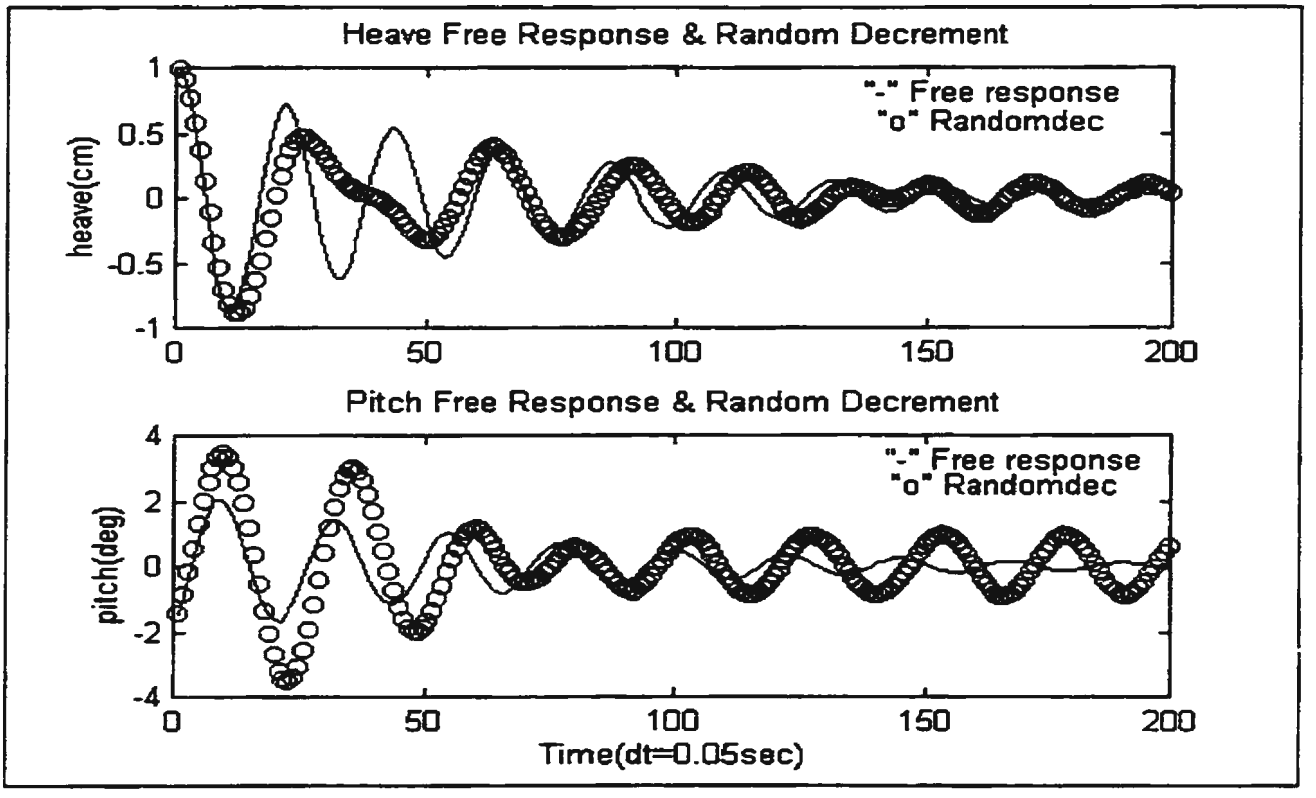

Figure 27: Comparison Between Free Response & Random Decrement Signature for ζ=0.08

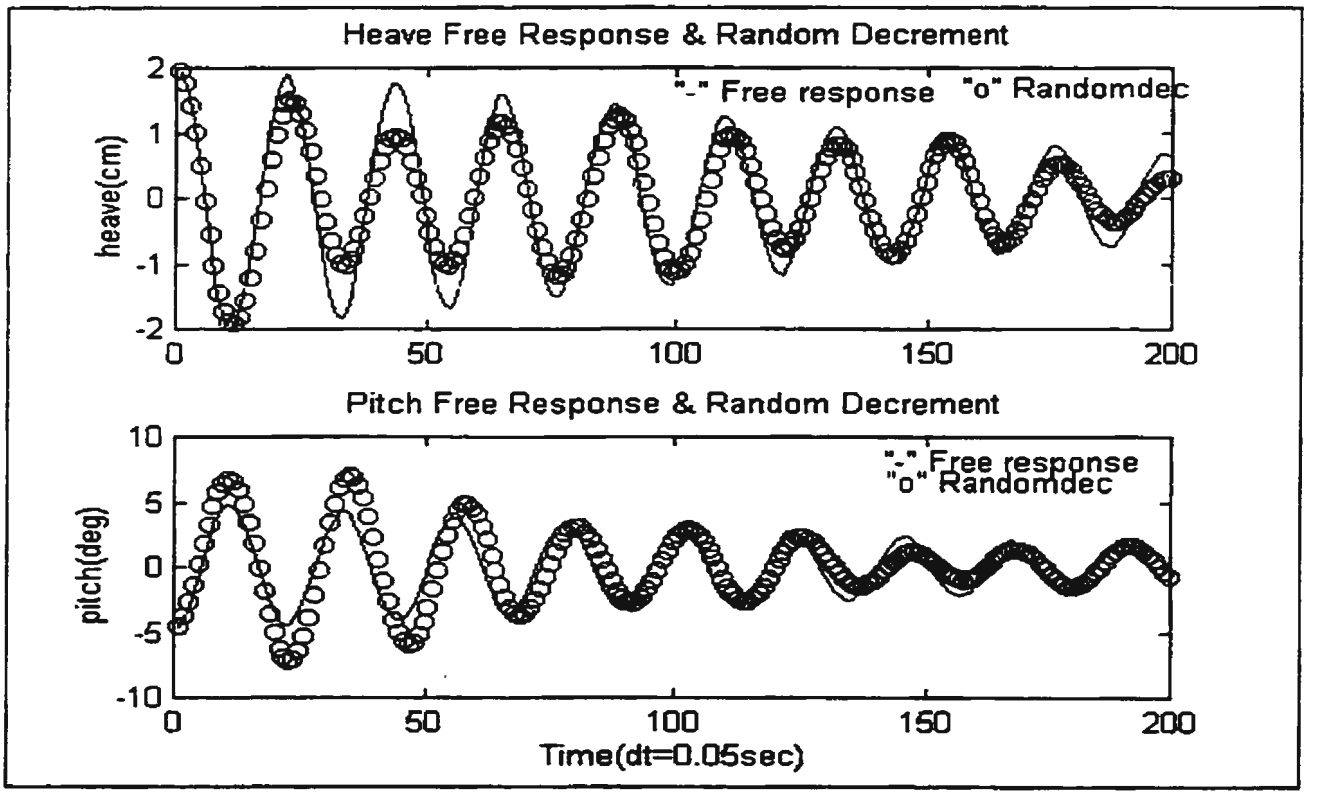

Figure 28: Comparison Between Free Response & Random Decrement Signature for ζ=0.04

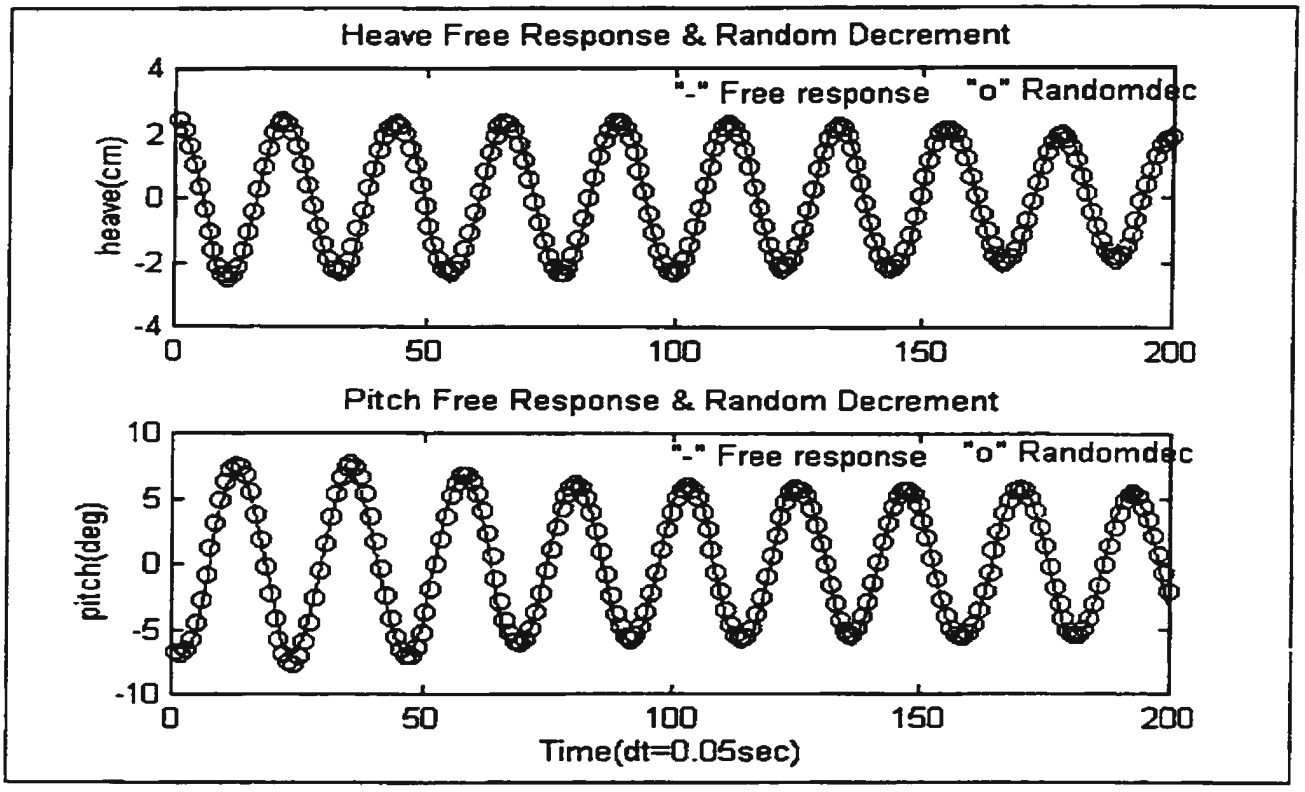

Figure 29: Comparison Between Free Response & Random Decrement Signature for ζ=0.02

3.2.2 Identification for Light Damping System

The coupled heave and pitch Random Decrement signatures obtained from the simulation of light damping system (ζ=0.02) were used to identify the Random Decrement equations. The Neural Network structure is similar to that shown in **Figure 5**. The identified weight values are tabulated in Table vi, and the training result is shown in Figure 30.

Table vi: Identification Results for Light Damping System Simulations

Weight Values for Identified Function $G_1(Z', Z, \theta', \theta)$						
β_I , i=0,1,2,3,4,5	-2.526	0.944	0.847	0.946	0.946	1.579
W_{1i} , i=0,1,2,3,4	-0.024	0.863	-1.387	-0.140	-0.828	
W_{2i} , i=0,1,2,3,4	-0.071	0.012	-3.592	-0.154	-0.944	
W_{3i} , i=0,1,2,3,4	-0.024	0.868	-1.379	-0.139	-0.831	
W_{4i} , i=0,1,2,3,4	-0.024	0.866	-1.381	-0.140	-0.830	
W_{5i} , i=0,1,2,3,4	0.043	0.698	-3.028	0.136	-2.067	
Weight Values for Identified Function $G_2(Z', Z, \theta', \theta)$						
β_I , i=0,1,2,3,4,5	-8.839	4.994	3.540	3.113	3.230	3.085
W_{1i} , i=0,1,2,3,4	-0.087	4.552	-1.514	1.167	-4.764	
W_{2i} , i=0,1,2,3,4	-0.860	5.702	-1.571	1.122	-9.906	
W_{3i} , i=0,1,2,3,4	-0.311	0.671	-3.745	0.030	-2.062	
W_{4i} , i=0,1,2,3,4	-0.760	5.242	-1.656	1.022	-9.166	
W_{5i} , i=0,1,2,3,4	-0.292	0.706	-3.697	0.040	-2.129	
Damped Frequencies for Heave and Pitch Random Decrement Signature						
Heave frequency ω_3	5.64781 (rad / sec)					
Pitch Frequency ω_5	5.58505 (rad / sec)					

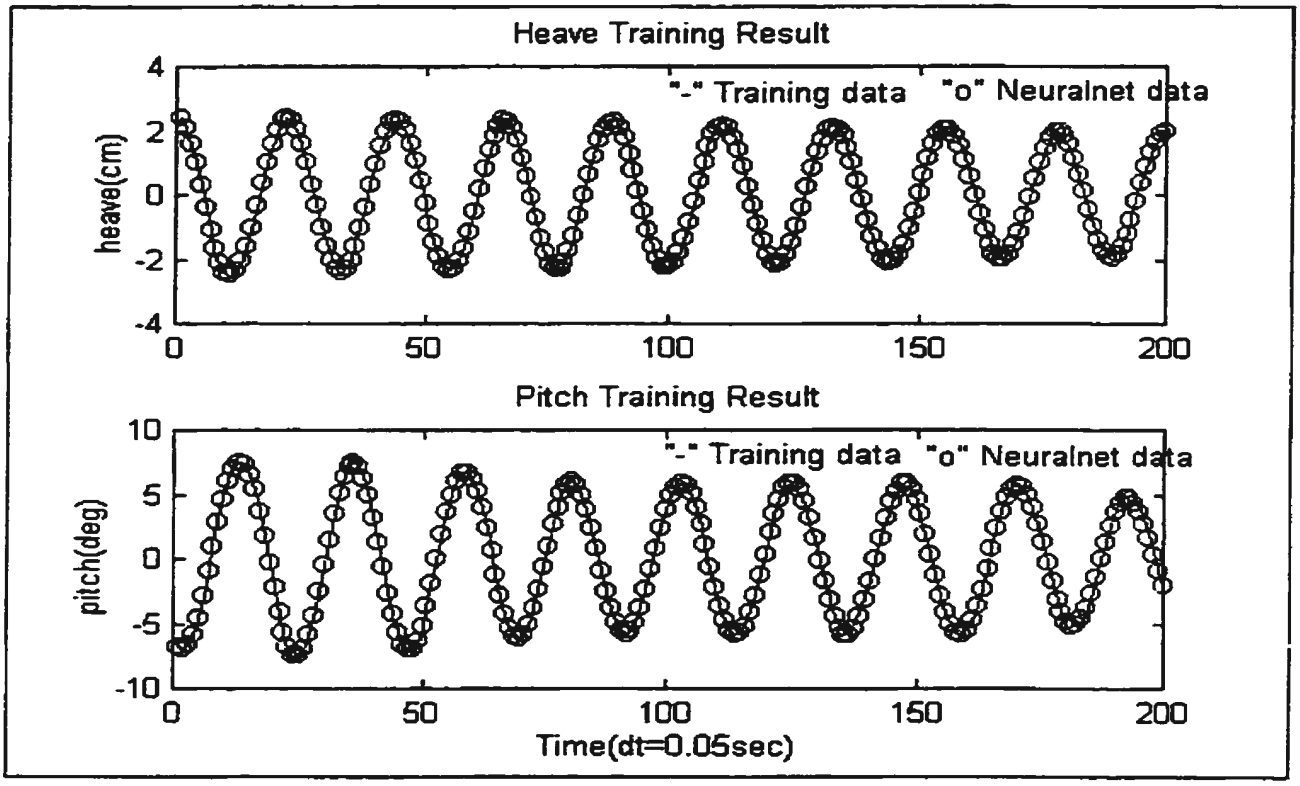

Figure 30: Neural Network Training Results for Light Damping System Simulations

3.2.3 Verification for Light Damping System

The first step was to verify the generalization of the identified Random Decrement equations by comparing the actual and the predicted Random Decrement signatures. The comparison results shown in Figure 31 to Figure 33 proved the generalization of the identified equations.

The second step was to verify the compatibility between the Random Decrement equations and free response signature. The solutions to the identified Random Decrement equations were compared with the free response signatures in Figure 34 to Figure 36.

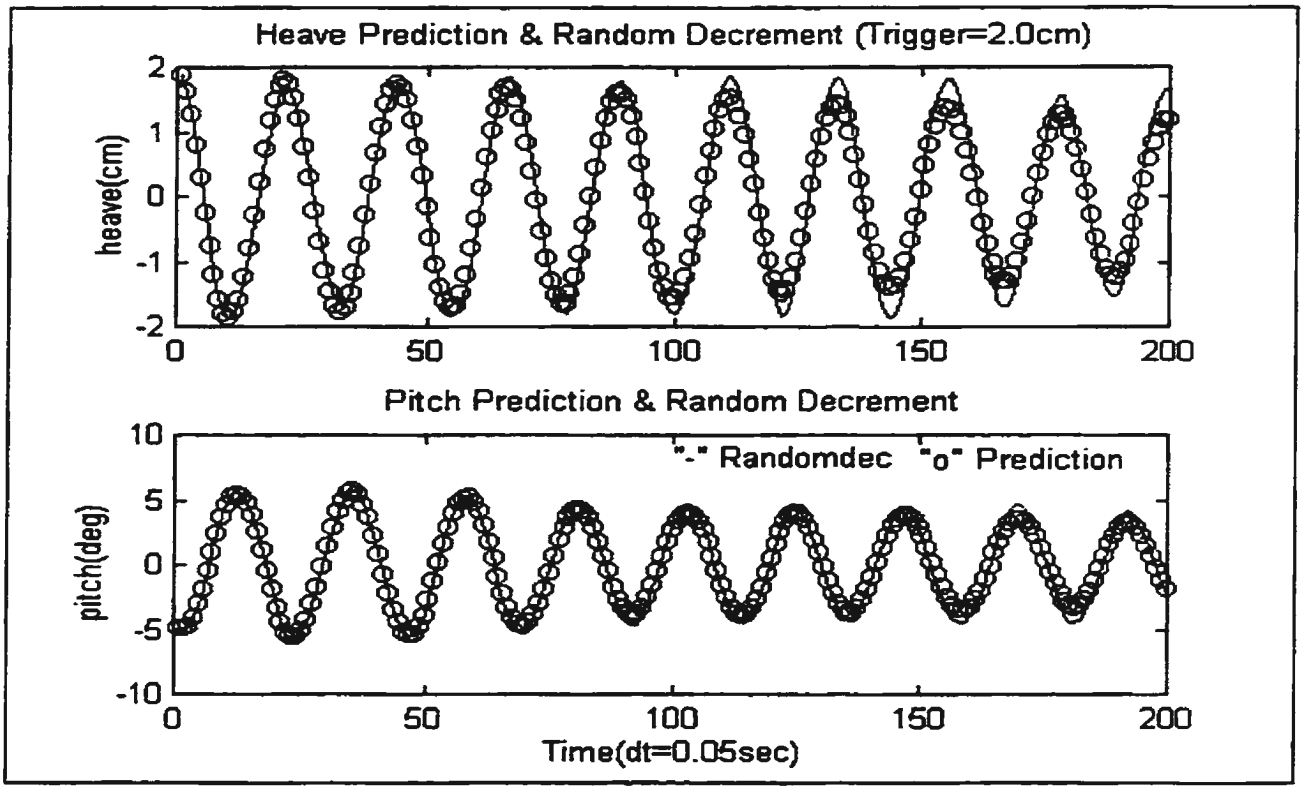

Figure 31: Comparison Between Predictions & Random Decrement Signature (Heave Trigger 2.0cm)

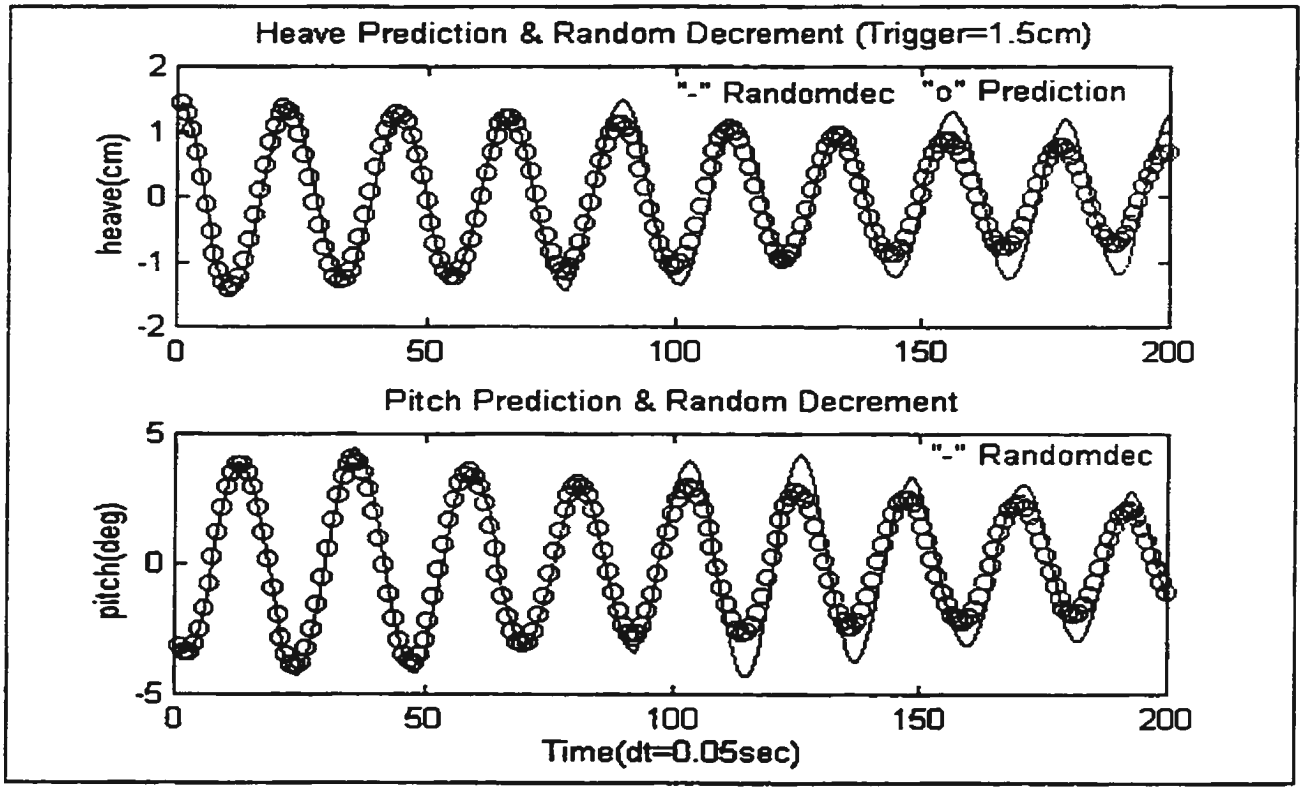

Figure 32: Comparison Between Predictions & Random Decrement Signature (Heave Trigger 1.5cm)

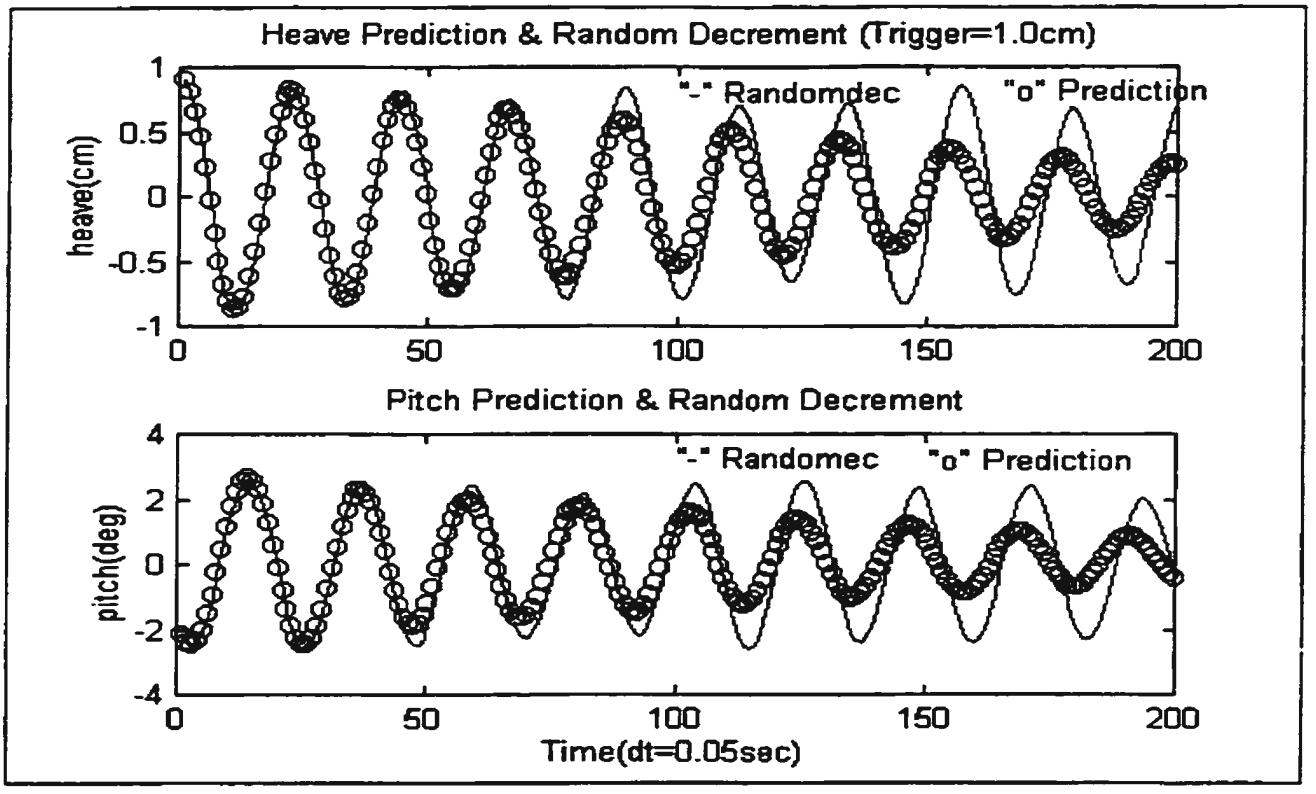

Figure 33: Comparison Between Predictions & Random Decrement Signature (Heave Trigger 1.0cm)

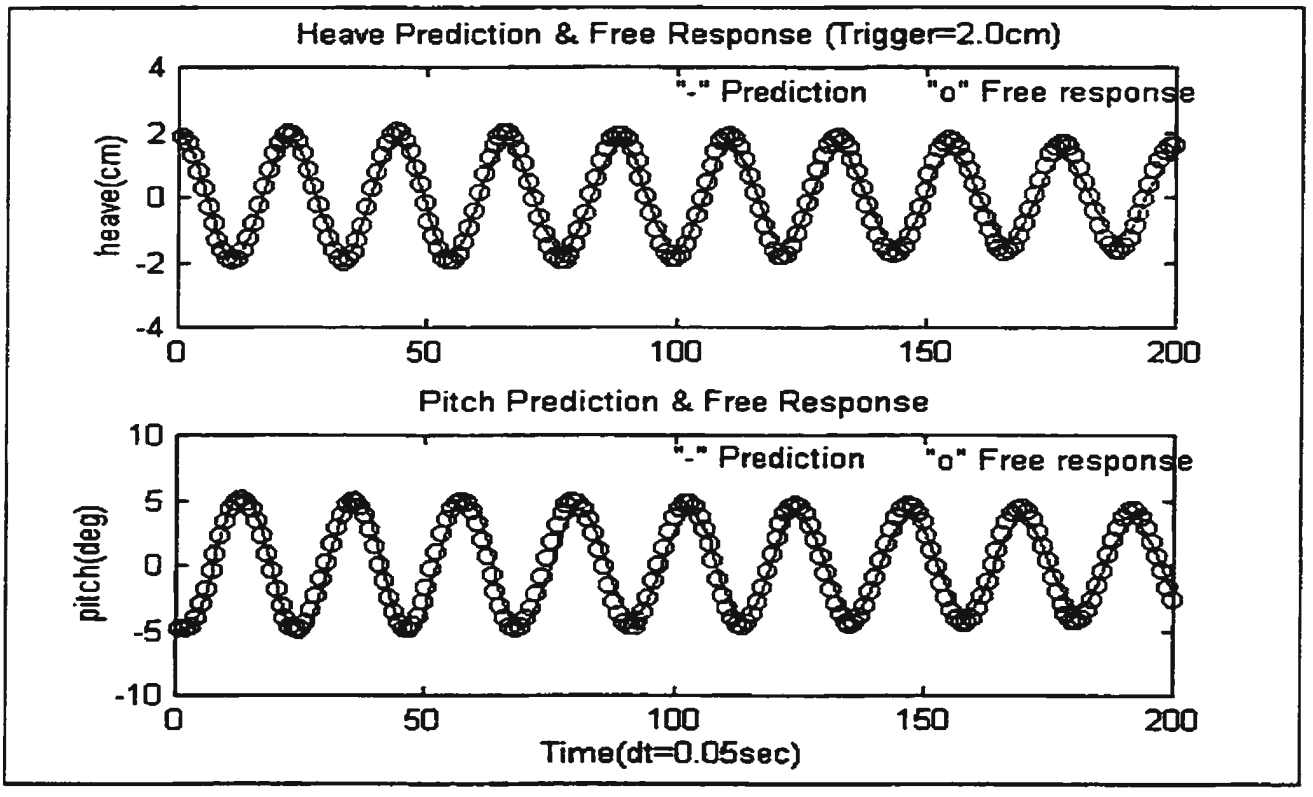

Figure 34: Comparison Between Predictions & Free Response (Heave Trigger 2.0cm)

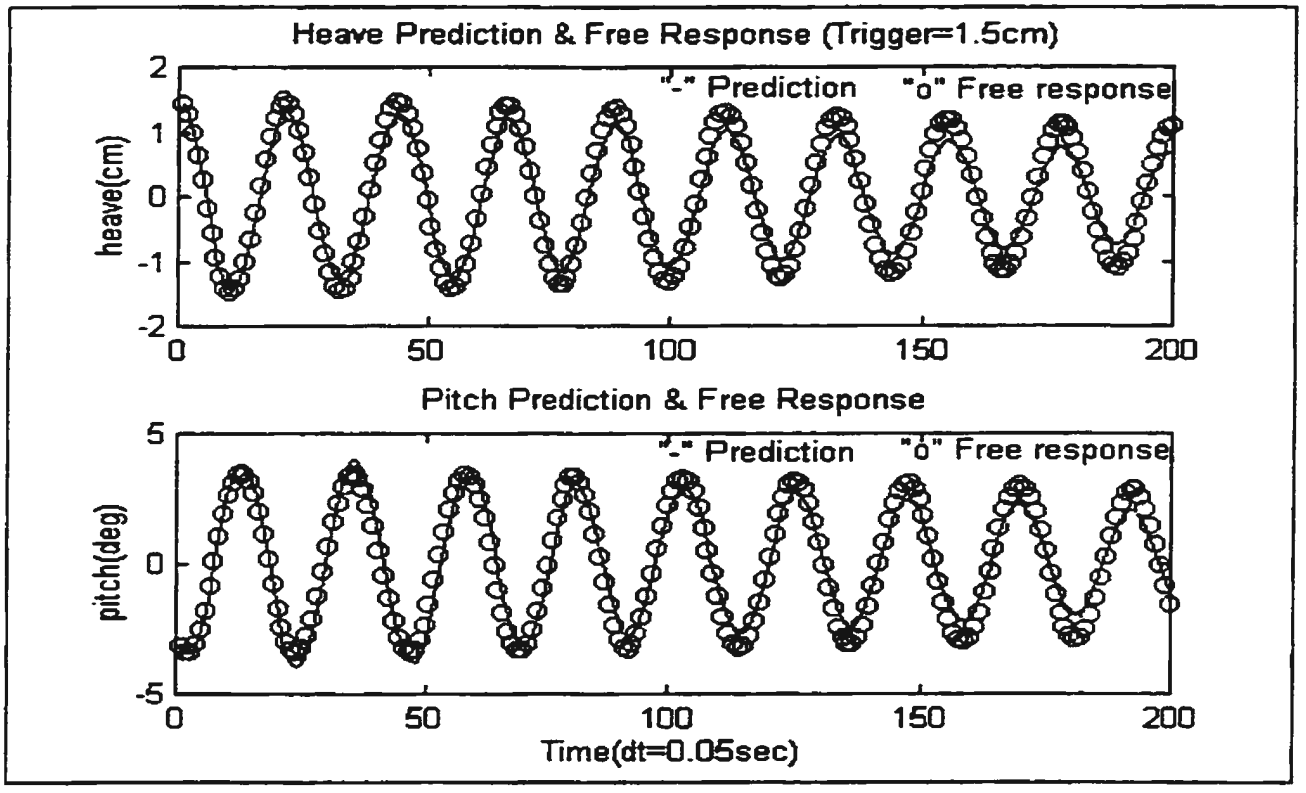

Figure 35: Comparison Between Predictions & Free Response (Heave Trigger 1.5cm)

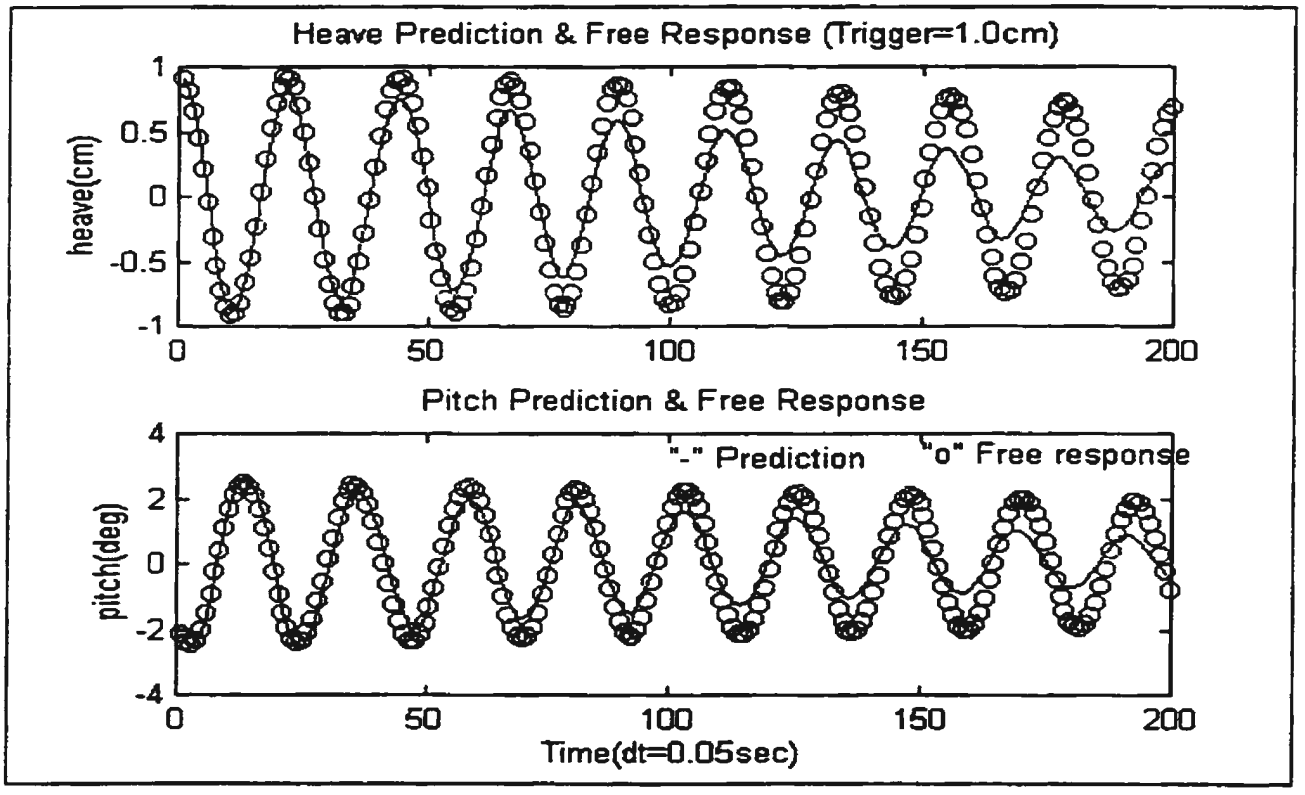

Figure 36: Comparison Between Predictions & Free Response (Heave Trigger 1.0cm)

3.3 Ship Model Simulation Results (White Noise)

For white noise excitation approximation, the random time series of force F(t) and moment M(t) were synthesized directly from the constant spectrum shown in Figure 3. The mathematical model for 'R-Class Icebreaker' motion (25) was employed to generate the motion time series, which was used later to obtain the heave and pitch Random Decrement signatures. This motion system is a heavy damping system.

3.3.1 Analysis of the Random Decrement Signatures

The heave and pitch Random Decrement signatures were analyzed by comparing with the free response signatures, which were obtained from the equation (26). Their agreement is the prerequisite to the validation of the identification results. The comparison results are shown in Figure 37 and Figure 38. The irregularity in the Random Decrement signatures was mainly caused by the insufficient segments selected from the motion time series. It had much more influence for the small value signatures. Even with such large interference, the required agreement was achieved in the first several periods. This agreement could be displayed more clearly using autocorrelation function. The heave autocorrelation function was scaled up to match the trigger value of the Random Decrement signature and compared with both heave Random Decrement signature and heave free response in Figure 39.

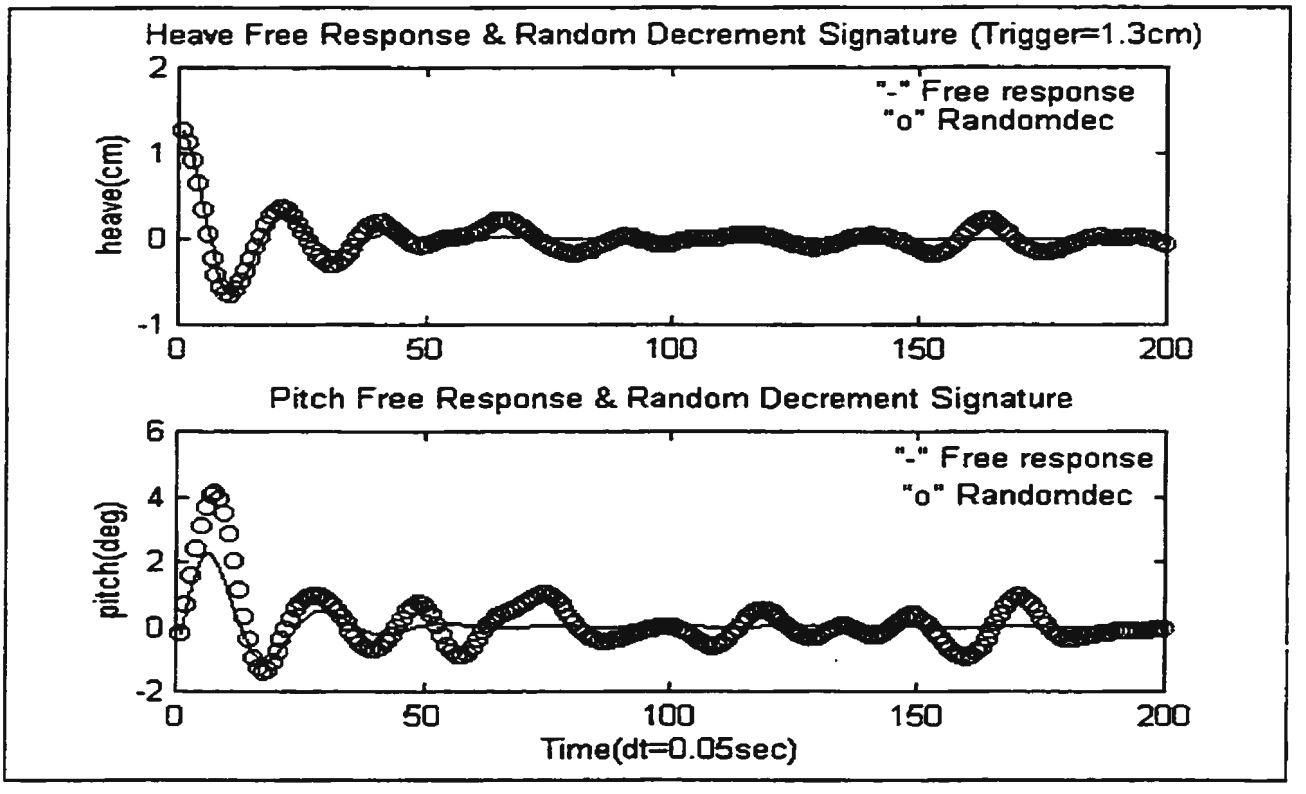

Figure 37: Comparison Between Free Response & Random Decrement Signature (Heave Trigger 1.3cm)

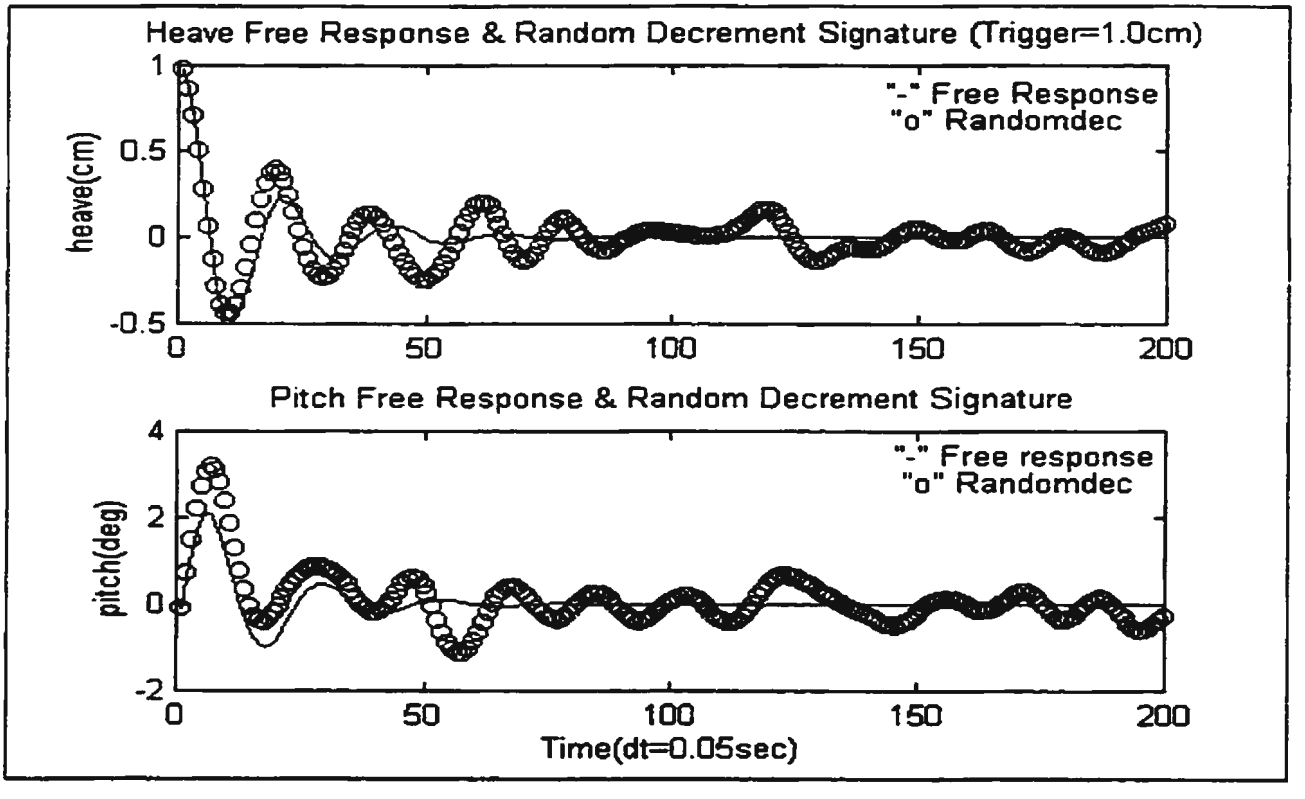

Figure 38: Comparison Between Free Response & Random Decrement Signature (Heave Trigger 1.0cm)

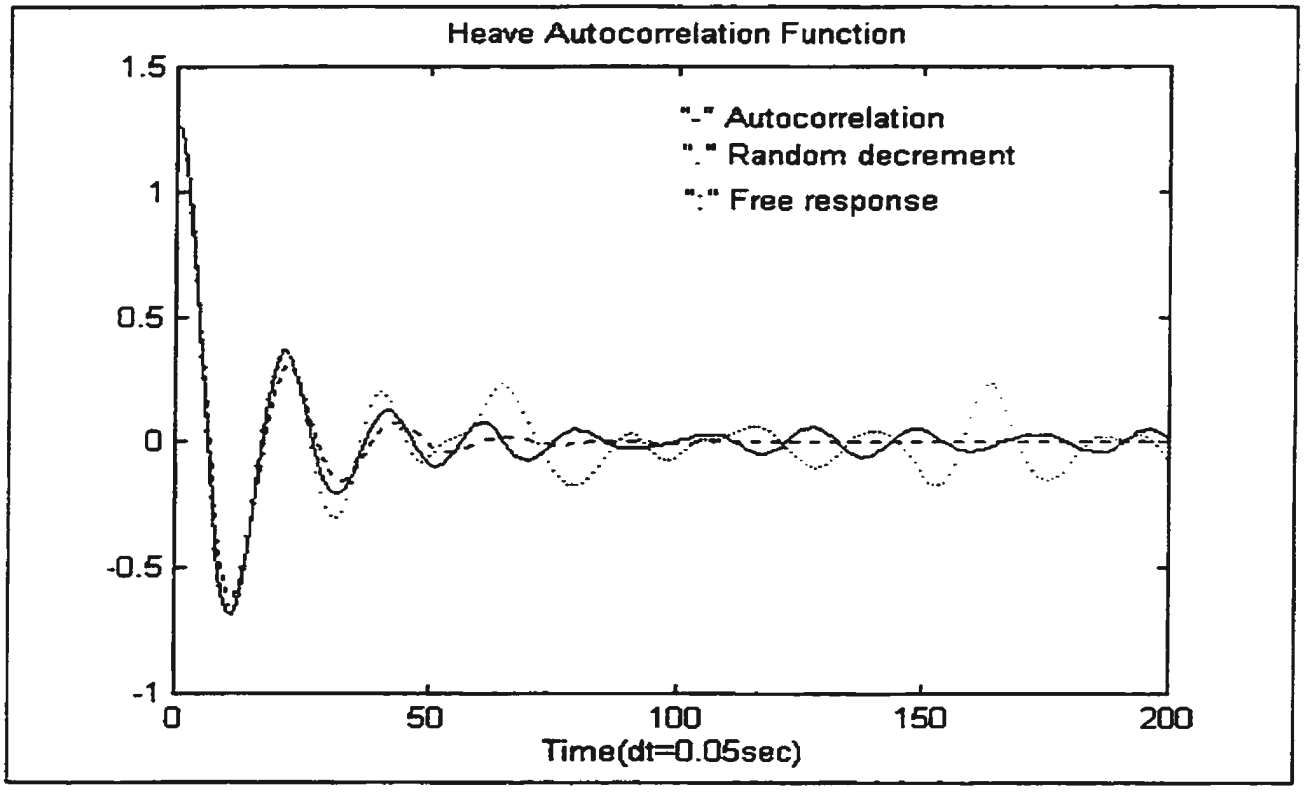

Figure 39: Comparison Between Heave Autocorrelation, Random Decrement, and Free Response

3.3.2 Identification Results

The Random Decrement signature with the heave trigger value 1.3cm was used for Neural Network training. The weight values and the damped frequencies identified from Neural Network training process are tabulated in Table vii. The training results are presented in Figure 40 and Figure 41. The training accuracy was not good due to the irregularity in the obtained Random Decrement signature. Only the first 50 points achieved the good agreement.

Table vii: Identification Results for White Noise Excitation

Weight Values for Identified Function $G_1(Z', Z, \theta', \theta)$						
β_I , i=0,1,2,3,4,5	2.842	-5.089	-5.089	-5.089	-5.089	-5.089
W_{1i} , i=0,1,2,3,4	2.693	0.953	-2.447	0.394	1.677	
W_{2i} , i=0,1,2,3,4	2.693	0.953	-2.447	0.394	1.677	
W_{3i} , i=0,1,2,3,4	2.693	0.953	-2.447	0.394	1.677	
W_{4i} , i=0,1,2,3,4	2.693	0.953	-2.447	0.394	1.677	
W_{5i} , i=0,1,2,3,4	2.693	0.953	-2.447	0.394	1.677	
Weight Values for Identified Function $G_2(Z', Z, \theta', \theta)$						
β_I , i=0,1,2,3,4,5	-64.431	8.996	10.457	18.790	19.715	18.991
W_{1i} , i=0,1,2,3,4	-0.948	1.843	-12.097	0.295	5.641	
W_{2i} , i=0,1,2,3,4	1.942	1.341	-22.639	1.583	-3.198	
W_{3i} , i=0,1,2,3,4	10.836	0.522	-14.913	0.889	-13.927	
W_{4i} , i=0,1,2,3,4	10.416	-10.130	-8.669	-0.450	-5.954	
W_{5i} , i=0,1,2,3,4	10.136	-9.737	-8.967	-0.400	-5.744	
Damped Frequencies for Heave and Pitch Random Decrement Signature						
Heave frequency ω_3	5.7776 (rad / sec)					
Pitch Frequency ω_5	5.4636 (rad / sec)					

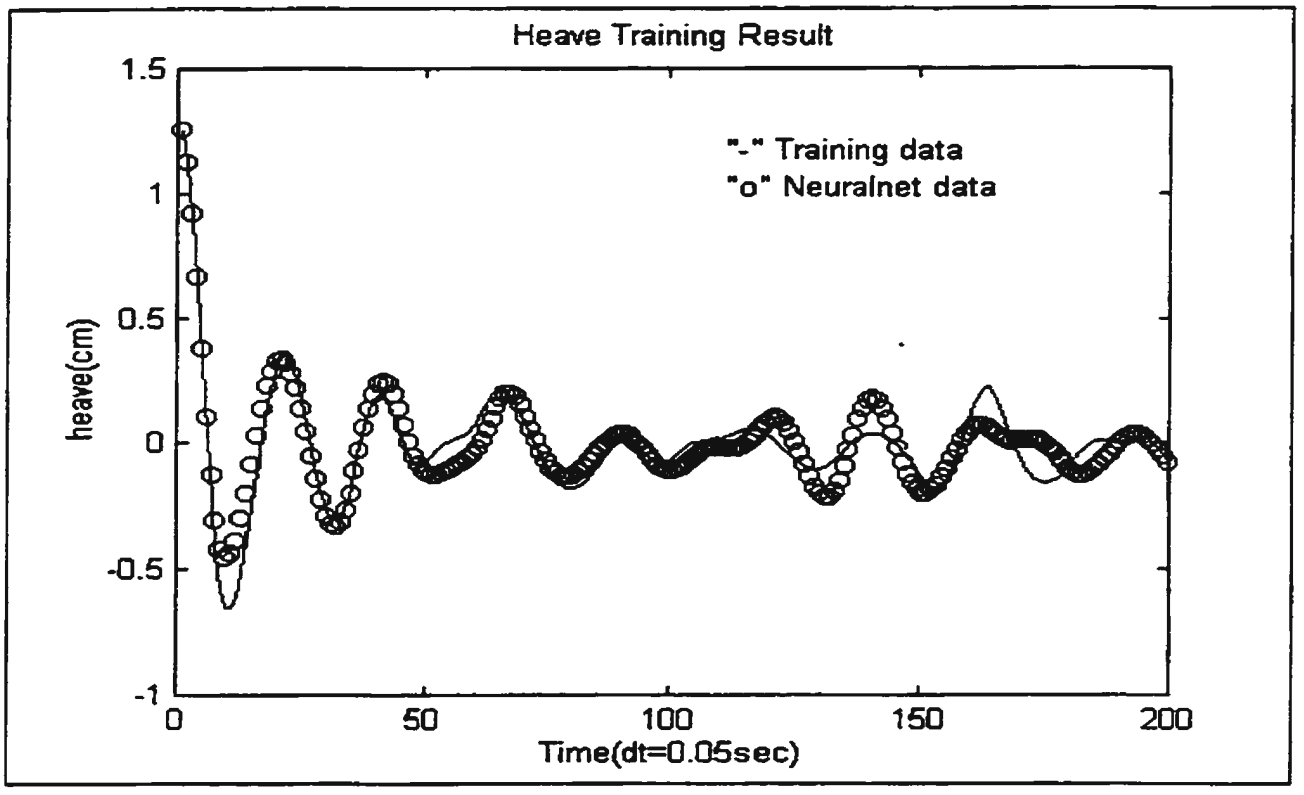

Figure 40: Heave Training Result for White Noise Simulations

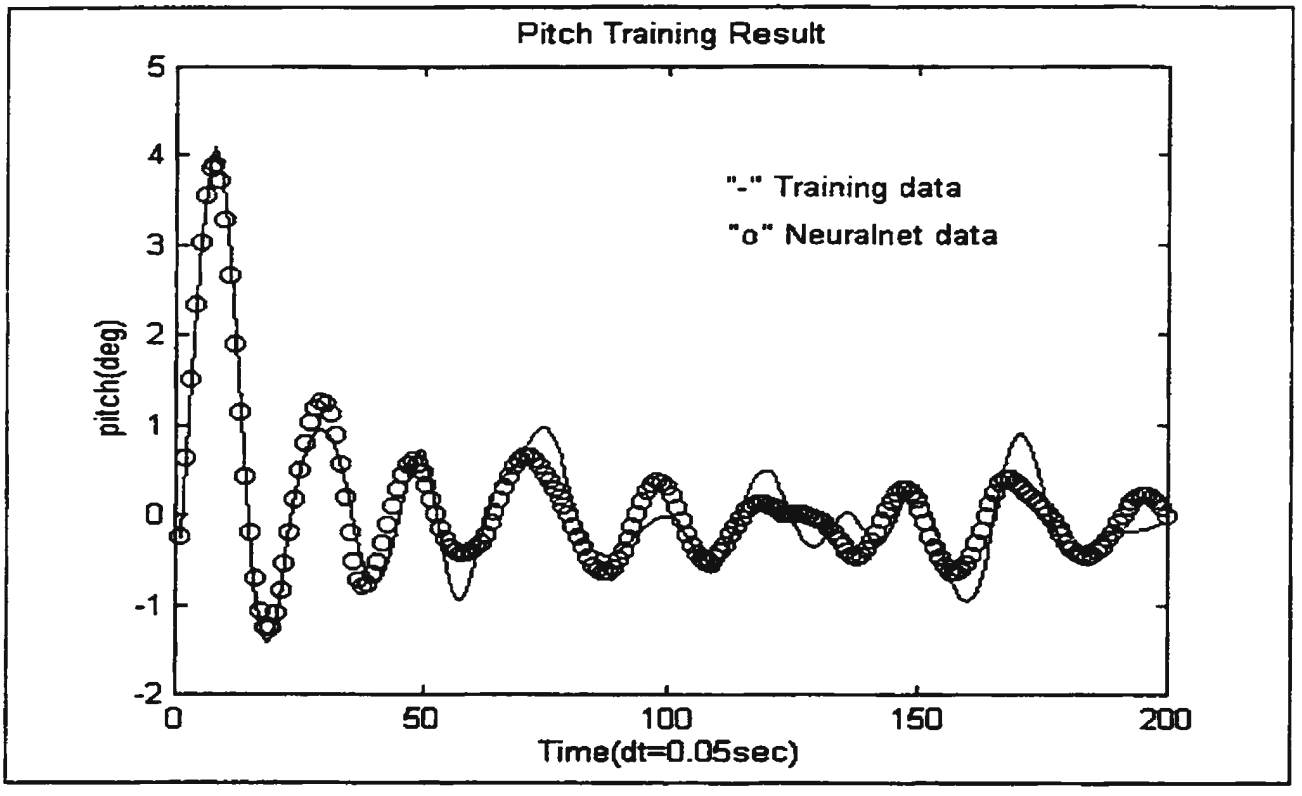

Figure 41: Pitch Training Result for White Noise Simulations

The identified Random Decrement equations are expressed as (28),

$$Z'' + 5.7776^2 Z + G_1(Z', Z, \theta', \theta) = 0$$
$$\theta'' + 5.4636^2 \theta + G_2(Z', Z, \theta', \theta) = 0 \qquad (28)$$

where the functions G_1 and G_2 are uniquely determined by the weight values in Table vii.

3.3.3 Verification Results

The generalization of the identified Random Decrement equations (28) was verified by the comparison between the predicted and the actual Random Decrement signatures. During the Neural Network training, only the agreement for the first 50 points was achieved. Thus the generalization was also verified by the comparison of the first 50 data points. The comparison results shown in Figure 42 and Figure 43 are not good due to the noise interference in both predictions and actual Random Decrement signatures. Obviously the identified equations expressed by equation (28) and Table vii was not acceptable. The lack of accuracy in the training data caused such failure of motion identification.

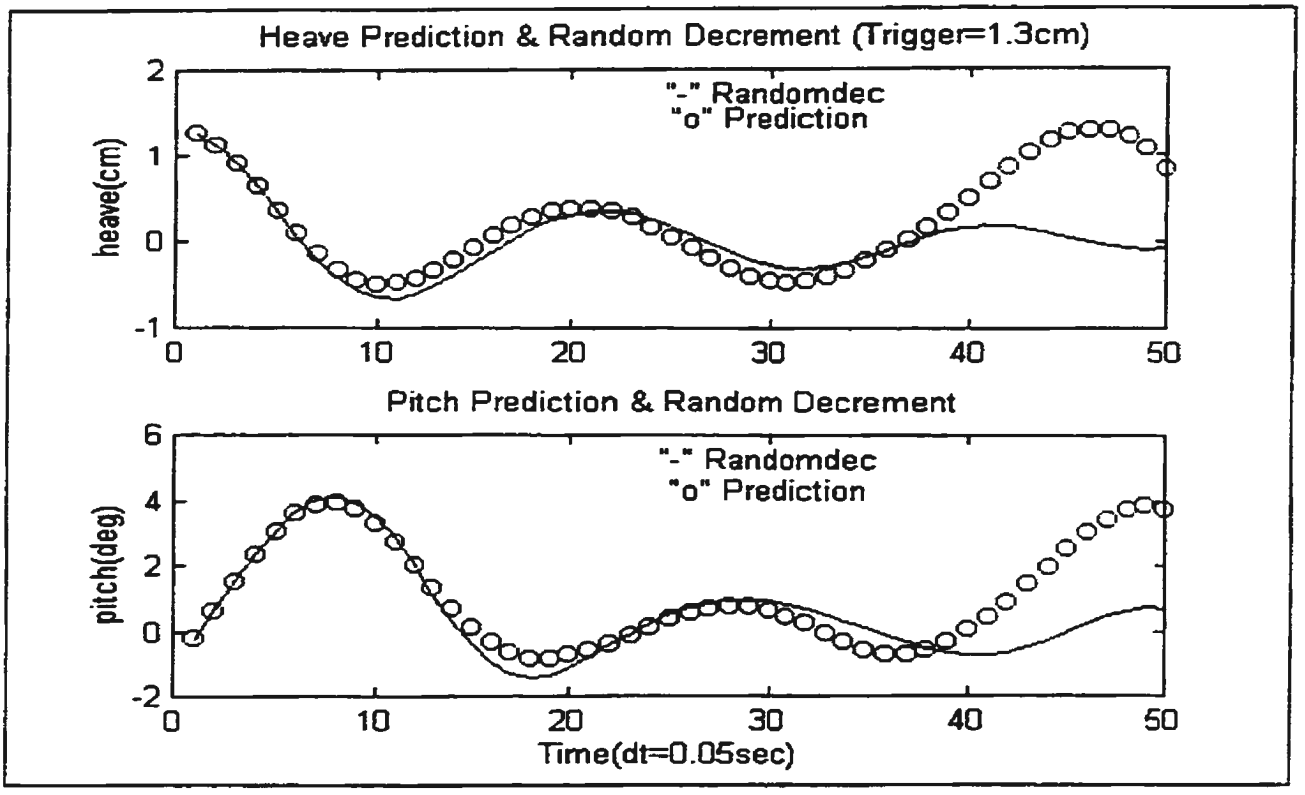

Figure 42: Comparison Between Predictions & Random Decrement Signature (Heave Trigger 1.3cm)

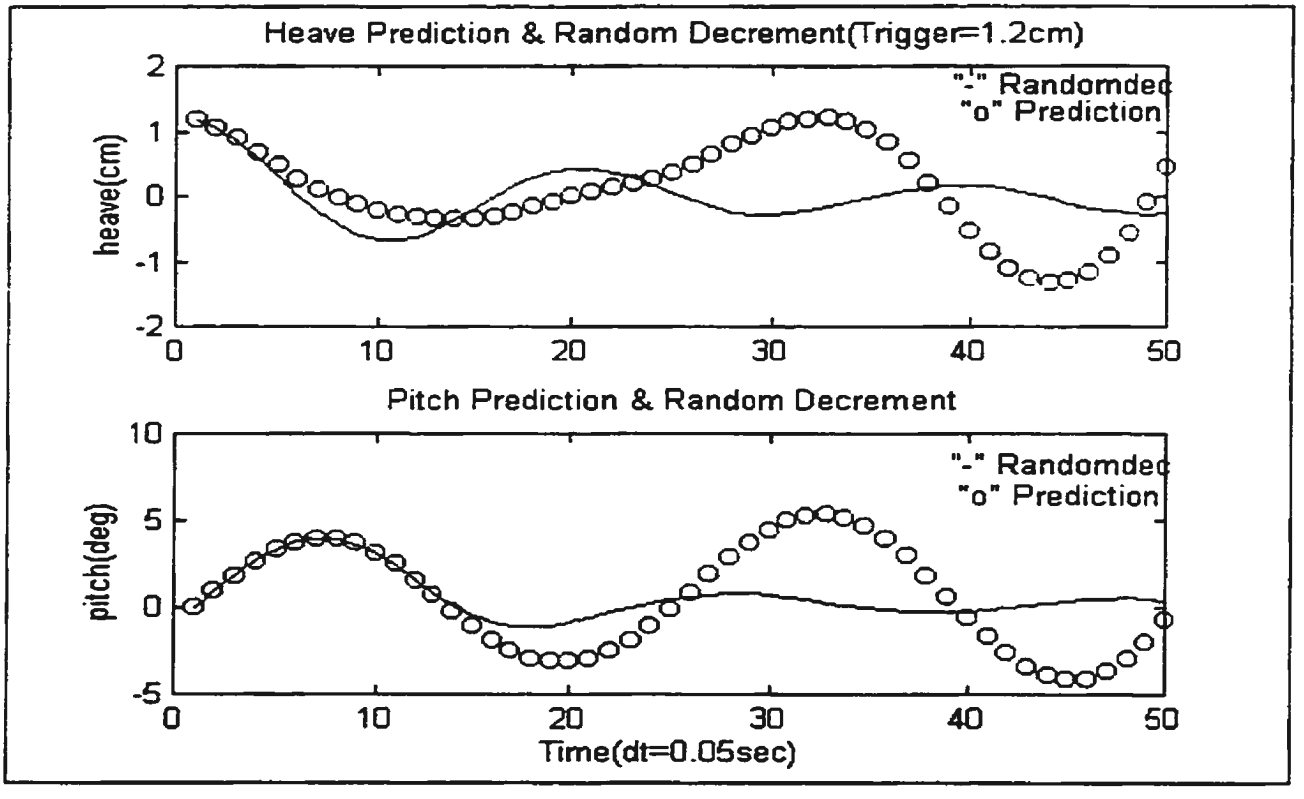

Figure 43: Comparison Between Predictions & Random Decrement Signature (HeaveTrigger 1.2cm)

4. Conclusions and Recommendations

A particular method was developed in this research to identify the ship coupled heave and pitch motions from the random motion histories. The two-degree Random Decrement technique and the Neural Networks technique were combined in the identification process. The application results suggested several points regarding the validation and effects of this identification method.

Both wave tank experiments and simulation results showed that under JONSWAP wave excitations the heave and pitch Random Decrement signatures did not agree with the free response signatures for 'R-Class Icebreaker' ship model. The obtained Random Decrement signatures demonstrated a light damping nature while the free responses had a heavy damping decay form. The identified Random Decrement equations thus did not represent the ship model free response equations that could be used for further seakeeping research.

More simulation results proved that under the JONSWAP wave excitations only the light damping systems were possible to achieve the required agreements between the Random Decrement signatures and the free response signatures. This agreement is the prerequisite to the validation of the identification results.

The broad-band constant excitation spectrum, which approximated the white noise excitations in the research, was used in another simulation for 'R-Class Icebreaker' ship model. Although the obtained Random Decrement signatures were severely damaged by some noise, they did agree with the free response signatures in the decay form. Both the

Random Decrement signatures and free response signatures displayed a heavy damping nature in this case.

Above results about the two-degree Random Decrement signatures are compatible with the one-degree conclusions presented by Vandiver et al.(1982),

- For a linear, time-invariant system excited by a zero-mean, stationary, Gaussian random process, the system response will also be a zero-mean, stationary, Gaussian random process. If the input is also a white noise, the Random Decrement signature of the output will exactly represent the transient decay of the system from the specified set of initial conditions.

- If the excitation for the same system is not white noise, but sufficiently broad-band, the above conclusion will apply well.

- For a band limited excitation spectrum, a lightly damped system often yields the results which to sufficient accuracy are equivalent to the response of a white noise input.

For the ship heave and pitch motions, the system is usually heavily damped. In this case the JONSWAP wave spectrum is too narrow-banded to achieve the required agreement between the Random Decrement signatures and free response signatures. Only the broad-band excitations could yield the acceptable results.

For two-degree Random Decrement signature, the proportional relationship that exists between the autocorrelation function and single-degree Random Decrement signature only applied to the leading signal of the two-degree Random Decrement signature. Thus

the autocorrelation function could not be used for motion identification even the obtained Random Decrement signature was not accurate.

Besides the nature of the Random Decrement signatures, the quality of Neural Networks training is another factor for the validation of identification results. In this research the Multilayer Perceptron networks simplified the identification problem by lumping a large number of the unknown parameters into a function. This unknown function was identified through the Neural Network training. It did provide a means for identification of the complicated systems. The quality of the training results was determined by several factors.

The accuracy of the Neural Network training results was mainly dependent on the quality of the selected training data. Too much noise in the training samples was not acceptable in any case, particularly for the small value signature. In this research the 8001 data points in motion series were not enough for selecting sufficient segments to form the Random Decrement signature. More motion data should be collected in practical application. However, too many training data with a relatively small network also caused the lack of accuracy in the training results.

The generalization of the Neural Networks identification is another concern for the quality of the training results. The good generalization is to ensure that the different Random Decrement signatures with the varying initial conditions will all satisfy the same identified equations. It is mainly dependent on the Neural Network structure. Too small network could not achieve good accuracy. Too capable network with too many neurons and weights will not yield good generalization. In that case the identified equations are

possibly not the true equations even the training results are perfect. From Hush and Horne(1993), a useful rule of thumb is that the number of training samples should be approximately ten times the number of the weights. The Neural Networks adopted in this research have 31 weights and 200 training data with their ratio around 7, which yielded the good results.

Generally the developed method will produce the acceptable identification results under the broad-band wave excitations. It is particularly valuable for the case where the complete wave knowledge is unavailable. Since the Random Decrement technique and the Neural Network technique are basically empirical methods, the careful verification and analyses are always necessary for any practical application.

References

Bhattacharyya, R. (1978). *Dynamics of Marine Vehicles*, John Wiley & Sons, Inc.

Cole, H.A.,Jr. (1971). "Failure Detection of a Space Shuttle Wing Flutter Model by Random Decrement", *NASA TMX-62, 041*, May 1971.

Haddara, M.R. and Hinchey, M. (1995). "On the Use of Neural Network Techniques in the Analysis of Free Roll Decay Curves", *International Shipbuilding Progress*, Vol. 42, No. 430, pp.166-178.

Haddara, M.R. and Wang, Y. (1996). "Parametric Identification of Coupled Sway and Yaw Motions", *Proceedings of the Fifteen International Conference on Offshore Mechanics and Arctic Engineering*, vol. I, Florence, Italy, pp. 267-273.

Haddara, M.R. and Wu, X. (1993). "Parameter Identification of Nonlinear Rolling Motion in Random Seas", *International Shipbuilding Progress*, Vol. 40, No. 423, pp. 247-260.

Haddara, M.R. and Xu, Jinsong. (1997). "Identification of Ship Coupled Heave-Pitch Motion Using Neural Networks", to be published.

Hush, D.R. and Horne, B.G. (1993). "Progress in Supervised Neural Networks", *IEEE Signal Processing Magazine*, January 1993, pp.8-39.

Ibrahim, S.R. (1977). "Random Decrement Technique for Modal Identification of Structures", *Journal of Spacecraft*, Vol. 14, No. 11, pp. 696-700.

Lloyd, A.R.J.M. (1989). *Seakeeping: Ship Behavior in Rough Weather*, Ellis Horwood Series in Marine Technology.

Lloyd, A.R.J.M. (1991). "Seakeeping", *Philosophical Transactions of the Royal Society of London*. Series A. pp.253-264.

Vandiver, J.K.; Dunwoody, A.B.; Campbell, R.B.; Cook, M.F. (1982). "A Mathematical Basis for the Random Decrement Vibration Signature Analysis Technique", *Journal of Mechanical Design*, April 1982, Vol. 104, pp.307-313.

Appendix A Parameter Calculations

The following calculations were based on the algorithm in Chapter Nine (pp.183-198) of *Dynamics of Marine Vehicles* by Bhattacharyya (1978).

The hull offsets of the ship model 'R-Class Icebreaker' are tabulated below, which are the geometric data for the parameter calculations.

OFFSETS TABLE OF 'R-CLASS ICEBREAKER' MODEL

Sta. X(cm) / Z(cm)	0 -110	1 -99	2 -88	3 -77	4 -66	5 -55	6 -44	7 -33	8 -22	9 -11	10 0
0	0	0.64	1.13	1.42	1.62	1.62	1.62	1.62	1.62	1.62	1.62
2.54	0	0.64	1.91	3.22	5.21	10.24	15.67	18.33	19.91	20.62	20.83
5.08	0	0.64	3.02	5.51	8.52	14.47	18.34	20.60	21.89	22.54	22.75
7.62	0	0.64	4.65	8.14	11.70	16.89	19.93	21.74	22.85	23.28	23.29
10.16	0	0.73	7.10	11.22	14.50	18.78	21.12	22.44	23.30	23.56	23.56
12.70	0	3.33	11.27	14.40	16.89	20.15	21.98	23.00	23.66	23.81	23.81
15.24	0	8.62	14.80	17.07	18.80	21.19	22.60	23.47	23.98	24.06	24.06
17.78	5.79	12.50	17.20	18.83	20.15	21.96	23.05	23.83	24.26	24.32	24.32
20.32	9.30	14.85	18.61	19.96	21.02	22.52	23.40	24.06	24.42	24.46	24.26
22.86	11.40	16.17	19.46	20.67	21.60	22.9	23.56	23.99	24.29	24.31	24.31
25.4	12.38	16.84	19.96	21.09	21.97	23.08	23.60	23.89	24.11	24.12	24.12
Sta. X(cm) / Z(cm)	11 11	12 22	13 33	14 44	15 55	16 66	17 77	18 88	19 99	20 110	
0	1.62	1.62	1.62	1.62	1.62	1.62	1.50	0	0	0	
2.54	20.80	20.46	19.51	17.77	15.09	11.50	7.04	2.15	0	0	
5.08	22.58	22.27	21.66	20.44	18.33	15.07	10.27	4.20	0	0	
7.62	23.29	23.09	22.69	21.85	20.19	17.42	12.99	6.48	0	0	
10.16	23.56	23.56	23.28	22.68	21.44	19.15	15.23	9.08	1.00	0	
12.70	23.81	23.81	23.68	23.27	22.36	20.47	17.10	11.86	4.53	0	
15.24	24.06	24.06	24.01	23.73	23.01	21.45	18.62	14.17	7.95	0.53	
17.78	24.32	24.32	24.30	24.08	23.46	22.16	19.83	15.97	10.66	4.47	
20.32	24.46	24.46	24.46	24.30	23.70	22.68	20.76	17.53	12.87	7.06	
22.86	24.31	24.31	24.31	24.19	23.81	23.06	21.51	18.84	14.66	8.87	
25.40	24.12	24.12	24.12	24.08	23.82	23.29	22.06	19.85	16.03	10.36	

The general equations for the coupled heave and pitch motions were expressed as below,

$$(m + a_z)Z'' + bZ' + cZ + d\theta'' + e\theta' + h\theta = F(t)$$
$$(I_{yy} + A_{yy})\theta'' + B\theta' + C\theta + DZ'' + EZ' + HZ = M(t)$$

The equation parameters for the 'R-Class Icebreaker' ship model were calculated in the following tables.

TABLE 1 CALCULATIONS FOR a_z AND A_{yy}

(1) station	(2)	(3)	(4)	(5)	(6)	(7)	(8)	(9)	(10)
0	0	0.1790	0	-1.092	0	0	0	0	0
5	0.4392	0.1763	0.0574	-0.542	0.4139	2.491	0.077	0.746	0.76
10	0.4864	0.1735	0.0762	0.008	0.4582	2.803	0.084	0.908	0.90
15	0.4692	0.1705	0.0650	0.558	0.4422	2.752	0.080	0.812	0.76
20	0	0.1675	0	1.108	0	0	0	0	0
station No.	(11)	(12)	(13)	(14)	(15)	(16)	(17)	(18)	(19)
0	0	0	0	1	0	1.192	0	1	0
5	0.1929	75.752	57.572	4	230.29	0.294	16.926	4	67.704
10	0.2366	92.913	83.622	2	167.24	0	0	2	0
15	0.2201	86.433	65.689	4	262.76	0.311	20.429	4	81.716
20	0	0	0	1	0	1.228	0	1	0
				SUM1	660.29			**SUM2**	149.42

Descriptions of Table 1

Column No.	*Description*	*Column No.*	*Description*
(1)	Station Number	(10)	Added Mass Coefficient from Fig.4.4 of *Dynamics of Marine Vehicles.*
(2)	Beam at Station, B_n (m)	(11)=(2)×(2)	Beam squared, B_n^2
(3)	Draft at Station, Tn (m)	(12)	$(\rho\pi/8)\times B_n^2$
(4)	Sectional Area at Station, S_n (m^2)	(13)=(12)×(10)	Sectional Added Mass, $a_n = C\times(\rho\pi/8)\times B_n^2$
(5)	Lever Arm from Longitudinal Center of Buoyancy, ξ (m)	(14)	Simpson's Multiplier
(6)	$\omega^2/(2g)\times B_n$, ω was peak frequency of the wave	(15)=(14)×(13)	Simpson's Product

	spectrum in calculation		
(7)=(2)/(3)	Beam Draft Ratio=B_n / T_n	(16)=(5)×(5)	Lever Arm Squared, ξ^2
(8)=(2)×(3)	$B_n \times T_n$	(17)=(13)×(16)	$a_n \times \xi^2$
(9)=(4)/(8)	Sectional Area Coefficient, $S_n /(B_n \times T_n)$	(19)=(17)×(18)	Simpson's Product

Added Mass for heaving, a_z

$a_z = \int a_n \, d\xi = (1/3) \times S \times SUM1$

$= (1/3) \times 0.55 \times 660.29 = 121.053(kg)$

Added mass moment of inertia for pitching,

$A_{yy} = \int (a_n \xi^2) \, d\xi = (1/3) \times S \times SUM2$

$= (1/3) \times 0.55 \times 149.42 = 27.394(kg\ m^2)$

TABLE 2 CALCULATIONS FOR b AND B

(1) station	(2)	(3)	(4)	(5)	(6)	(7)	(8)	(9)	(10)
0	0	0	0	0	0	0	1	0	1.192
5	0.4139	2.491	0.746	0.52	0.2704	326.63	4	1306.5	0.294
10	0.4582	2.803	0.908	0.54	0.2916	352.24	2	704.47	0
15	0.4422	2.752	0.812	0.60	0.3600	434.86	4	1739.4	0.311
20	0	0	0	0	0	0	1	0	1.228
							SUM1	3750.4	
station No.	**(11)**	**(12)**	**(13)**						
0	0	1	0						
5	96.029	4	384.12						
10	0	2	0						
15	135.24	4	540.96						
20	0	1	0						
		SUM2	925.08						

Description of Table 2

Column No.	*Description*	*Column No.*	*Description*
(1)	Station Number	(7)=$(\rho g^2/\omega^3) \times (6)$	Sectional Damping Coefficient, b_n

(2)	$\omega^2/(2g)\times B_n$, ω was peak frequency of the wave spectrum in calculation	(8)	Simpson's Multiplier
(3)	Beam Draft Ratio=B_n / T_n	(9)=(7)×(8)	Simpson's Product
(4)	Sectional Area Coefficient, S_n /(B_n × T_n)	(10)	Lever Arm Squared, ξ^2
(5)	Amplitude Ratio for Heaving, found from Fig. 4.6 of *Dynamics of Marine Vehicles*	(11)=(7)×(10)	$b_n\times\xi^2$
(6)= (5)×(5)	Square of Amplitude Ratio	(13)=(11)×(12)	Simpson's Product

Damping coefficient for heaving, b

$b = \int b_n \, d\xi = (1/3)\times S\times SUM1$

$= (1/3)\times 0.55\times 3750.4 = 687.578$(kg/sec)

Damping coefficient for pitching, B

$A_{yy} = \int (b_n \xi^2) \, d\xi = (1/3)\times S\times SUM2$

$= (1/3)\times 0.55\times 925.08 = 169.598$(kg m^2/sec)

TABLE 3 CALCULATIONS FOR c AND C

(1) station	(2)	(3)	(4)	(5)	(6)	(7)	(8)	(9)
0	0	0	1	0	1.192	0	1	0
5	0.4392	4304.2	4	17217	0.294	1265.4	4	5061.7
10	0.4864	4766.7	2	9533.4	0	0	2	0
15	0.4692	4598.2	4	18393	0.311	1430.0	4	5720.1
20	0	0	1	0	1.228	0	1	0
			SUM1	45142			**SUM2**	10782

Description of Table 3

Column No.	*Description*	*Column No.*	*Description*
(1)	Station Number	(5)=(3)×(4)	Simpson's Product
(2)	Beam, B_n (m)	(6)	Lever Arm Squared, ξ^2

(3)=ρg×(2)	Sectional Restoring Force Coefficient, $c_n=\rho g B_n$	(7)=(3)×(6)	$c_n\times\xi^2$
(4)	Simpson's Multiplier	(9)=(7)×(8)	Simpson's Product

Restoring force coefficient for heaving, c

$c = \int c_n \, d\xi = (\rho g A_w) = (1/3)\times S \times SUM1$

$=(1/3)\times 0.55 \times 45142 = 8276.165 (kg/sec^2)$

Restoring moment coefficient for pitching,

$C = \int c_n \, \xi^2 \, d\xi$ - uE (u was model speed 0)

$= (1/3)\times S \times SUM2 - 0$

$=(1/3)\times 0.55 \times 10782 = 1976.66 (kg\ m^2/sec^2)$

TABLE 4 CALCULATIONS FOR d, e, h, D, E, AND H

(1) station	(2)	(3)	(4)	(5)	(6)	(7)	(8)	(9)	(10)
0	-1.092	0	0	1	0	0	0	1	0
5	-0.542	57.572	-31.20	4	-124.8	326.63	-177.0	4	-708.1
10	0.008	83.622	0.669	2	1.338	352.24	2.818	2	5.636
15	0.558	65.689	36.654	4	146.62	434.86	242.65	4	970.61
20	1.108	0	0	1	0	0	0	1	0
				SUM1	23.138			**SUM2**	268.12
station No.	**(11)**	**(12)**	**(13)**	**(14)**					
0	0	0	1	0					
5	4304.2	-2333	4	-9331					
10	4766.7	38.134	2	76.268					
15	4598.2	2565.8	4	10263					
20	0	0	1	0					
			SUM3	1007.9					

Description of Table 4

Column No.	*Description*	*Column No.*	*Description*
(1)	Station Number	(8)=(2)×(7)	$b_n\times\xi$
(2)	Lever Arm, ξ	(9)	Simpson's

(3)=(13) of Table 1	Sectional Added Mass Coefficient, a_n	(10)=(8)×(9)	Multiplier Simpson's Product
(4)=(2)×(3)	$a_n \times \xi$	(11)=(3) of Table 3	Sectional Restoring Force Coefficient, c_n
(5)	Simpson's Multiplier	(12)=(2)×(11)	$c_n \times \xi$
(6)=(4)×(5)	Simpson's Product	(13)	Simpson's Multiplier
(7)=(7) of Table 2	Sectional Damping Coefficient, b_n	(14)=(12)×(13)	Simpson's Product

$d = \int a_n \xi \, d\xi = (1/3) \times S \times SUM1$

$= (1/3) \times 0.55 \times 23.138 = 4.242$ (kg m)

$D = d = 4.242$ (kg m)

$e = \int b_n \xi \, d\xi + ua$ (u is model speed 0)

$= (1/3) \times S \times SUM2 = (1/3) \times 0.55 \times 268.12$

$= 49.155$ (kg m/sec)

$E = \int b_n \xi \, d\xi - ua$ (u is model speed 0)

$= (1/3) \times S \times SUM2 = (1/3) \times 0.55 \times 268.12$

$= 49.155$ (kg m/sec)

$h = \int c_n \xi \, d\xi + ub$ (u is model speed 0)

$= (1/3) \times S \times SUM3 = (1/3) \times 0.55 \times 1007.9$

$= 184.789$ (kg m/sec^2)

$H = \int c_n \xi \, d\xi - ub$ (u is model speed 0)

$= (1/3) \times S \times SUM3 = (1/3) \times 0.55 \times 1007.9$

$= 184.789$ (kg m/sec^2)

Mass of 'R-Class Icebreaker' ship model' is m = 121.6 kg. The mass moment of inertia I_{yy} was approximated as follows,

$$I_{yy} = mk_{yy}^2 \approx m(0.25L)^2 = 121.6 \times (0.25 \times 2.2)^2 = 36.784(kgm^2)$$

Substitute the calculated parameter values into the 'R-Class Icebreaker' heave and pitch motion equations.

$$242.653Z'' + 687.578Z' + 8276.165Z + 4.242\theta'' + 49.155\theta' + 184.789\theta = F(t)$$
$$64.178\theta'' + 169.598\theta' + 1976.66\theta + 4.242Z'' + 49.155Z' + 184.789Z = M(t)$$

Rewrite the motion equations into the matrix form,

$$\begin{pmatrix} 242.653 & 4.242 \\ 4.242 & 64.178 \end{pmatrix}\begin{pmatrix} Z'' \\ \theta'' \end{pmatrix} + \begin{pmatrix} 687.578 & 49.155 \\ 49.155 & 169.598 \end{pmatrix}\begin{pmatrix} Z' \\ \theta' \end{pmatrix} + \begin{pmatrix} 8276.165 & 184.789 \\ 184.789 & 1976.66 \end{pmatrix}\begin{pmatrix} Z \\ \theta \end{pmatrix} = \begin{pmatrix} F(t) \\ M(t) \end{pmatrix}$$

Multiply the above equations by $\begin{pmatrix} 242.653 & 4.242 \\ 4.242 & 64.178 \end{pmatrix}^{-1}$,

$$\begin{pmatrix} Z'' \\ \theta'' \end{pmatrix} + \begin{pmatrix} 2.824 & 0.158 \\ 0.580 & 2.632 \end{pmatrix}\begin{pmatrix} Z' \\ \theta' \end{pmatrix} + \begin{pmatrix} 34.092 & 0.238 \\ 0.629 & 30.780 \end{pmatrix}\begin{pmatrix} Z \\ \theta \end{pmatrix} = \begin{pmatrix} 0.0041258 & -0.000273 \\ -0.000273 & 0.0155997 \end{pmatrix}\begin{pmatrix} F(t) \\ M(t) \end{pmatrix}$$

If the units for Z, θ, F(t) and M(t) were (cm), (rad), (N), and (Nm) respectively, the equations for 'R-Class Icebreaker' ship model heave and pitch motions were converted into the following form,

$$Z'' + 2.824Z' + 34.092Z + 0.158\theta' + 0.238\theta = 100 \times (0.0041258F(t) - 0.000273M(t))$$
$$\theta'' + 0.580Z' + 0.629Z + 2.632\theta' + 30.780\theta = 100 \times (-0.000273F(t) + 0.0155997M(t))$$

This is the mathematical model for ship motion simulations in this research.

Appendix B Exciting Forces Calculations

The following calculations for wave induced forces and moments were based on the algorithm in Chapter Nine (pp.183-198) of *Dynamics of Marine Vehicles* by Bhattacharyya (1978).

TABLE CALCULATIONS FOR EXCITING FORCES AND MOMENTS

(1) station	(2)	(3)	(4)	(5)	(6)	(7)	(8)	(9)	(10)
0	-1.092	-2.156	-0.834	-0.552	0	0	1.00	0	0
5	-0.542	-1.070	-0.877	0.480	0.1306	0.2578	0.772	4304.2	107.60
10	0.008	0.016	0.016	1.00	0.1567	0.3093	0.734	4766.7	119.17
15	0.558	1.101	0.892	0.453	0.1385	0.2734	0.761	4598.2	114.95
20	1.108	2.187	0.816	-0.578	0	0	1.00	0	0
station No.	(11)	(12)	(13)	(14)	(15)	(16)	(17)	(18)	(19)
0	0	0	0	104.68	0	0	0	0	0
5	57.572	-27.84	79.764	76.020	0	35.913	35.913	-69.95	17.238
10	83.622	-40.44	78.732	7.379	0	38.728	38.728	1.260	38.728
15	65.689	-31.77	83.189	-76.02	0	47.813	47.813	74.205	21.659
20	0	0	0	-119.4	0	0	0	0	0
station No.	(20)	(21)	(22)	(23)	(24)	(25)	(26)	(27)	(28)
0	0	0	0	0	0	1	0	0	1
5	-52.72	38.287	-31.50	69.781	-40.70	4	-162.8	53.941	4
10	39.988	78.732	0.620	78.112	29.351	2	58.702	57.334	2
15	95.864	37.685	42.649	-4.964	72.953	4	291.81	-3.778	4
20	0	0	0	0	0	1	0	0	1
						SUM1	187.73		
station No.	(29)	(30)	(31)	(32)	(33)	(34)	(35)		
0	0	0	1	0	0	1	0		
5	215.76	22.057	4	88.228	-29.24	4	-116.9		
10	114.67	0.235	2	0.47	0.459	2	0.918		
15	-15.11	40.708	4	162.83	-2.108	4	-8.432		
20	0	0	1	0	0	1	0		
SUM2	315.45		**SUM3**	251.53		**SUM4**	-124.6		

Description of Table

Column No.	*Description*	*Column No.*	*Description*
(1)	Station Number	(17)=(16)-(15)	
(2)	Lever Arm, ξ(m)	(18)=(13)×(4)	
(3)	$k\xi=(2\pi/L_w)\times\xi$ $L_w=2\pi g/\omega^2$, ω was peak frequency in this table	(19)=(17)×(5)	
(4)	$\sin(k\xi)$	(20)=(18)×(19)	
(5)	$\cos(k\xi)$	(21)=(13)×(5)	
(6)	Mean Draft, T_m(m)	(22)=(17)×(4)	
(7)=k×(6)	$k\times T_m$	(23)=(21)-(22)	
(8)	$\exp(-k\times T_m)$	(24)=(20)×(8)	dF_1 / dx
(9)=(3) of Table 3 in Appendix A	Sectional Restoring Coefficient, c_n	(25)	Simpson's Multiplier
(10)=(9)×ζ_a	$c_n\times\zeta_a$, wave amplitude ζ_a was 2.5cm in this table	(26)=(24)×(25)	Simpson's Product
(11)=(13) of Table 1 in Appendix A	Sectional Added Mass, a_n	(27)=(23)×(8)	dF_2 / dx
(12)	$a_n\times(-\zeta_a\times\omega^2)$, ζ_a was wave amplitude 2.5cm in this table	(29)=(27)×(28)	Simpson's Product
(13)=(12)+(10)		(30)=(24)×(2)	dM_1 / dx
(14)	Slope of the added mass curve, $da_n/d\xi$ (numerical differentiation)	(32)=(30)×(31)	Simpson's Product
(15)=u$\zeta_a\omega$×(14)	u was the model speed 0 in this table	(33)=(27)×(2)	dM_2 / dx
(16)	$b_n\zeta_a\omega$	(35)=(34)×(33)	Simpson's Product

Exciting force component F_1 and F_2,

$F_1=(1/3)\times S\times SUM1=(1/3)\times 0.55\times 187.73$

$=34.417$ (N)

Exciting moment component M_1 and M_2,

$M_1=(1/3)\times S\times SUM3=(1/3)\times 0.55\times 251.53$

$=46.114$(Nm)

$F_2 = (1/3) \times S \times SUM2 = (1/3) \times 0.55 \times 315.15$

$= 57.776(N)$

$F_0 = \sqrt{F_1^2 + F_2^2} = 67.21(N)$

Ratio between force and wave amplitude,

$r_f = F_0 / \zeta_a = 67.21 / 2.5 = 26.88$ (N/cm)

The phase difference between force and wave,

$\sigma = \tan^{-1}(F_2/F_1) = 1.034(rad)$

$M_2 = (1/3) \times S \times SUM4 = (1/3) \times 0.55 \times (-124.6)$

$= -22.83((Nm)$

$M_0 = \sqrt{M_1^2 + M_2^2} = 51.45(Nm)$

Ratio between moment and wave amplitude,

$r_m = M_0 / \zeta_a = 51.45/2.5 = 20.58(Nm/cm)$

The phase difference between moment and wave

$\tau = \tan^{-1}(M_2/M_1) = -0.460(rad)$

The above results are excitation forces of 'R-Class Icebreaker' ship model in the regular wave with frequency 0.7Hz. For different wave frequencies ω, there will be different values for amplitude ratios r_f, r_m and phase difference σ, τ. This group of functions $r_f(\omega)$, $r_m(\omega)$, $\sigma(\omega)$, and $\tau(\omega)$ are excitation transform functions which can be used to deduce the random excitation forces from the wave spectrum. The following FORTRAN 77 program RATIO.FOR was used in this research to calculate the excitation transform functions of 'R-Class Icebreaker' ship model. The results were plotted after the program.

RATIO.FOR

```
      PROGRAM TRANSFORM FUNCTION
      REAL DS,X(5),T(5),A(5),B(5),C(5)
```

```
      REAL FRE(800),SPEC(800),K(800)
      REAL DF1(5,800),DF2(5,800),DM1(5,800),DM2(5,800)
      REAL F1(800),F2(800),M1(800),M2(800)
      REAL F(800),FANGLE(800),M(800),MANGLE(800)
      DATA X/-1.092,-0.542,0.008,0.558,1.108/
      DATA T/0.0,0.1306,0.1567,0.1385,0.0/
      DATA A/0.0,57.572,83.622,65.689,0.0/
      DATA B/0.0,326.628,352.236,434.860,0.0/
      DATA C/0.0,4304.16,4766.72,4598.16,0.0/
      DS=0.55
      OPEN (UNIT=11,FILE='spec1.d',STATUS='UNKNOWN')
      READ (11,*) (FRE(I),SPEC(I),I=1,800)
      CLOSE(11)
      DO 10 I=1,800
      K(I)=(2*3.1415926*FRE(I))**2/9.8
      DO 20 J=1,5
      DF1(J,I)=((-A(J)*(2*3.1415926*FRE(I))**2+C(J))*sin(K(I)*X(J))
     $ +B(J)*(2*3.1415926*FRE(I))*cos(K(I)*X(J)))*exp(-K(I)*T(J))
      DF2(J,I)=((-A(J)*(2*3.1415926*FRE(I))**2+C(J))*cos(K(I)*X(J))
     $ -B(J)*(2*3.1415926*FRE(I))*sin(K(I)*X(J)))*exp(-K(I)*T(J))
      DM1(J,I)=DF1(J,I)*X(J)
      DM2(J,I)=DF2(J,I)*X(J)
20    CONTINUE
      F1(I)=DS/300.0*(DF1(1,I)+4*DF1(2,I)+2*DF1(3,I)+4*DF1(4,I)+
     $ DF1(5,I))
      F2(I)=DS/300.0*(DF2(1,J)+4*DF2(2,I)+2*DF2(3,I)+4*DF2(4,I)+
     $ DF2(5,I))
      M1(I)=DS/300.0*(DM1(1,I)+4*DM1(2,I)+2*DM1(3,I)+4*DM1(4,I)+
     $ DM1(5,I))
      M2(I)=DS/300.0*(DM2(1,I)+4*DM2(2,I)+2*DM2(3,I)+4*DM2(4,I)+
     $ DM2(5,I))
      F(I)=sqrt(F1(I)**2+F2(I)**2)
      FANGLE(I)=ATAN(F2(I)/F1(I))
      M(I)=SQRT(M1(I)**2+M2(I)**2)
      MANGLE(I)=ATAN(M2(I)/M1(I))
10    CONTINUE
      OPEN (UNIT=21,FILE='ratio.d',STATUS='UNKNOWN')
      DO 30 I=1,800
      WRITE (21,*) F(I),FANGLE(I),M(I),MANGLE(I)
30    CONTINUE
      CLOSE(21)
      END
```

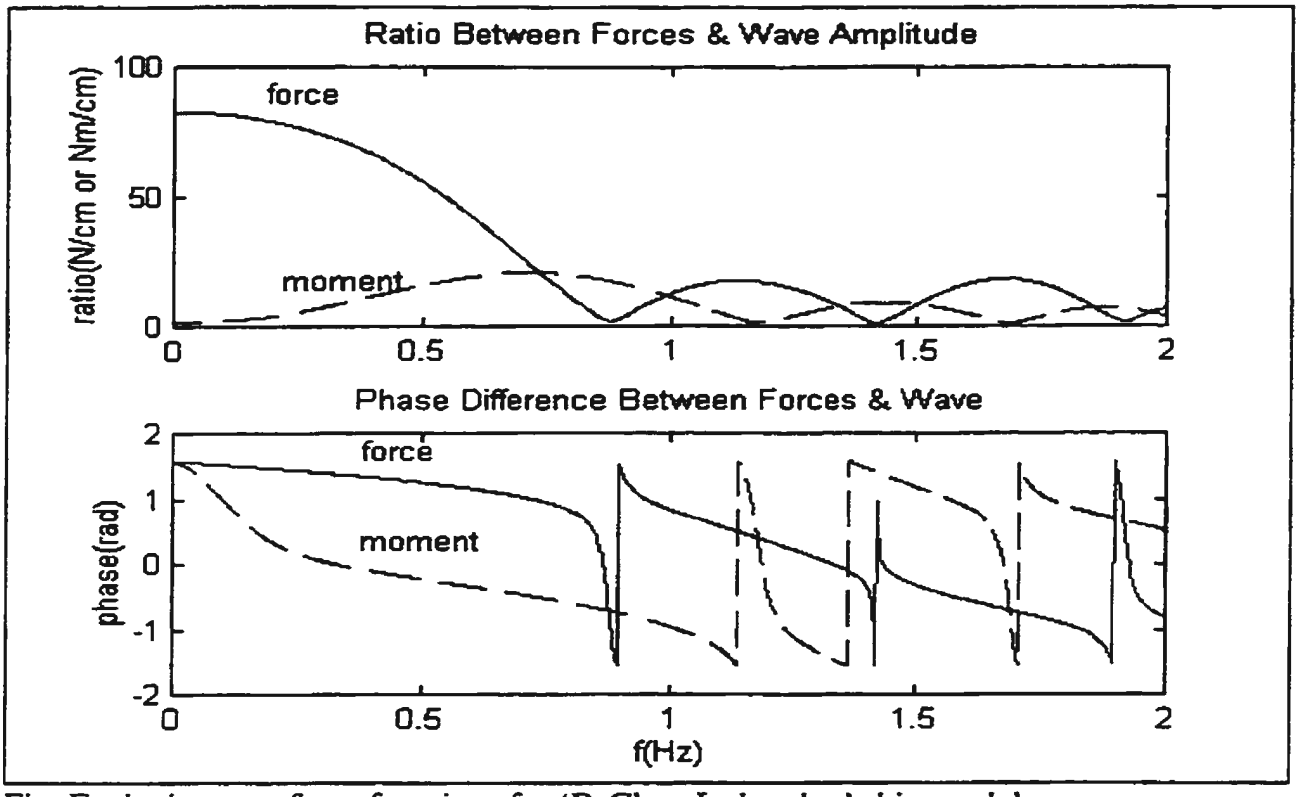

Fig. Excitation transform functions for 'R-Class Icebreaker' ship model

The following FORTRAN 77 program FORCE.FOR was used in this research to generate the random time series of the wave excitation forces through the combination of the wave spectrum and the excitation transform functions.

FORCE.FOR

```
PROGRAM SIMULATION OF EXCITATION FORCES
REAL FRE(800),SPEC(800),ANGLE(800),AMPLI(800),DFRE
REAL WAVE(8001),F(8001),M(8001),DT
REAL FRATIO(800),FANGLE(800),MRATIO(800),MANGLE(800)
OPEN (UNIT=11,FILE='spec1.d',STATUS='UNKNOWN')
READ (11,*) (FRE(I),SPEC(I),I=1,800)
CLOSE(11)
OPEN (UNIT=21,FILE='angle.d',STATUS='UNKNOWN')
READ (21,*) (ANGLE(I),I=1,800)
CLOSE(21)
OPEN (UNIT=31,FILE='ratio.d',STATUS='UNKNOWN')
READ (31,*) (FRATIO(I),FANGLE(I),MRATIO(I),MANGLE(I),I=1,800)
CLOSE(31)
```

```
      PRINT *, 'INPUT FREQUENCY BAND!'
      READ (*,*) DFRE
      DT=0.05
      DO 10 I=1,800
      AMPLI(I)=sqrt(2*SPEC(I)*DFRE)
      DO 20 J=1,8001
      WAVE(J)=WAVE(J)+AMPLI(I)*cos(2*3.1415926*FRE(I)*(J-1)*DT
     $ +ANGLE(I))
      F(J)=F(J)+FRATIO(I)*AMPLI(I)*cos(2*3.1415926*FRE(I)*(J-1)*DT
     $ +ANGLE(I)+FANGLE(I))
      M(J)=M(J)+MRATIO(I)*AMPLI(I)*cos(2*3.1415926*FRE(I)*(J-1)*DT
     $ +ANGLE(I)+MANGLE(I))
20    CONTINUE
10    CONTINUE
      OPEN (UNIT=41,FILE='force.d',STATUS='UNKNOWN')
      DO 30 I=1,8001
      WRITE (41,*) WAVE(I),F(I),M(I)
30    CONTINUE
      CLOSE(41)
      END
```

For White Noise excitation case, the random time series of the excitation forces were generated directly from the White Noise spectrum. The following FORTRAN 77 program WHITE.FOR was used for this generation.

WHITE.FOR

```
      PROGRAM SIMULATION OF WHITE EXCITATION
      REAL FRE(800),SPEC(800),ANGLE(800),AMPLI(800),DFRE
      REAL WAVE(8001),F(8001),M(8001),DT
      REAL FANGLE(800),MANGLE(800),FRATIO(800),MRATIO(800)
      OPEN (UNIT=11,FILE='spec1.d',STATUS='UNKNOWN')
      READ (11,*) (FRE(I),SPEC(I),I=1,800)
      CLOSE(11)
      OPEN (UNIT=21,FILE='angle.d',STATUS='UNKNOWN')
      READ (21,*) (ANGLE(I),I=1,800)
      CLOSE(21)
      OPEN (UNIT=31,FILE='ratio.d',STATUS='UNKNOWN')
      READ (31,*) (FRATIO(I),FANGLE(I),MRATIO(I),MANGLE(I),I=1,800)
      CLOSE(31)
      PRINT *, 'INPUT FREQUENCY BAND!'
      READ (*,*) DFRE
```

```
      DT=0.05
      DO 10 I=1,800
* Test of white noise excitation!
      SPEC(I)=3.0
      AMPLI(I)=sqrt(2*SPEC(I)*DFRE)
      DO 20 J=1,8001
      WAVE(J)=WAVE(J)+AMPLI(I)*cos(2*3.1415926*FRE(I)*(J-1)*DT
     $ +ANGLE(I))
      F(J)=F(J)+20.0*AMPLI(I)*cos(2*3.1415926*FRE(I)*(J-1)*DT
     $ +ANGLE(I)+FANGLE(I))
      M(J)=M(J)+20.0*AMPLI(I)*cos(2*3.1415926*FRE(I)*(J-1)*DT
     $ +ANGLE(I)+MANGLE(I))
20    CONTINUE
10    CONTINUE
      OPEN (UNIT=41,FILE='force.d',STATUS='UNKNOWN')
      DO 30 I=1,8001
      WRITE (41,*) WAVE(I),F(I),M(I)
30    CONTINUE
      CLOSE(41)
      END
```

Appendix C Data Processing Programs

The following FORTRAN 77 program SIMU.FOR was used to generate the heave and pitch motion history from the random excitation forces. The program CG.FOR was used to convert the experiment data into the motion data of the ship model CG (center of gravity). The program RANDEC.FOR was used to obtain the two-degree Random Decrement signatures from the heave and pitch motion history.

SIMU.FOR

```
      PROGRAM MOTION SIMULATION BY STRIP THEORY
      DOUBLE PRECISION RHO(1:8001),RPO(1:8001),VHO(1:8001),VPO(1:8001)
      DOUBLE PRECISION F1(1:8001),F2(1:8001),WAVE(0:8001)
      DOUBLE PRECISION A1,B1,C1,D1,E1,DT
      DOUBLE PRECISION A2,B2,C2,D2,E2
      DOUBLE PRECISION GH,GP
      DOUBLE PRECISION K1,K2,K3,K4,L1,L2,L3,L4
      DOUBLE PRECISION M1,M2,M3,M4,N1,N2,N3,N4
* Input initial value for motion signature!
      DT=0.05
      PRINT *, 'INPUT INITIAL VALUES FOR HEAVE!'
      READ (*,*) RHO(1),VHO(1)
      PRINT *, 'INPUT INITIAL VALUES FOR PITCH!'
      READ (*,*) RPO(1),VPO(1)
* Input heave coefficients from strip theory!
      PRINT *, 'INPUT HEAVE COEFFICIENTS A1,B1,C1,D1!'
      READ (*,*) A1,B1,C1,D1
* Input pitch coefficients from strip theory!
      PRINT *,'INPUT PITCH COEFFICIENTS A2,B2,C2,D2!'
      READ (*,*) A2,B2,C2,D2
* Calculation of the excitation forces!
      OPEN (UNIT=11,FILE='force.d',STATUS='UNKNOWN')
      READ (11,*) (WAVE(I),F1(I),F2(I),I=1,8001)
      CLOSE(11)
      DO 10 I=1,8001
      F1(I)=0.4125878*F1(I)-0.02727*F2(I)
      F2(I)=-0.02727*F1(I)+1.5599688*F2(I)
10    CONTINUE
* Prediction of coupled heave & pitch motion!
```

```
      DO 20 I=1,8000
      CALL NEURAL(GH,A1,B1,C1,D1,RHO(I),VHO(I),RPO(I),VPO(I))
      CALL NEURAL(GP,A2,B2,C2,D2,RHO(I),VHO(I),RPO(I),VPO(I))
      K1=DT*VHO(I)
      L1=DT*(F1(I)-GH)
      M1=DT*VPO(I)
      N1=DT*(F2(I)-GP)
      CALL
NEURAL(GH,A1,B1,C1,D1,RHO(I)+0.5*K1,VHO(I)+0.5*L1,RPO(I)+0.5*M1,
     $  VPO(I)+0.5*N1)
      CALL
NEURAL(GP,A2,B2,C2,D2,RHO(I)+0.5*K1,VHO(I)+0.5*L1,RPO(I)+0.5*M1,
     $  VPO(I)+0.5*N1)
      K2=DT*(VHO(I)+0.5*L1)
      L2=DT*((F1(I)+F1(I+1))/2.0-GH)
      M2=DT*(VPO(I)+0.5*N1)
      N2=DT*((F2(I)+F2(I+1))/2.0-GP)
      CALL
NEURAL(GH,A1,B1,C1,D1,RHO(I)+0.5*K2,VHO(I)+0.5*L2,RPO(I)+0.5*M2,
     $  VPO(I)+0.5*N2)
      CALL
NEURAL(GP,A2,B2,C2,D2,RHO(I)+0.5*K2,VHO(I)+0.5*L2,RPO(I)+0.5*M2,
     $  VPO(I)+0.5*N2)
      K3=DT*(VHO(I)+0.5*L2)
      L3=DT*((F1(I)+F1(I+1))/2.0-GH)
      M3=DT*(VPO(I)+0.5*N2)
      N3=DT*((F2(I)+F2(I+1))/2.0-GP)
      CALL
NEURAL(GH,A1,B1,C1,D1,RHO(I)+K3,VHO(I)+L3,RPO(I)+M3,VPO(I)+N3)
      CALL
NEURAL(GP,A2,B2,C2,D2,RHO(I)+K3,VHO(I)+L3,RPO(I)+M3,VPO(I)+N3)
      K4=DT*(VHO(I)+L3)
      L4=DT*(F1(I+1)-GH)
      M4=DT*(VPO(I)+N3)
      N4=DT*(F2(I+1)-GP)
      RHO(I+1)=RHO(I)+(K1+2.0*K2+2.0*K3+K4)/6.0
      VHO(I+1)=VHO(I)+(L1+2.0*L2+2.0*L3+L4)/6.0
      RPO(I+1)=RPO(I)+(M1+2.0*M2+2.0*M3+M4)/6.0
      VPO(I+1)=VPO(I)+(N1+2.0*N2+2.0*N3+N4)/6.0
20    CONTINUE
* Output of predicted heave & pitch motion!
      OPEN (UNIT=41,FILE='cg.d',STATUS='UNKNOWN')
      DO 30 I=1,8001
      WRITE (41,*) WAVE(I),RPO(I),RHO(I)
30    CONTINUE
```

```
      CLOSE(41)
      END

      SUBROUTINE NEURAL(G,A,B,C,D,RH,VH,RP,VP)
      DOUBLE PRECISION G,RH,VH,RP,VP
      DOUBLE PRECISION A,B,C,D
      G=A*VH+B*RH+C*VP+D*RP
      RETURN
      END
```

CG.FOR

```
      PROGRAM CGMOTION
      REAL WAVE(8001),PITCH(8001),HEAVE(8001),MW,MP,MH,HEAD,LCG
      OPEN(UNIT=11,FILE='data.d',STATUS='OLD')
      READ(11,*) (WAVE(I),PITCH(I),HEAVE(I), I=1,8001)
      CLOSE(11)
      MW=0.0
      MP=0.0
      MH=0.0
      PRINT *, 'INPUT WAVE DIRECTION VALUE!
     $ /HEADING=1.0,FOLLOWING=-1.0'
      READ (*,*) HEAD
      PRINT *,'INPUT LONGITUDINAL POSITION OF CG!
     $ /FORWARD OF MIDSHIP(cm)'
      READ (*,*) LCG
      DO 10 I=1,8001
      WAVE(I)=0.000553835845*WAVE(I)-18.5869461
      PITCH(I)=0.00210797726*PITCH(I)-69.3330754
      MP=MP+PITCH(I)
      MW=MW+WAVE(I)
10    CONTINUE
      MP=MP/8001.0
      MW=MW/8001.0
      DO 20 I=1,8001
      PITCH(I)=-HEAD*(PITCH(I)-MP)
      HEAVE(I)=-0.00277451443*HEAVE(I)+134.034007
      HEAVE(I)=HEAVE(I)-LCG*sin(PITCH(I)/180.0*3.1415926)
      MH=MH+HEAVE(I)
20    CONTINUE
      MH=MH/8001.0
      DO 30 I=1,8001
      HEAVE(I)=HEAVE(I)-MH
```

```
      WAVE(I)=WAVE(I)-MW
30    CONTINUE
      OPEN(UNIT=12,FILE='cg.d',STATUS='OLD')
      DO 40 I=1,8001
      WRITE (12,*) WAVE(I),PITCH(I),HEAVE(I)
40    CONTINUE
      CLOSE(12)
      PRINT *, 'MEAN VALUE OF WAVE(cm),PITCH(deg),HEAVE(cm) FOR CG!'
      PRINT *,'MW=',MW,'MP=',MP,'MH=',MH
      END
```

RANDEC.FOR

```
      PROGRAM HEAVE RANDOM DECREMENT
      REAL WAVE(8001),PITCH(8001),HEAVE(8001),RP(0:201),RH(0:201)
      REAL TRIGGER
      INTEGER SP(50),SN(50)
      OPEN (UNIT=11, FILE='cg.d',STATUS='OLD')
      READ (11,*) (WAVE(I),PITCH(I),HEAVE(I), I=1,8001)
      CLOSE(11)
      M=0
      N=0
      PRINT *, 'INPUT TRIGGER VALUE FOR HEAVE RANDOMDEC!'
      READ (*,*) TRIGGER
      DO 10 I=1,7800
      IF (HEAVE(I).LE.TRIGGER.AND.HEAVE(I+1).GT.TRIGGER) THEN
      M=M+1
      SP(M)=I
      IF (ABS(HEAVE(I)-TRIGGER).GT.ABS(HEAVE(I+1)-TRIGGER)) SP(M)=I+1
      I=I+201
      END IF
10    CONTINUE
      DO 20 I=1,7800
      IF (HEAVE(I).GE.TRIGGER.AND.HEAVE(I+1).LT.TRIGGER) THEN
      N=N+1
      SN(N)=I
      IF(ABS(HEAVE(I)-TRIGGER).GT.ABS(HEAVE(I+1)-TRIGGER)) SN(N)=I+1
      I=I+201
      END IF
20    CONTINUE
      K=M
      IF(M.GT.N) K=N
      DO 30 I=1,K
```

```
      DO 40 J=0,201
      RH(J)=RH(J)+HEAVE(SP(I)+J)
      RH(J)=RH(J)+HEAVE(SN(I)+J)
      RP(J)=RP(J)+PITCH(SP(I)+J)
      RP(J)=RP(J)+PITCH(SN(I)+J)
40    CONTINUE
30    CONTINUE
      OPEN (UNIT=12, FILE='randec.d',STATUS='OLD')
      DO 50 J=0,201
      RH(J)=RH(J)/(2.0*K)
      RP(J)=RP(J)/(2.0*K)
      WRITE(12,100) RP(J),RH(J)
100   FORMAT (1X,2F15.6)
50    CONTINUE
      PRINT *,'NUMBER FOR BOTH POSITIVE AND NEGATIVE SEGMENTS!'
      PRINT *, 'K=',K
      END
```

Appendix D Neural Network Training Program

The following FORTRAN 77 program NEURAL.FOR was used for Neural Network training to identify the unknown function in the heave motion equation. For pitch motion identification, the pitch motion data was input instead of the heave data in the program.

NEURAL.FOR

```
      PROGRAM NEURAL TRAINING FOR HEAVE
      DOUBLE PRECISION RH(0:201),RP(0:201),VH(1:200),VP(1:200)
      DOUBLE PRECISION WB(0:5),WA(1:5,0:4),DWA(1:5,0:4),DWB(0:5)
      DOUBLE PRECISION SWA(1:5,0:4),SWB(0:5),RO(200),ROP(200),RON(200)
      DOUBLE PRECISION JT,JTP,JTN,RATE,DT,DJW,FRE,TIME
      OPEN (UNIT=11, FILE='randec.d', STATUS='OLD')
      READ (11,*) (RP(I),RH(I),I=0,201)
      CLOSE(11)
* Numerical differentiation for randomdec signature!
      DT=0.05
      DO 10 I=1,200
      VH(I)=(RH(I+1)-RH(I-1))/(2.0*DT)
      VP(I)=(RP(I+1)-RP(I-1))/(2.0*DT)
10    CONTINUE
* Identification of damped heave frequency!
      IK=0
      DO 200 I=1,100
      IF((RH(I)-RH(I-1))*(RH(I+1)-RH(I)).LT.0.0) THEN
      IF(IK.EQ.0) IS=I
      TIME=DT*(I-IS)
      IK=IK+1
      END IF
200   CONTINUE
      TIME=TIME/(IK-1)*2.0
      FRE=2.0*3.1415926/TIME
      PRINT *,'DAMPED HEAVE FREQUENCY FRE =',FRE
* Set initial weight values for training!
      OPEN(UNIT=21,FILE='initial.d',STATUS='OLD')
      PRINT *,'PLEASE INPUT THE INITIAL WEIGHT VALUES!'
      READ (21,*) (WB(I),I=0,5)
      PRINT *,'WEIGHT VALUES BETWEEN OUTPUT AND HIDDEN NODES'
      WRITE (*,*) (WB(I),I=0,5)
      READ (21,*) (WA(1,I),I=0,4)
```

```
      PRINT *,'WEIGHT VALUES BETWEEN FIRST HIDDEN NODE & INPUTS'
      WRITE (*,*) (WA(1,I),I=0,4)
      READ (21,*) (WA(2,I),I=0,4)
      PRINT *,'WEIGHT VALUES BETWEEN SECOND HIDDEN NODE & INPUT'
      WRITE (*,*) (WA(2,I),I=0,4)
      READ (21,*) (WA(3,I),I=0,4)
      PRINT *,'WEIGHT VALUES BETWEEN THIRD HIDDEN NODE & INPUTS'
      WRITE (*,*) (WA(3,I),I=0,4)
      READ (21,*) (WA(4,I),I=0,4)
      PRINT *,'WEIGHT VALUES BETWEEM FOURTH HIDDEN NODE & INPUT'
      WRITE (*,*) (WA(4,I),I=0,4)
      READ (21,*) (WA(5,I),I=0,4)
      PRINT *,'WEIGHT VALUES BETWEEN FIFTH HIDDEN NODE & INPUTS'
      WRITE (*,*) (WA(5,I),I=0,4)
      PRINT *,'PLEASE INPUT SEARCH RATE !'
      READ (*,*) RATE
* Net training using set of training data by iteration!
      DO 150 K=1,100000
      IF (K.EQ.K/100*100) PRINT *, 'ITERATION TIME =', K
      JT=0.0
      DO 15 J=0,5
      WB(J)=WB(J)-RATE*DWB(J)
15    CONTINUE
      DO 20 M=1,5
      DO 30 N=0,4
      WA(M,N)=WA(M,N)-RATE*DWA(M,N)
30    CONTINUE
20    CONTINUE
      CALL NEURAL(RH,RP,VH,VP,RO,FRE,WA,WB,DT)
      DO 40 I=1,200
      JT=JT+(RO(I)-RH(I))**2
40    CONTINUE
      IF (K.EQ.K/100*100) PRINT *,'THE TOTAL ERROR JT=',JT
      IF(JT.LT.0.1D-05) GOTO 155
* Numerical differentiation of total error to every weight!
      DO 50 I=0,5
      SWB(I)=0.01*WB(I)
      WB(I)=WB(I)+SWB(I)
      CALL NEURAL(RH,RP,VH,VP,ROP,FRE,WA,WB,DT)
      JTP=0.0
      DO 60 J=1,200
      JTP=JTP+(ROP(J)-RH(J))**2
60    CONTINUE
      WB(I)=WB(I)-2.0*SWB(I)
      CALL NEURAL(RH,RP,VH,VP,RON,FRE,WA,WB,DT)
```

```
      JTN=0.0
      DO 70 J=1,200
      JTN=JTN+(RON(J)-RH(J))**2
70    CONTINUE
      WB(I)=WB(I)+SWB(I)
      DWB(I)=(JTP-JTN)/(2.0*SWB(I))
50    CONTINUE
      DO 80 M=1,5
      DO 90 N=0,4
      SWA(M,N)=0.01*WA(M,N)
      WA(M,N)=WA(M,N)+SWA(M,N)
      CALL NEURAL(RH,RP,VH,VP,ROP,FRE,WA,WB,DT)
      JTP=0.0
      DO 100 J=1,200
      JTP=JTP+(ROP(J)-RH(J))**2
100   CONTINUE
      WA(M,N)=WA(M,N)-2.0*SWA(M,N)
      CALL NEURAL(RH,RP,VH,VP,RON,FRE,WA,WB,DT)
      JTN=0.0
      DO 110 J=1,200
      JTN=JTN+(RON(J)-RH(J))**2
110   CONTINUE
      WA(M,N)=WA(M,N)+SWA(M,N)
      DWA(M,N)=(JTP-JTN)/(2.0*SWA(M,N))
90    CONTINUE
80    CONTINUE
      DJW=0.0
      DO 120 I=0,5
      DJW=DJW+DWB(I)**2
120   CONTINUE
      DO 130 M=1,5
      DO 140 N=0,4
      DJW=DJW+DWA(M,N)**2
140   CONTINUE
130   CONTINUE
      IF (K.EQ.K/100*100) THEN
      PRINT *,'THE SQUARE TOTAL OF PARTIAL DERIVATIVES DJW=',DJW
      END IF
      IF (DJW.LE.0.1D-10) GOTO 155
      IF (K.EQ.K/1000*1000) THEN
      OPEN (UNIT=12,FILE='weight.d',STATUS='OLD')
      WRITE(12,*) (WB(I),I=0,5)
      WRITE(12,*) (WA(1,I),I=0,4)
      WRITE(12,*) (WA(2,I),I=0,4)
      WRITE(12,*) (WA(3,I),I=0,4)
```

```
      WRITE(12,*) (WA(4,I),I=0,4)
      WRITE(12,*) (WA(5,I),I=0,4)
      CLOSE(12)
      END IF
150   CONTINUE
155   OPEN (UNIT=12, FILE='weight.d',STATUS='OLD')
      PRINT *, 'THE FINAL WEIGHT VALUES!'
      PRINT *, (WB(I), I=0,5)
      WRITE(12,*) (WB(I), I=0,5)
      PRINT *, 'FIRST HIDDEN NODE - INPUTS'
      PRINT *, (WA(1,I), I=0,4)
      WRITE(12,*) (WA(1,I), I=0,4)
      PRINT *, 'SECOND HIDDEN NODE - INPUTS'
      PRINT *, (WA(2,I), I=0,4)
      WRITE(12,*) (WA(2,I), I=0,4)
      PRINT *, 'THIRD HIDDEN NODE - INPUTS'
      PRINT *, (WA(3,I), I=0,4)
      WRITE (12,*) (WA(3,I),I=0,4)
      PRINT *, 'FOURTH HIDDEN NODE - INPUTS'
      PRINT *, (WA(4,I), I=0,4)
      WRITE(12,*) (WA(4,I),I=0,4)
      PRINT *, 'FIFTH HIDDEN NODE - INPUTS'
      PRINT *, (WA(5,I),I=0,4)
      WRITE(12,*) (WA(5,I),I=0,4)
      CLOSE(12)
      OPEN (UNIT=13,FILE='neural.d',STATUS='OLD')
      WRITE (13,*) 'DAMPED HEAVE FREQUENCY FRE =',FRE
      WRITE (13,*) 'THE TOTAL ERROR JT =',JT
      WRITE (13,*) 'THE TOTAL SQUARE PARTIAL DERIVATIVES DJW =',DJW
      WRITE (13,*) 'THE PARTIAL DERIVATIVES ARE AS FOLLOWING:'
      WRITE (13,*) (DWB(I),I=0,5)
      WRITE (13,*) (DWA(1,I),I=0,4)
      WRITE (13,*) (DWA(2,I),I=0,4)
      WRITE (13,*) (DWA(3,I),I=0,4)
      WRITE (13,*) (DWA(4,I),I=0,4)
      WRITE (13,*) (DWA(5,I),I=0,4)
      WRITE (13,*) 'THE TARGET VALUE RH(I) AND OUTPUT VALUE RO(I)!'
      DO 160 I=1,200
      WRITE (13,*) RH(I),RO(I)
160   CONTINUE
      CLOSE(13)
      END

      SUBROUTINE NEURAL(RH,RP,VH,VP,RO,FRE,WA,WB,DT)
      DOUBLE PRECISION RH(0:201),RP(0:201),VH(1:200),VP(1:200),RO(1:200)
```

```
      DOUBLE PRECISION WA(1:5,0:4),WB(0:5),G(1:200),UH(1:5),VO(1:200)
      DOUBLE PRECISION FRE,DT,X,K1,K2,K3,K4
      DOUBLE PRECISION RHM(1:199),RPM(1:199),VHM(1:199),VPM(1:199)
      DOUBLE PRECISION UHM(1:5),GM(1:199)
      f(X)=1.0/(1.0+exp(-X))
* Calculation for neural-net outputs!
      DO 150 K=1,200
      DO 10 J=1,5
      UH(J)=f(WA(J,0)*1.0+WA(J,1)*VH(K)+WA(J,2)*RH(K)+WA(J,3)*VP(K)
     $   +WA(J,4)*RP(K))
10    CONTINUE
      G(K)=WB(0)*1.0+WB(1)*UH(1)+WB(2)*UH(2)+WB(3)*UH(3)+WB(4)*UH(4)
     $  +WB(5)*UH(5)
150   CONTINUE
* Calculation for neural-net output midpoints!
      DO 20 I=1,199
      RHM(I)=(RH(I)+RH(I+1))/2.0
      VHM(I)=(VH(I)+VH(I+1))/2.0
      RPM(I)=(RP(I)+RP(I+1))/2.0
      VPM(I)=(VP(I)+VP(I+1))/2.0
      DO 30 J=1,5
      UHM(J)=f(WA(J,0)*1.0+WA(J,1)*VHM(I)+WA(J,2)*RHM(I)
     $   +WA(J,3)*VPM(I)+WA(J,4)*RPM(I))
30    CONTINUE
      GM(I)=WB(0)*1.0+WB(1)*UHM(1)+WB(2)*UHM(2)+WB(3)*UHM(3)
     $   +WB(4)*UHM(4)+WB(5)*UHM(5)
20    CONTINUE
* Numerical integration for differential equation!
      RO(1)=RH(1)
      VO(1)=VH(1)
      DO 160 I=1,199
      K1=DT*(-G(I)-FRE**2*RO(I))
      K2=DT*(-GM(I)-FRE**2*(RO(I)+DT*VO(I)/2.0+DT*K1/8.0))
      K3=DT*(-GM(I)-FRE**2*(RO(I)+DT*VO(I)/2.0+DT*K2/8.0))
      K4=DT*(-G(I+1)-FRE**2*(RO(I)+DT*VO(I)+DT*K3/2.0))
      RO(I+1)=RO(I)+DT*(VO(I)+(K1+K2+K3)/6.0)
      VO(I+1)=VO(I)+(K1+2.0*K2+2.0*K3+K4)/6.0
160   CONTINUE
      RETURN
      END
```

Appendix E Verification Programs

The following programs were used to verify the identification results in this research. The program PREDIC.FOR was used to get the prediction signatures from the identified Random Decrement equations and make a comparison with the .actual Random Decrement signatures. The program FREE.FOR was used in simulation case to obtain the free response signatures and compare with the Random Decrement signatures.

PREDIC.FOR

```
      PROGRAM MOTION PREDICTION
      DOUBLE PRECISION RH(0:201),RP(0:201),VH(1:200),VP(1:200)
      DOUBLE PRECISION RHO(1:200),RPO(1:200),VHO(1:200),VPO(1:200)
      DOUBLE PRECISION WAH(1:5,0:4),WBH(0:5),FREH,DT
      DOUBLE PRECISION WAP(1:5,0:4),WBP(0:5),FREP
      DOUBLE PRECISION GH,GP
      DOUBLE PRECISION K1,K2,K3,K4,L1,L2,L3,L4
      DOUBLE PRECISION M1,M2,M3,M4,N1,N2,N3,N4
      OPEN (UNIT=11,FILE='randec.d',STATUS='OLD')
      READ (11,*) (RP(I),RH(I),I=0,201)
      CLOSE(11)
      PRINT *, 'PLEASE INPUT DAMPED FREQUENCY FOR HEAVE!'
      READ (*,*) FREH
      PRINT *, 'PLEASE INPUT DAMPED FREQUENCY FOR PITCH!'
      READ (*,*) FREP
* Numerical differentiation for randomdec signature!
      DT=0.05
      DO 10 I=1,200
      VH(I)=(RH(I+1)-RH(I-1))/(2.0*DT)
      VP(I)=(RP(I+1)-RP(I-1))/(2.0*DT)
10    CONTINUE
* Input heave weight values obtained from training!
      OPEN (UNIT=21,FILE='weight.d',STATUS='OLD')
      READ (21,*) (WBH(I),I=0,5)
      READ (21,*) (WAH(1,I),I=0,4)
      READ (21,*) (WAH(2,I),I=0,4)
      READ (21,*) (WAH(3,I),I=0,4)
      READ (21,*) (WAH(4,I),I=0,4)
      READ (21,*) (WAH(5,I),I=0,4)
```

```
      CLOSE(21)
* Input pitch weight values obtained from training!
      OPEN (UNIT=31,FILE='pweight.d',STATUS='OLD')
      READ (31,*) (WBP(I),I=0,5)
      READ (31,*) (WAP(1,I),I=0,4)
      READ (31,*) (WAP(2,I),I=0,4)
      READ (31,*) (WAP(3,I),I=0,4)
      READ (31,*) (WAP(4,I),I=0,4)
      READ (31,*) (WAP(5,I),I=0,4)
      CLOSE(31)
* Prediction of coupled heave & pitch motion!
      RHO(1)=RH(1)
      VHO(1)=VH(1)
      RPO(1)=RP(1)
      VPO(1)=VP(1)
      DO 20 I=1,199
      CALL NEURAL(GH,WBH,WAH,RHO(I),VHO(I),RPO(I),VPO(I))
      CALL NEURAL(GP,WBP,WAP,RHO(I),VHO(I),RPO(I),VPO(I))
      K1=DT*VHO(I)
      L1=DT*(-FREH**2*RHO(I)-GH)
      M1=DT*VPO(I)
      N1=DT*(-FREP**2*RPO(I)-GP)
      CALL NEURAL(GH,WBH,WAH,RHO(I)+0.5*K1,
     S  VHO(I)+0.5*L1,RPO(I)+0.5*M1,VPO(I)+0.5*N1)
      CALL NEURAL(GP,WBP,WAP,RHO(I)+0.5*K1,
     S  VHO(I)+0.5*L1,RPO(I)+0.5*M1,VPO(I)+0.5*N1)
      K2=DT*(VHO(I)+0.5*L1)
      L2=DT*(-FREH**2*(RHO(I)+0.5*K1)-GH)
      M2=DT*(VPO(I)+0.5*N1)
      N2=DT*(-FREP**2*(RPO(I)+0.5*M1)-GP)
      CALL NEURAL(GH,WBH,WAH,RHO(I)+0.5*K2,
     S  VHO(I)+0.5*L2,RPO(I)+0.5*M2,VPO(I)+0.5*N2)
      CALL NEURAL(GP,WBP,WAP,RHO(I)+0.5*K2,
     S  VHO(I)+0.5*L2,RPO(I)+0.5*M2,VPO(I)+0.5*N2)
      K3=DT*(VHO(I)+0.5*L2)
      L3=DT*(-FREH**2*(RHO(I)+0.5*K2)-GH)
      M3=DT*(VPO(I)+0.5*N2)
      N3=DT*(-FREP**2*(RPO(I)+0.5*M2)-GP)
      CALL NEURAL(GH,WBH,WAH,RHO(I)+K3,
     S  VHO(I)+L3,RPO(I)+M3,VPO(I)+N3)
      CALL NEURAL(GP,WBP,WAP,RHO(I)+K3,
     S  VHO(I)+L3,RPO(I)+M3,VPO(I)+N3)
      K4=DT*(VHO(I)+L3)
      L4=DT*(-FREH**2*(RHO(I)+K3)-GH)
      M4=DT*(VPO(I)+N3)
```

```
        N4=DT*(-FREP**2*(RPO(I)+M3)-GP)
        RHO(I+1)=RHO(I)+(K1+2.0*K2+2.0*K3+K4)/6.0
        VHO(I+1)=VHO(I)+(L1+2.0*L2+2.0*L3+L4)/6.0
        RPO(I+1)=RPO(I)+(M1+2.0*M2+2.0*M3+M4)/6.0
        VPO(I+1)=VPO(I)+(N1+2.0*N2+2.0*N3+N4)/6.0
20      CONTINUE
* Output of predicted heave & pitch motion!
        OPEN (UNIT=41,FILE='comp.d',STATUS='UNKNOWN')
        DO 30 I=1,200
        WRITE (41,*) RH(I),RHO(I)
30      CONTINUE
        CLOSE(41)
        OPEN (UNIT=51,FILE='pcomp.d',STATUS='UNKNOWN')
        DO 40 I=1,200
        WRITE (51,*) RP(I),RPO(I)
40      CONTINUE
        CLOSE(51)
        OPEN (UNIT=61,FILE='predic.d',STATUS='UNKNOWN')
        DO 50 I=1,200
        WRITE (61,100) RPO(I),RHO(I)
100     FORMAT(1X,2F15.6)
50      CONTINUE
        CLOSE(61)
        END

        SUBROUTINE NEURAL(G,WB,WA,RH,VH,RP,VP)
        DOUBLE PRECISION G,RH,VH,RP,VP
        DOUBLE PRECISION WB(0:5),WA(1:5,0:4),UH(1:5),X
        f(x)=1.0/(1.0+exp(-x))
        DO 10 J=1,5
        UH(J)=f(WA(J,0)*1.0+WA(J,1)*VH+WA(J,2)*RH+WA(J,3)*VP+WA(J,4)*RP)
10      CONTINUE
        G=WB(0)*1.0+WB(1)*UH(1)+WB(2)*UH(2)+WB(3)*UH(3)+WB(4)*UH(4)+
     S  WB(5)*UH(5)
        RETURN
        END
```

FREE.FOR

```
        PROGRAM MOTION FREE RESPONSE
        DOUBLE PRECISION RH(0:201),RP(0:201),VH(1:200),VP(1:200)
        DOUBLE PRECISION RHO(1:200),RPO(1:200),VHO(1:200),VPO(1:200)
        DOUBLE PRECISION A1,B1,C1,D1,DT
```

```
      DOUBLE PRECISION A2,B2,C2,D2
      DOUBLE PRECISION GH,GP
      DOUBLE PRECISION K1,K2,K3,K4,L1,L2,L3,L4
      DOUBLE PRECISION M1,M2,M3,M4,N1,N2,N3,N4
      OPEN (UNIT=11,FILE='randec.d',STATUS='OLD')
      READ (11,*) (RP(I),RH(I),I=0,201)
      CLOSE(11)
* Numerical differentiation for randomdec signature!
      DT=0.05
      DO 10 I=1,200
      VH(I)=(RH(I+1)-RH(I-1))/(2.0*DT)
      VP(I)=(RP(I+1)-RP(I-1))/(2.0*DT)
10    CONTINUE
* Input heave coefficients from strip theory!
      PRINT *, 'INPUT HEAVE COEFFICIENTS A1,B1,C1,D1!'
      READ (*,*) A1,B1,C1,D1
* Input pitch coefficients from strip theory!
      PRINT *,'INPUT PITCH COEFFICIENTS A2,B2,C2,D2!'
      READ (*,*) A2,B2,C2,D2
* Free response of coupled heave & pitch motion!
      RHO(1)=RH(1)
      VHO(1)=VH(1)
      RPO(1)=RP(1)
      VPO(1)=VP(1)
      DO 20 I=1,199
      CALL NEURAL(GH,A1,B1,C1,D1,RHO(I),VHO(I),RPO(I),VPO(I))
      CALL NEURAL(GP,A2,B2,C2,D2,RHO(I),VHO(I),RPO(I),VPO(I))
      K1=DT*VHO(I)
      L1=DT*(-GH)
      M1=DT*VPO(I)
      N1=DT*(-GP)
      CALL NEURAL(GH,A1,B1,C1,D1,RHO(I)+0.5*K1,
     $ VHO(I)+0.5*L1,RPO(I)+0.5*M1,VPO(I)+0.5*N1)
      CALL NEURAL(GP,A2,B2,C2,D2,RHO(I)+0.5*K1,
     $ VHO(I)+0.5*L1,RPO(I)+0.5*M1,VPO(I)+0.5*N1)
      K2=DT*(VHO(I)+0.5*L1)
      L2=DT*(-GH)
      M2=DT*(VPO(I)+0.5*N1)
      N2=DT*(-GP)
      CALL NEURAL(GH,A1,B1,C1,D1,RHO(I)+0.5*K2,
     $ VHO(I)+0.5*L2,RPO(I)+0.5*M2,VPO(I)+0.5*N2)
      CALL NEURAL(GP,A2,B2,C2,D2,RHO(I)+0.5*K2,
     $ VHO(I)+0.5*L2,RPO(I)+0.5*M2,VPO(I)+0.5*N2)
      K3=DT*(VHO(I)+0.5*L2)
      L3=DT*(-GH)
```

```
      M3=DT*(VPO(I)+0.5*N2)
      N3=DT*(-GP)
      CALL NEURAL(GH,A1,B1,C1,D1,RHO(I)+K3,
     $  VHO(I)+L3,RPO(I)+M3,VPO(I)+N3)
      CALL NEURAL(GP,A2,B2,C2,D2,RHO(I)+K3,
     $  VHO(I)+L3,RPO(I)+M3,VPO(I)+N3)
      K4=DT*(VHO(I)+L3)
      L4=DT*(-GH)
      M4=DT*(VPO(I)+N3)
      N4=DT*(-GP)
      RHO(I+1)=RHO(I)+(K1+2.0*K2+2.0*K3+K4)/6.0
      VHO(I+1)=VHO(I)+(L1+2.0*L2+2.0*L3+L4)/6.0
      RPO(I+1)=RPO(I)+(M1+2.0*M2+2.0*M3+M4)/6.0
      VPO(I+1)=VPO(I)+(N1+2.0*N2+2.0*N3+N4)/6.0
20    CONTINUE
* Output of predicted heave & pitch motion!
      OPEN (UNIT=41,FILE='comp.d',STATUS='UNKNOWN')
      DO 30 I=1,200
      WRITE (41,*) RH(I),RHO(I)
30    CONTINUE
      CLOSE(41)
      OPEN (UNIT=51,FILE='pcomp.d',STATUS='UNKNOWN')
      DO 40 I=1,200
      WRITE (51,*) RP(I),RPO(I)
40    CONTINUE
      CLOSE(51)
      OPEN (UNIT=61,FILE='strip.d',STATUS='UNKNOWN')
      DO 50 I=1,200
      WRITE (61,100) RPO(I),RHO(I)
100   FORMAT (1X,2F15.6)
50    CONTINUE
      CLOSE(61)
      END

      SUBROUTINE NEURAL(G,A,B,C,D,RH,VH,RP,VP)
      DOUBLE PRECISION G,RH,VH,RP,VP
      DOUBLE PRECISION A,B,C,D
      G=A*VH+B*RH+C*VP+D*RP
      RETURN
      END
```